

**The Role of PTPN1 in the Progression of  
JAK2V617F-induced Myeloproliferative  
Neoplasms**

Bao Le

A Dissertation for the Degree of Doctor of Philosophy in  
Biochemistry and Molecular Genetics at the University of Virginia

## Acknowledgments

Firstly, I would like to express my appreciation to my Ph.D. mentor, Dr. Golam Mohi. Since the beginning of my Ph.D. journey in 2016 until its completion, he has provided invaluable support that has nurtured not only my curiosity for scientific knowledge but also my personal growth as a scientist. As a result, I am confident that I will be well-prepared for whatever the future holds. For this, I am deeply grateful.

Next, I would like to thank my committee members, Dr. Yuh-Hwa Wang, Dr. Hao Jiang, and Dr. Adam Goldfarb for being on my committee and allocating their time to support me. I greatly appreciate their valuable feedback and advice.

To the former and current lab members, I thank you for your support. Dr. Dipmoy Nath and Dr. Avik Dutta, thank you for your help and training during my early years. Dr. Yue Yang, thank you for your numerous contributions to support my project and for always being there to lend a hand throughout my journey. Dr. Patrick Faughnan, thanks for being a great roommate throughout this journey and providing a lively atmosphere in the lab. Dr. Ferdous Ur-Rahman, thanks for your guidance and advice throughout. Dr. Mohammed Abu Sayem, Dr. Abbas Salar, Dr. Chandrajeet Singh, and Fahim Ather, thank you for being great colleagues and supporting me whenever things become overburdensome.

I would also like to give thanks to the BMG department and the University of Virginia, especially Debbie, Nancy, Carolyn, Sonya, and Helen, for always providing assistance and support through all the tedious bureaucratic activities.

Finally, I would like to thank my family and friends for their patience throughout my long journey while remaining highly supportive. My sister, Thuy, thank you for always listening and providing me with valuable suggestions and guidance. To my nieces and nephew, Kiera, Tiana, Ella, and Emmet, who grew up with very little presence from this uncle, that will change soon. I would like to thank my parents for providing boundless love and support no matter the difficulties I have faced. I also give thanks to my aunt and uncles who supported me throughout this journey. Finally, Ha Vi, thank you for always supporting me throughout my Ph.D. journey and providing encouragement and motivation. For that, I just want to say, I love you all.

# Dissertation Abstract

## The Role of PTPN1 in the Progression of JAK2V617F-induced Myeloproliferative Neoplasms

Bao Le

Sponsor: Golam Mohi, Ph.D

The deletion of chromosome 20q (del20q) is a common karyotypic abnormality associated with myeloid malignancies, including 15% of myeloproliferative neoplasms (MPN), 10% of myelodysplastic syndrome (MDS), 5% of MDS/MPN overlapping diseases, and 5% of acute myeloid leukemia (AML). Myelofibrosis (MF), the deadliest among MPNs, exhibits the most frequent association with del20q. In MPN, the oncogenic JAK2V617F mutation was detected in approximately 97% of patients with polycythemia vera (PV), and 50-60% of patients with essential thrombocythemia (ET) and myelofibrosis. We have observed a significant co-occurrence of the JAK2V617F mutation and del20q abnormality involving PTPN1 deletion in patients with MF. Therefore, we hypothesize that PTPN1 deficiency may cooperate with JAK2V617F in the progression to MF.

In this study, we investigated the effects of PTPN1 deficiency in JAK2V617F-induced MPN using a conditional knockout allele for PTPN1 and a mouse model of MPN with knock-in JAK2V617F mutation. Mice expressing heterozygous JAK2V617F ( $JAK2^{V617F/+}$ ) exhibit a PV-like MPN characterized by an increase in red blood cells (RBC), white blood cells (WBC), neutrophils, and platelets in the peripheral blood. Heterozygous deletion of PTPN1 significantly increased WBC, neutrophil, and

platelet counts but reduced RBC and hemoglobin levels in JAK2<sup>V617F/+</sup> mice. Flow cytometric analysis showed significantly increased myeloid (Gr-1<sup>+</sup>Mac-1<sup>+</sup>) and megakaryocytic (CD41<sup>+</sup>CD61<sup>+</sup>) precursors in the BM and spleens of PTPN1-deficient JAK2<sup>V617F/+</sup> mice compared with JAK2<sup>V617F/+</sup> mice. Additionally, deletion of PTPN1 significantly increased hematopoietic stem cells and myeloid progenitors in the BM and spleens of PTPN1-deficient JAK2<sup>V617F/+</sup> mice compared to JAK2<sup>V617F/+</sup> mice. Spleen weight was significantly increased in JAK2<sup>V617F/+</sup> mice, while deletion of PTPN1 further enhanced splenomegaly in PTPN1-deficient JAK2<sup>V617F/+</sup> mice. Moreover, PTPN1 deletion significantly enhanced bone marrow fibrosis in JAK2<sup>V617F/+</sup> mice. Bone marrow transplantation assays confirmed that the phenotypes observed in PTPN1-deficient JAK2<sup>V617F/+</sup> mice are cell intrinsic. Furthermore, the hematopoietic stem cells (HSC) from PTPN1-deficient JAK2<sup>V617F/+</sup> mice display greater clonal advantage than the HSC of JAK2<sup>V617F/+</sup> mice. Deletion of both alleles of PTPN1 resulted in more robust and accelerated development of myelofibrosis in JAK2<sup>V617F/+</sup> mice. The cooperative effects of JAK2V617F and PTPN1 deficiency in myelofibrotic transformation are associated with increased production of proinflammatory cytokines, including IL-1 $\beta$ , IL-6, and TGF- $\beta$ .

Biochemical analyses revealed greater activation of STAT1, STAT3, STAT5, ERK1/2, and NF-kB signaling in bone marrow of PTPN1-deficient JAK2V617F/+ mice compared with bone marrow of JAK2V617F/+ or WT mice. CRISPR/Cas9-mediated deletion of PTPN1 also resulted in increased proliferation and enhanced activation of these signaling molecules in JAK2V617F-positive hematopoietic cells. RNA-sequencing analysis showed enrichment of genes related to hematopoietic stem cells, MAPK cascade, cell cycle, and WNT signaling pathways in PTPN1-deficient JAK2<sup>V617F/+</sup> LSK

cells, which have significant overlap with genes enriched in hematopoietic cells of patients with myelofibrosis. Furthermore, deletion of PTPN1 significantly reduced ruxolitinib sensitivity against JAK2V617F-positive hematopoietic cells, suggesting that del20q involving PTPN1 deletion may alter the ruxolitinib response in MPN. Overall, this study demonstrates that PTPN1 is an important target in del20q-associated MPN, and deficiency of PTPN1 collaborates with JAK2V617F in the progression to myelofibrosis.

## List of Abbreviations

293T	Human Embryonic Kidney 293T cells
AGM	Aorta-Gonad-Mesonephros
AKT	Protein Kinase B
AML	Acute myeloid leukemia
ANOVA	Analysis of variance
AXL	Tyrosine-protein kinase receptor UFO
Ba/F3 VF	Ba/F3 expressing human EPOR and JAK2V617F mutation
BCR-ABL1	Oncogenic fusion protein p210
BFU-E	Burst-forming units erythroid
BLVRB	Biliverdin reductase
BM	Bone Marrow
BMT	Bone marrow transplantation
BTK	Bruton's tyrosine kinase
CALR	Calreticulin
CD11b	Mac-1
CD41a	glycoprotein IIb/IIIa
CD42b	glycoprotein Ib
CD61	glycoprotein IIIa
CD71	Transferrin receptor 1
CFU	Colony-forming units
CFU-E	Colony-forming units erythroid
CFU-GEMM	Colony forming unit – granulocyte, erythrocyte, monocyte, and megakaryocyte

CFU-GM	Colony-forming unit granulocyte-monocyte
CFU-Mk	Colony-forming unit megakaryocytes
CFU-Mk	Colony-forming unit megakaryocyte
CLL	Chronic lymphocytic leukemia
CLP	Common lymphoid progenitor
CML	Chronic myeloid leukemia
CMP	Common myeloid progenitor
COL1A1	Collagen I
CRISPR	Clustered regularly interspaced short palindromic repeats
DAG	Diacylglycerol
DAPI	4',6-diamidino-2-phenylindole
del20q	Deletion of the q-arm of chromosome 20
DIPPS	Dynamic international prognostic scoring system
DMEM	Dulbecco's Modified Eagle Medium
DMS / IMS	Demarcation membrane system / Invaginated membrane system
EDTA	Ethylenediaminetetraacetic acid
ELISA	Enzyme-linked immunosorbent assay
EMH	Extramedullary hematopoiesis
EMT	epithelial-to-mesenchymal transition
EPO	Erythropoietin
EPOR	erythropoietin receptor
ERK	Extracellular Signal-Related Kinases
ESA	Erythropoietin-stimulating agent



ET	Essential thrombocythemia
FERM	4.1 protein, Ezrin, Radixin, Moesin
FLI1	Friend leukemia integration 1
FLT3	FMS-like tyrosine kinase 3
FOG1	Friend of GATA 1
GAPDH	Glyceraldehyde-3-phosphate dehydrogenase
GATA1	GATA-binding factor 1
GIPSS	Genetically-inspired international prognostic scoring system
GM-CSF	Granulocyte-monocyte colony-stimulating factor
GMP	Granulocyte-monocyte progenitor
Gr-1	Ly6G/Ly6C
GSEA	Gene Set Enrichment Analysis
H&E	Hematoxylin and Eosin
Hb	Hemoglobin
HCT	Hematocrit
HEL	Human erythroid leukemic cells
HMGA2	High-mobility group AT-hook 2
HPRT1	Hypoxanthine-guanine phosphoribosyltransferase
HSC	Hematopoietic Stem Cells
HU	Hydroxyurea
IFN- $\alpha$	Interferon- $\alpha$
IFN- $\gamma$	Interferon- $\gamma$
IL1B	Interleukin-1 $\beta$
IL-3	Interleukin-3

IL-6	Interleukin-6
IP	Immunoprecipitation
IP3	Inositol-1,4,5-trisphosphate
IPSS	International prognostic scoring system
IR	Insulin receptor
IWG-MRT	International Working Group for Myelofibrosis Research and Treatment
JAK	Janus Kinase
JAK2V617F	JAK2 mutation with valine to phenylalanine at position 617
JH1/2	Janus homology domain 1/2
KLF1	Kruppel-like factor 1
KO	Knockout
LK	Lineage Negative; c-Kit positive; Sca-1 negative
LSK	Lineage Negative, Sca-1 positive, and c-Kit positive cells
LTHSC	Long-term hematopoietic stem cells
MAPK	Mitogen-activated protein kinases
M-CSF	Macrophage colony-stimulating factor
MD5SUM	Message Digest Algorithm 5 checksum
MDS	Myelodysplastic syndrome
MEP	Megakaryocyte-erythrocyte progenitor
MET	Tyrosine-kinase MET
MF	Myelofibrosis
MIPSS70	Mutation-enhanced international prognostic scoring system
MK	Megakaryocyte

MkP	Megakaryocyte progenitor
MO	Monocytes
MPN	Myeloproliferative neoplasms
MPP	Multipotent progenitor
MSC	Mesenchymal stromal cells
NE	Neutrophil
NEAA	Non-essential amino acids
NK	Natural killer cells
NOTCH3	Neurogenic locus notch homolog protein 3
OX	Overexpression
PBS	Phosphate Buffer Saline
PDGF	Platelet-derived growth factor
Ph+/-	Philadelphia chromosome positive/negative
PI3K	Phosphoinositide 3-kinase
PIP2	Phospholipid phosphatidylinositol-4,5-bisphosphate
pIpC	polyinosine-polycytosine
PLCG2	1-Phosphatidylinositol-4,5-bisphosphate phosphodiesterase gamma-2
PLT	Platelets
PMF	Primary myelofibrosis
PTK2B	Protein Tyrosine Kinase 2B
PTPN1	Protein tyrosine phosphatase non-receptor type 1
PTPN1-DA / PTPN1-D181A	PTPN1 protein with mutation of aspartic acid to alanine at position 181
PV	Polycythemia vera

RBC	Red Blood Cells
RNA	Ribonucleic acid
RNA-Seq	RNA-Sequencing
ROS	Reactive oxygen species
RPMI	Roswell Park Memorial Institute Medium
RT-qPCR	Reverse transcription real-time polymerase chain reaction
RUNX1	Runt-related transcription factor 1
RUX	Ruxolitinib
SCF	Stem cell factor
SDS	Sodium dodecyl sulfate
SET-2	Human megakaryoblast leukemic cells
sgRNA	Short Guide RNA
SH2	Src homology 2 domains
SRC	Proto-oncogene tyrosine-protein kinase Src (short for sarcoma)
STAT	Signal transducer and activator of transcription
STHSC	Short-term hematopoietic stem cells
TER119	Ly-76 (Glycophorin A-associated protein)
TGF $\beta$	Transforming growth factor $\beta$
TPO	Thrombopoietin
TPOR / MPL	thrombopoietin receptor / Myeloproliferative Leukemia Protein
WBC	White Blood Cells
WHO	World Health Organization
WT	Wild-type

## Table of Contents

<b>Chapter I – Introduction</b> .....	1
1.1 - Hematopoiesis.....	1
Hematopoietic Stem Cells (HSC) .....	3
Hematopoietic Differentiation Hierarchy.....	4
Erythropoiesis.....	6
Megakaryopoiesis.....	8
Myelopoiesis.....	12
1.2 - Myeloproliferative Neoplasms (MPN) .....	14
Polycythemia vera (PV) .....	15
Myelofibrosis (MF) .....	18
1.3 - JAK2-STAT Signaling.....	24
Janus Kinase 2 (JAK2) .....	24
Signal Transducers and Activators of Transcription (STATs) .....	26
JAK2V617F Mutation.....	28
1.4 - Deletion of Chromosome 20q (del20q) .....	30
1.5 - Protein Tyrosine Phosphatase Non-Receptor Type 1 (PTPN1/PTP1B)...	33
Regulation of PTPN1.....	34
PTPN1 role in metabolism.....	39
PTPN1 role in pathologies.....	39

1.6 - References.....	41
<b>Chapter II - PTPN1 deficiency accelerates the progression of JAK2V617F-induced myeloproliferative neoplasms.....</b>	<b>57</b>
2.1 – Introduction.....	58
2.2 - Results.....	61
Deletion of PTPN1 in del20q is frequently observed with JAK2 mutation.....	61
PTPN1 expression modulates the proliferation of JAK2V617F-positive hematopoietic cell lines.....	63
Heterozygous deletion of PTPN1 in JAK2V617F-mice displays progressive leukocytosis and thrombocytosis.....	65
Ptpn1-deficient Jak2V617F/+ mice exhibit greater disease burden and poor survival.....	67
Ptpn1+/-Jak2V617F/+ mice exhibit increased hematopoietic stem cells with a preference for myeloid and megakaryocyte lineage cells.....	70
The phenotypic effects of Ptpn1-deficient Jak2V617F/+ are cell intrinsic.....	73
JAK2V617F-positive Ptpn1-deficient cells exhibit greater clonal advantages than JAK2V617F mutation alone.....	76
Heterozygous deletion of Ptpn1 in mice exhibits splenomegaly and platelet-lineage expansion after a protracted period.....	78
Homozygous deletion of Ptpn1 results in faster progression to myelofibrosis in Jak2V617F-positive mice.....	80
2.3 - Methods.....	83
2.4 - References.....	89

<b>Chapter III - The mechanistic basis for synergy between PTPN1 deficiency and JAK2V617F mutation in myeloproliferative neoplasms.....</b>	<b>91</b>
3.1 - Introduction.....	92
3.2 - Results.....	94
Megakaryocytes from Ptpn1-deficient Jak2V617F mice exhibit increased proliferation and induce collagen expression in BM-derived mesenchymal stromal cells (MSC).....	94
RNA-sequencing analysis to determine the effects of Ptpn1-deficiency on gene expression changes in Jak2V617F mice hematopoietic progenitors.....	97
PTPN1 deficiency hyperactivates JAK-STAT signaling.....	101
Identification of novel targets of PTPN1 as a potential contributing factor to MPN progression.....	103
The deficiency of PTPN1 reduces sensitivity to Ruxolitinib.....	107
PTK2B modulates the proliferation of PTPN1-deleted JAK2V617F-positive cells.....	109
AXL expression demonstrates an inverse relationship with PTPN1 expression and can serve as a therapeutic target for cases of PTPN1 deficiency.....	110
3.3 – Methods.....	112
3.4 – References.....	117
<b>Chapter IV – Discussion.....</b>	<b>119</b>
Future works.....	131
4.1 – References.....	134
<b>Appendix.....</b>	<b>140</b>

The role of MYBL2 in myeloproliferative neoplasms.....	140
Interleukin-1 contributes to clonal expansion and progression of bone marrow fibrosis in JAK2V617F-induced myeloproliferative neoplasm.....	144
U2af1 is required for survival and function of hematopoietic stem/progenitor cells .....	150

## List of Figures

### Chapter I - Introduction

Figure 1 - Developmental hematopoiesis.....	2
Figure 2 - Models of hematopoiesis hierarchy.....	5
Figure 3 - Overview of erythropoiesis.....	7
Figure 4 - Overview of megakaryopoiesis.....	8
Figure 5 - Megakaryocytes endomitosis.....	9
Figure 6 - Overview of platelet formation from MK.....	11
Figure 7 - Overview of myelopoiesis.....	13
Figure 8 - Diagram of generalized PV treatment options.....	18
Figure 9 - Generalized myelofibrosis treatment stratified by risk.....	23
Figure 10 - JAK2 structural domain and the "sliding" model of activation.....	26
Figure 11 - JAK2 signaling pathway with and without V617F mutation.....	30
Figure 12 - Commonly deleted region (CDR) on the q-arm of chromosome 20.....	31



Figure 13 - Structural domain of PTPN1.....	34
Figure 14 - Chemical reaction of vanadate to pervanadate and EDTA-complex.....	36
Figure 15 - PTPN1 involvement in insulin, leptin, and HER2 signaling pathway...	38
<b>Chapter II - PTPN1 deficiency accelerates the JAK2V617F-induced disease progression to myelofibrosis</b>	
Figure 1 - PTPN1 deletion frequency and expression in MPNs.....	62
Figure 2 - PTPN1 expression modulates the proliferation of JAK2V617F-positive hematopoietic cell lines.....	64
Figure 3 - Heterozygous deletion of Ptpn1 in Jak2V617F-mice display progressive leukocytosis and thrombocytosis.....	66
Figure 4 - Ptpn1 <sup>+/-</sup> Jak2V617F/+ mice exhibit poorer survival, increase the splenic burden, and elevated serum proinflammatory cytokines with a reduction in thrombopoietin (Tpo).....	68
Figure 5 - Bone marrow (BM) and spleen of Ptpn1 <sup>+/-</sup> Jak2V617F/+ mice showed greater deposition of fibrosis and abundance megakaryocytes (MK) clusters.....	69
Figure 6 - Ptpn1 <sup>+/-</sup> -Jak2V617F/+ mice exhibit increased stemness with the expansion of myeloid and megakaryocyte lineages.....	72
Figure 7 - BMT cells from Ptpn1 <sup>+/-</sup> -Jak2V617F/+ mice exhibit increased WBC, NE, MO, platelets, and spleen size but the reduction in RBC, HCT, and Hb.....	74
Figure 8 - Hematopoietic stem cells and megakaryocytes are significantly elevated with robust fibrosis in the bone marrow of transplanted Ptpn1 <sup>+/-</sup> -Jak2V617F/+ mice.....	75
Figure 9 - Ptpn1 <sup>+/-</sup> -Jak2V617F/+-derived cells exhibit greater clonal advantages than Jak2V617F/+ alone.....	77
Figure 10 - The clonal advantaged given by Ptpn1 <sup>+/-</sup> -Jak2V617F/+-derived cells also expanded myeloid, megakaryocytes, HSC, and myeloid progenitor	

cells.....	78
Figure 11 - Heterozygous loss of Ptpn1 in absence of Jak2V617F mutation can induce protracted development of megakaryopoiesis and spleen enlargement...	79
Figure 12 - Deletion of PTPN1 in Jak2V617F/+ mice results in significantly higher disease burden and morbidity.....	81
Figure 13 - Jak2V617F/+ -positive Ptpn1 knockout mice have greater stem, myeloid, and megakaryocytes expansion with severe fibrosis of the BM and spleen.....	82
 <b>Chapter III - The mechanistic role of PTPN1-induced Jak2V617F/+ disease progression to myelofibrosis</b>	
Figure 1 - Ptpn1+/- Jak2V617F/+-derived megakaryocytes exhibited increased growth and induce collagen expression BM-derived mesenchymal stromal cells (MSC).....	96
Figure 2 - RNA-sequencing analysis of LSK cells from Ptpn1+/- Jak2V617F/+ and Jak2V617F/+ mice.....	99
Figure 3 - Examining the overlapping differentially expressed genes in LSK derived from Ptpn1-deficient Jak2V617F-mice to MF patients and validation of differentially expressed genes in LSK and MEP population .....	100
Figure 4 - PTPN1 deficiency results in hyperphosphorylation of JAK2 signaling...	102
Figure 5 - Two-system co-immunoprecipitation provides a robust method to pulldown PTPN1 substrates.....	105
Figure 6 - The identification of multiple targets including PTK2B as a direct substrate of PTPN1 and are robustly phosphorylated in PTPN1-deficiency.....	106
Figure 7 - PTPN1 deficiency reduces ruxolitinib sensitivity.....	108
Figure 8 - PTK2B modulates the proliferation of PTPN1-deleted JAK2V617F-positive cells .....	109
Figure 9 - AXL expression demonstrates inverse relationship with PTPN1	

expression and can serve as a therapeutic target to cases of PTPN1 deficiency..... 111

## **Appendix**

Figure 1 – MYBL2 expression on the proliferation of JAK2V617F-positive hematopoietic cell lines, HEL and SET2..... 141

Figure 2 – Heterozygous deletion of MYBL2 in context of JAK2V617F mutation exhibits no significant alteration in the disease progression..... 142

Figure 3 – Expression of IL-1 is elevated in MPN..... 145

Figure 4 – Effects of IL-1 $\beta$  on gene expression in Jak2V617F mice hematopoietic progenitors..... 146

Figure 5 – Effects of IL-1 on gene expression changes and collagen expression in BM mesenchymal..... 148

Figure 6 – Effect of U2af1 deletion on gene expression profile in HSPC..... 151

Figure 7 – Effect of U2af1 deletion on RNA splicing..... 153

## List of Tables

### Chapter I - Introduction

Table 1 - World Health Organization (WHO) MPN classification.....	14
Table 2 - WHO criteria for PV diagnosis.....	16
Table 3 - WHO criteria for the distinction of primary MF.....	19
Table 4 - Myelofibrosis grading score with corresponding human BM reticulin-stained images.....	20
Table 5 - Myelofibrosis scoring systems with associated risk strata and patient's median survival.....	22

### Chapter II - PTPN1 deficiency accelerates the JAK2V617F-induced disease progression to myelofibrosis

sgRNA Primer Table.....	88
RT-qPCR Primer Table.....	88

### Chapter III - The mechanistic role of PTPN1-induced Jak2V617F/ disease progression to myelofibrosis

sgRNA Primer Table.....	115
RT-qPCR Primer Table.....	116

# CHAPTER I

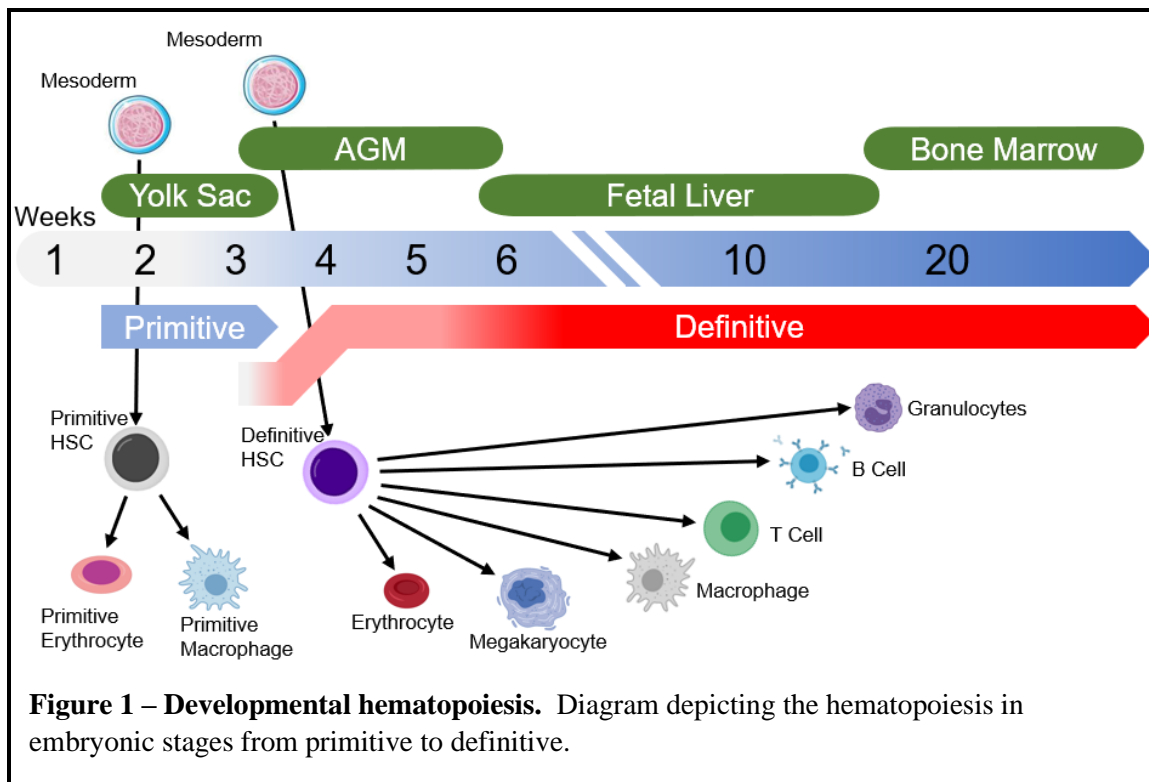
## Introduction

### 1.1 – Hematopoiesis

The human body is composed of approximately 30 trillion cells, of which 80-90% are hematopoietic cells<sup>1</sup>. Of these cells, approximately 1% or  $0.3 \times 10^{12}$  cells are replaced daily<sup>2</sup>. This highlights the important role of hematopoiesis in maintaining homeostasis. Hematopoiesis is a dynamic process by which blood cellular components are formed with continuous coordination and balance throughout the organism's lifespan. It is derived from the Greek words *haima* (blood) and *poiēsis* (to produce something). All hematopoietic cells are produced in a hierarchal structure of differentiation originating from hematopoietic stem cells (HSC). These HSCs have a robust capacity for self-renewal and the maintenance of multipotency<sup>3</sup>. The endpoint of the differentiation gives rise to two distinct populations of hematopoietic cells: myeloid and lymphoid. The population of myeloid cells includes erythrocytes (RBC), megakaryocytes, monocytes/macrophages, and granulocytes. While the lymphoid cells include T-cells, B-cells, and natural killer (NK) cells. The focus of this research is primarily on myeloid lineages and their pathologies. The majority of the hematopoiesis process occurs in the bone marrow (BM). The hematopoiesis process that occurs elsewhere, such as in the spleen, is termed extramedullary hematopoiesis.

In vertebrates, the hematopoietic processes occur in two distinct waves: primitive and definitive<sup>4</sup>. The primitive wave is a transient phase of hematopoiesis during the

embryonic stage, which primarily gives rise to nucleated erythrocytes with embryonic globin and macrophages<sup>5</sup>. These “primitive” erythrocytes and macrophages are products of primitive HSC-like cells, derived from mesoderm, which are neither pluripotent nor capable of self-renewal. The definitive wave of hematopoiesis follows the primitive wave at approximately 27 days of gestation and gives rise to definitive HSC, also derived from mesoderm. These HSCs are capable of self-renewal and differentiation into all hematopoietic cells. In humans, the hematopoiesis process begins in the yolk sac with the primitive wave, follows by the definitive wave marked by the birth of definitive HSCs from the aorta-gonad-mesonephros (AGM). The HSCs then colonize the fetal liver before transitioning to their permanent residence within the bone marrow<sup>6,7</sup>.



## Hematopoietic Stem Cells (HSC)

Our understanding of HSC existence came to light in the 1950s during the heights of nuclear irradiation research when lethality irradiated patients and mice were rescued in bone marrow or spleen transplantation<sup>8-10</sup>. While still unidentified, in 1961, James Till and Ernest McCulloch transplanted BM cells into the spleen and identified clumps of cells that are proportional to the total number of bone marrow cells transplanted. They coin these clumps “colony-forming unit” or CFU<sup>11</sup>. The investigations that follow were able to characterize these CFUs as stem cells by their capacity for proliferation, differentiation, and self-renewal<sup>12,13</sup>. However, it was not until the advent use of flow cytometry in the 1980s that the isolation and characterization of HSC and other hematopoietic cells were probed at greater depth<sup>14,15</sup>. This is in due part to hematopoietic cells being identified by the presence or absence of specific surface antigen(s) that can immunologically be targeted or immunophenotyping<sup>16,17</sup>. HSC is identified by Lin<sup>-</sup> c-kit<sup>+</sup> Sca-1<sup>+</sup> (LSK) markers<sup>18</sup>. Within the LSK population, HSCs are further subclassified into long-term HSC (LTHSC) [CD34<sup>-</sup>FLT3<sup>-</sup>], short-term HSC (STHSC) [CD34<sup>+</sup>FLT3<sup>-</sup>], and multipotent progenitor (MPP)[CD34<sup>+</sup>FLT3<sup>+</sup>]<sup>19,20</sup>. The distinction between these subclassifications is defined by the altered self-renewal potential post-transplantation but still preserving pluripotency. As such, the population of LTHSC has perpetual self-renewal; while the population of STHSC and MPP have ~6 weeks of self-renewal to extremely short and difficult to detect, respectively<sup>21</sup>.

## Hematopoietic Differentiation Hierarchy

The hematopoietic differentiation process is a structural hierarchy of distinct stages of transition toward maturation for a desired lineage. Upon early identification of individual population and their properties, a conventional lineage differentiation model was proposed with a linear path of HSC differentiation and myeloid/lymphoid fork immediately after<sup>22</sup>. This fork separates two progenitor populations, common myeloid progenitor (CMP) and common lymphoid progenitor (CLP). CLP gives rise to T-cells, B-cells, and natural killer cells (NK); while CMP can further separate into megakaryocyte-erythrocyte progenitor (MEP) and granulocyte-monocyte progenitor (GMP), which differentiate into their respective hematopoietic cells. However, challenges to the conventional model were quickly proposed based on the observation that MPP failed to produce significant megakaryocytes and erythrocytes population but gave rise to granulocytes, monocytes, B-cells, and T-cells<sup>23</sup>. This posed a question of the existence of CMP as MEP and GMP differentiation branched at different points. Multiple alternative models were proposed trying to rectify this with the most recent one proposed by using single-cell RNA-sequencing data<sup>24,25</sup>. These different differentiation models are outlined in Figure 2.



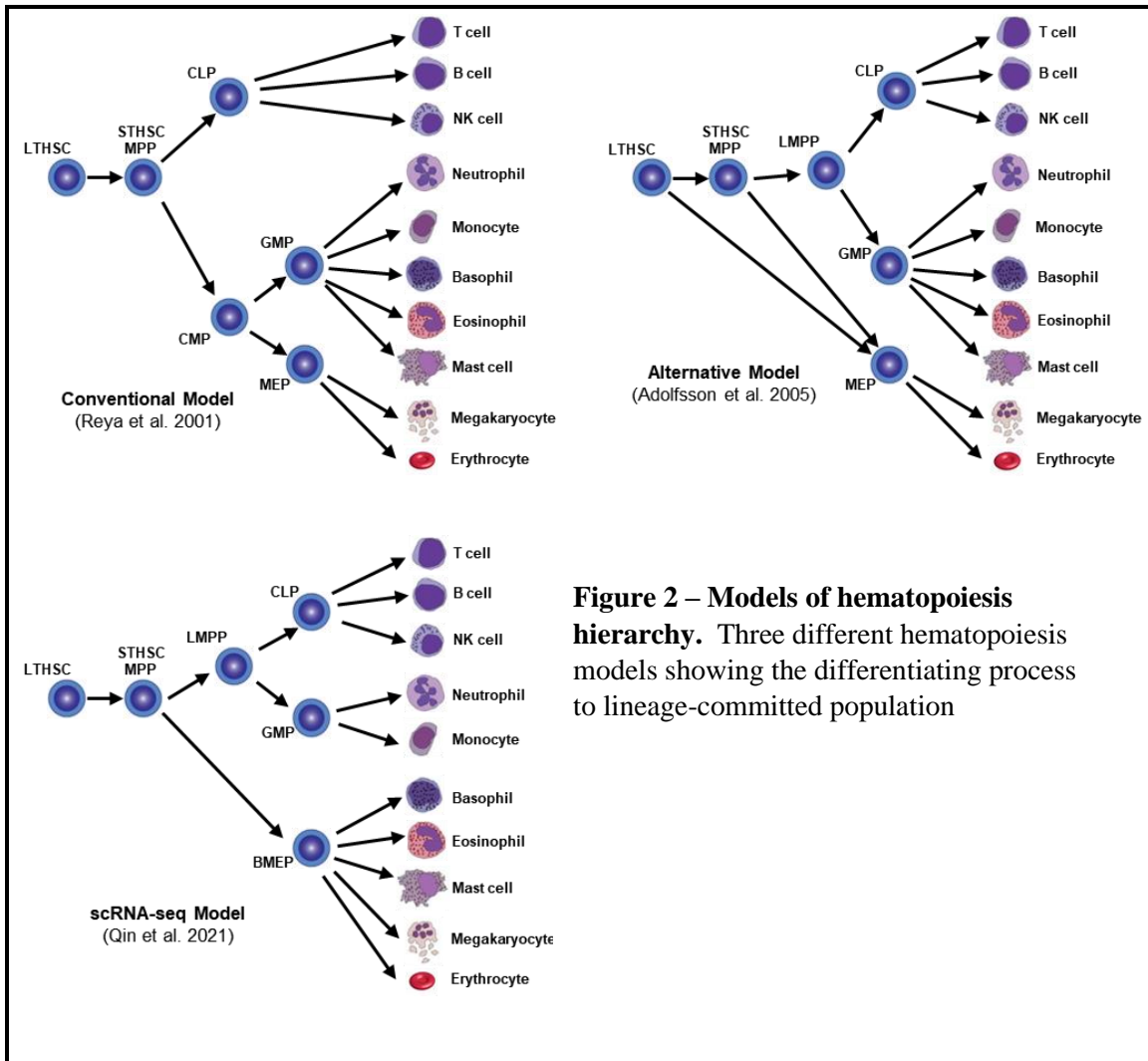


**Figure 2 – Models of hematopoiesis hierarchy.** Three different hematopoiesis models showing the differentiating process to lineage-committed population

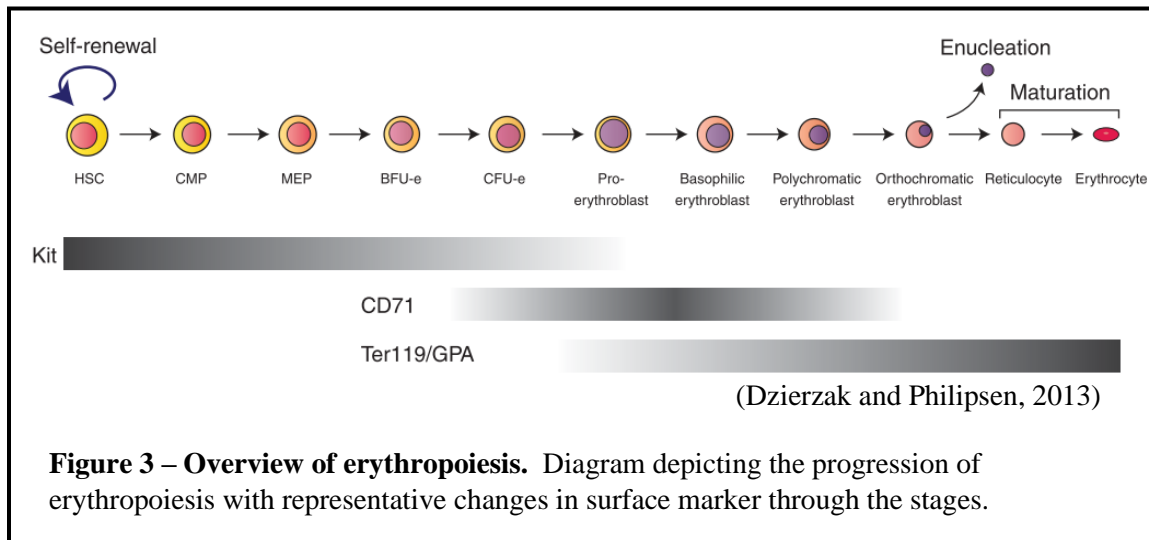
After committing to a specific lineage, the maturation process will see the cells undergo multiple additional steps before reaching their terminal stage that is observed in the blood. The factors that dictate lineage commitment in HSC are driven by the interaction with local microenvironment secretion of various cytokines, growth factors, and chemokines such as interleukin-3 (IL-3), interleukin-6 (IL-6), stem cell factor (SCF), erythropoietin (EPO), thrombopoietin (TPO), granulocyte-macrophage colony-

stimulating factors (GM-CSF), etc<sup>26,27</sup>. It is the fine-tuning of these and many other cytokines secretions, along with cell-cell interaction, that maintains the organism's balance in the distribution of the cell's lineages. The lack of a specific lineage or excessive production of a specific lineage by pathological changes such as JAK2 mutation is the disruption of this homeostasis. While we have been able to gauge some aspects of this process, many of the cellular decisions that drive the lineage commitment path is still being investigated.

## **Erythropoiesis**

Red blood cells or erythrocytes are the most abundant cells in the human body. They play a pivotal role in the transportation of gases (O<sub>2</sub> and CO<sub>2</sub>) around the body to sustain our metabolic needs<sup>28</sup>. The process that produces erythrocytes is known as erythropoiesis. After differentiation from HSC to MEP, erythroid development proceeds to the formation of burst-forming unit-erythroid (BFU-E)<sup>29</sup> and then colony-forming unit-erythroid (CFU-E)<sup>30</sup>. Subsequent development sees it through 4 stages of erythroblasts (proerythroblast, basophilic erythroblast, polychromatic erythroblast, and orthochromatic erythroblast), named by its appearance under Wright stain. This maturation process is also defined by its gradual decrease in the nucleus-to-cytoplasmic ratio, elimination of internal organelles, and accumulation of hemoglobin. The extrusion of the nucleus marks the formation of reticulocytes, an immature form of red blood cells that contain a reticular network of mRNA and lack the bi-concavity appearance. The final step sees reticulocytes undergo RNA elimination and membrane remodeling to generate mature

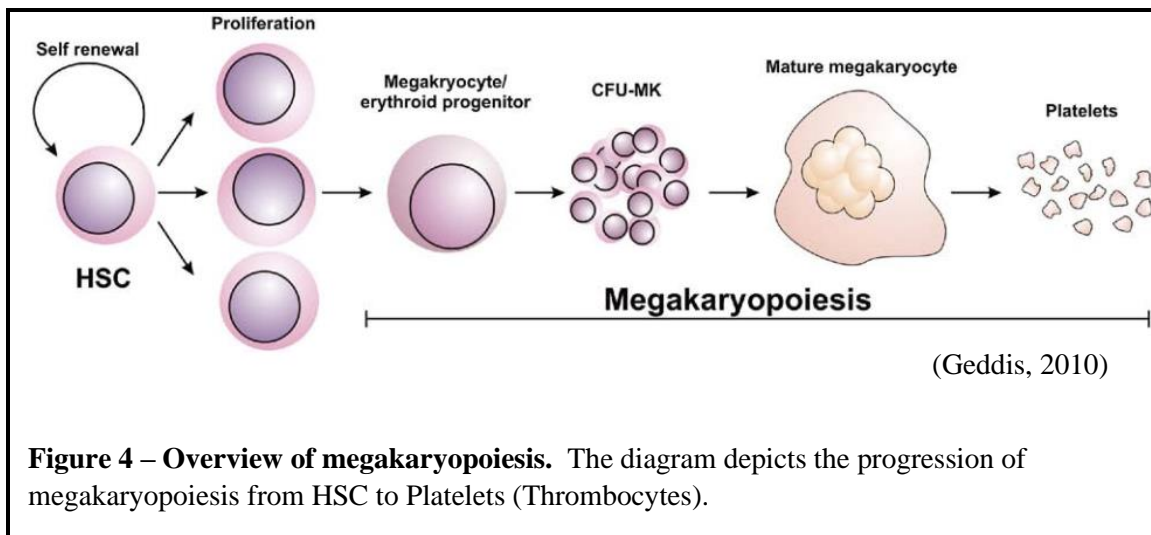
RBC or erythrocytes<sup>31</sup>. The changing expression of surface antigens, CD71 and Ter119, are signatures used for identification of this process by flow cytometry<sup>32,33</sup>.



The principal growth factor that drives erythropoiesis is erythropoietin (EPO). EPO existence was proposed in 1906 by Paul Carnot and Clotilde-Camille Deflandre after transplanting plasma to an anemic rabbit, which resulted in rapid elevation in erythrocytes<sup>34</sup>. Since then, EPO has been purified<sup>35</sup> and characterized<sup>36</sup> for the generation of recombinant protein accessible for therapeutic use<sup>37</sup>. EPO is produced primarily in the kidney and is essential to the proliferation, survival, and differentiation of erythroid development<sup>38</sup>. These effects are exerted through the interaction of EPO with its designated receptor, EPOR<sup>39</sup>. The activation of EPOR leads to the receptor for activation of JAK2/STAT signaling<sup>40,41</sup>. It is the modulation of EPO abundance and JAK2/STAT signaling that maintain homeostasis in RBC production. Dysregulation of either can result in anemia, lacking RBC, or polycythemia, excessive production of RBC.

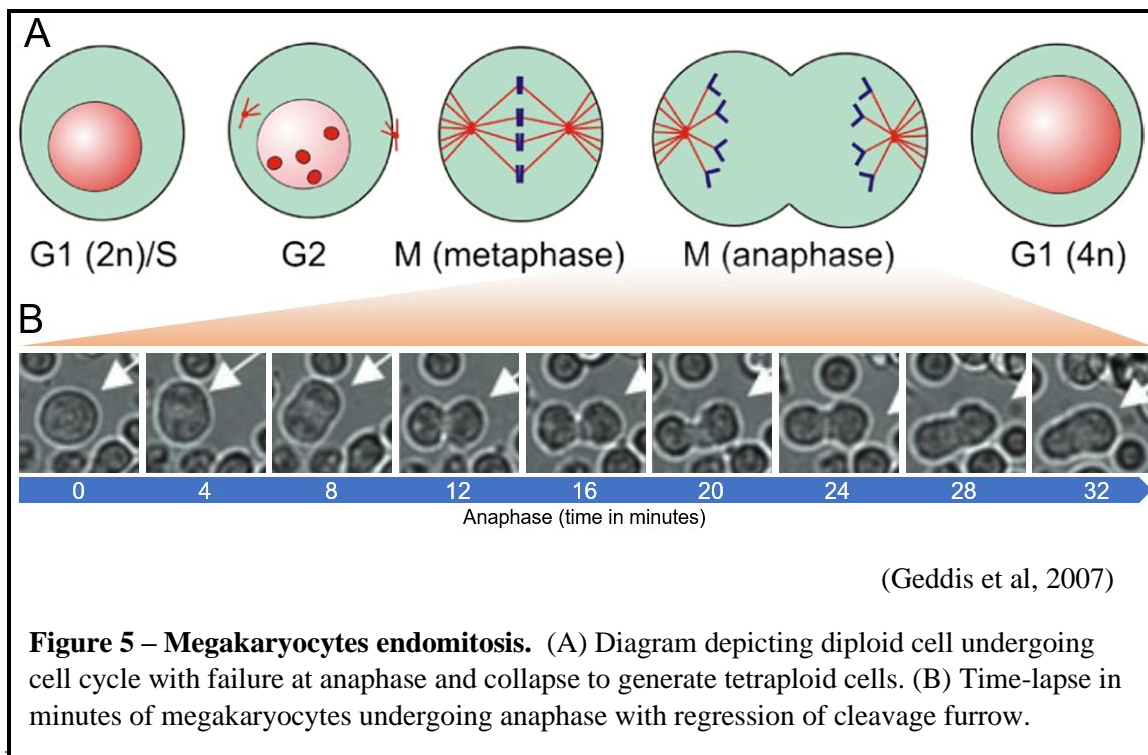
## Megakaryopoiesis

Platelets, or thrombocytes, are anucleated cytoplasmic fragments derived from megakaryocytes that function in clotting blood vessels during vascular injuries<sup>42</sup>. Furthermore, thrombocytes play a significant role in modulating wound healing and inflammation<sup>43</sup>. The process that gives rise to thrombocytes is called megakaryopoiesis. Similar to erythropoiesis, the differentiation of HSC to MEP is the initial step of megakaryopoiesis<sup>44</sup>. The mechanism behind the decision at lineage bifurcation of MEP is still poorly understood and remained an ongoing investigation. The rate of cell cycle has been proposed as one of the mechanisms for lineage decision<sup>45</sup>. The expression level of certain transcription factors like RUNX1, GATA1, FOG1, and FLI1 have been shown to play a pivotal role in regulating the differentiation of megakaryocytes<sup>46-51</sup>.

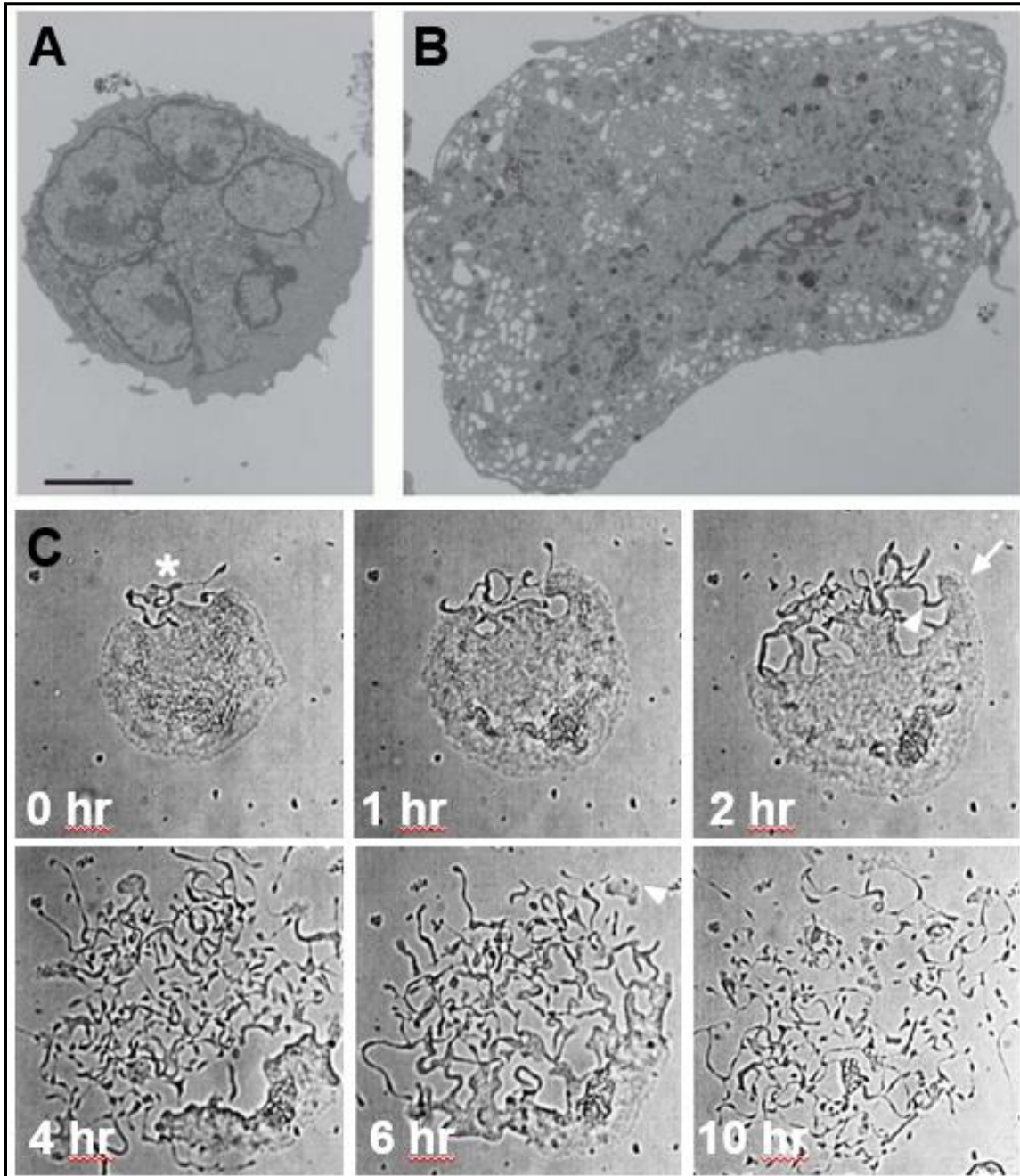


Upon commitment toward megakaryocytes, the first stage of maturation involves the formation of CFU-Mk, often references as megakaryocyte-committed progenitors (MkP)<sup>52</sup>. Interestingly, the sequential differentiation from HSC through MEP and then

MkP can be circumvented for a direct path to MkP from Mk-primed HSC under high thrombopoietin (TPO) concentration<sup>53</sup>. It is reasonable to assume that this high TPO bypass is a necessary mechanism for emergency megakaryopoiesis to recapitulate loss or insufficient platelets during tissue insult. Subsequent maturation of megakaryocytes sees cells undergoing polyploidization in which the chromosomal contents increase from 2N (diploid) upward to 128N, but average around 16N<sup>54</sup>. This process, called endomitosis, sees the megakaryocytes undergo cell cycles through G1, S, and G2, but incomplete M phases<sup>55,56</sup>. MK progression through M phases shows abortion of mitosis at anaphase with regression of the cleavage furrow during cytokinesis<sup>57</sup>. The failure results in a single cell with a polyploid nucleus and enlarged cytoplasm instead of two daughter cells. The continuous cell cycle and endomitosis gradually increase the cell's size and ploidy. Flow cytometric identification of MK utilizes glycoprotein IIb/IIIa (CD41a) and glycoprotein Ib (CD42b) or glycoprotein IIIa (CD61)<sup>58</sup>.



The formation of platelets from mature polyploid MK occurs in the blood with a single MK producing approximately 4000 platelets<sup>59</sup>. The thrombopoiesis process in MK follows its maturation through the internal formation of the demarcation membrane system (DMS) or invaginated membrane system (IMS), a membranous network that is formed from the invagination of the plasma membrane<sup>60</sup>. The DMS/IMS provides a significant increase in the surface area of the MK necessary for platelet formation<sup>61</sup>. At the zenith of maturation, the MK proceeds to form multiple elongated pseudopods called proplatelet shafts. This shaft breaks from the main body of the MK to generate proplatelets fragments that disassociate further to generate platelets<sup>62</sup>. The end of this process will leave only a small cytoplasm with the multilobed nuclei of the MK intact. This remnant/senescent MK will then be phagocytosed by macrophages<sup>63</sup>.



(Italiano Jr. et al., 1999)

**Figure 6 – Overview of platelet formation from MK.** (A) Electron microscope (EM) image of an immature MK lacking DMS/IMS internal structure. (B) EM image of a mature MK with numerous DMS/IMS observed within the cytoplasm. (C) A time-lapse on a light microscope of the formation of pseudopods in MK followed by the disassembly of proplatelet shaft.

The primary growth factor for megakaryopoiesis is thrombopoietin (TPO or THPO). TPO existence was demonstrated in 1958 within a complex serum mixture but was not isolated until 1994<sup>64,65</sup>. Interestingly, the TPO receptor, MPL, was isolated before TPO and was determined to have significant involvement with megakaryopoiesis<sup>66,67</sup>. TPO is primarily produced in the liver and kidney and is inversely proportional to platelet abundance<sup>68,69</sup>. This inverse relationship is due to the consumption of TPO when binding to MPL and thus removed from circulation<sup>70,71</sup>. Similar to EPOR, TPO binding to dimerized MPL results in the activation of JAK2/STAT signaling that promotes the proliferation, differentiation, and production of megakaryocytes/platelets<sup>72</sup>. While TPO/MPL signaling is mostly associated with megakaryocytes/platelets, they also play a significant proliferative role in HSC and are essential for their survival<sup>73</sup>.

## **Myelopoiesis**

Myelopoiesis is the maturation process that gives rise to myeloid leukocytes (granulocytes and monocytes) that plays a pivotal role in the innate immune system. Granulocytes are a population of polymorphonuclear leukocytes that encompasses neutrophils, basophils, and eosinophils; of which, neutrophils are the most abundant leukocytes. These cells are named by histological staining properties of their cytoplasm: eosino- (acidic/red), baso- (basic/blue), neutro- (neutral, white)<sup>74</sup>. The differentiation of these cells is term granulopoiesis which sees the maturation progression through multiple stages. Neutrophils, basophils, and eosinophils are lineage committed early in the process, after myeloblast, and differentiate uniquely to their mature form<sup>75</sup>. The other



myeloid lineage, monocyte, also diverges at the myeloblastic stage and proceeds through its own maturation step<sup>76</sup>. Mature monocytes circulate the blood and differentiate in macrophages/dendritic cells as they are recruited into the tissues by inflammatory signals. The standard detection of granulocytes and monocytes by flow cytometry is through the surface antigens Ly6G/Ly6C (Gr-1), CD11b (Mac-1), and F4/80<sup>77</sup>. A combination of Gr-1 and Mac-1 are present in granulocytes and a subset of monocytes<sup>78</sup>. Interestingly, Gr-1 expression is both high or low in monocytes, which can define the state of the monocytes as “inflammatory” (high) or “steady” (low)<sup>79</sup>. F4/80 is the marker that is typically used for the detection of mature tissue macrophages<sup>80</sup>.

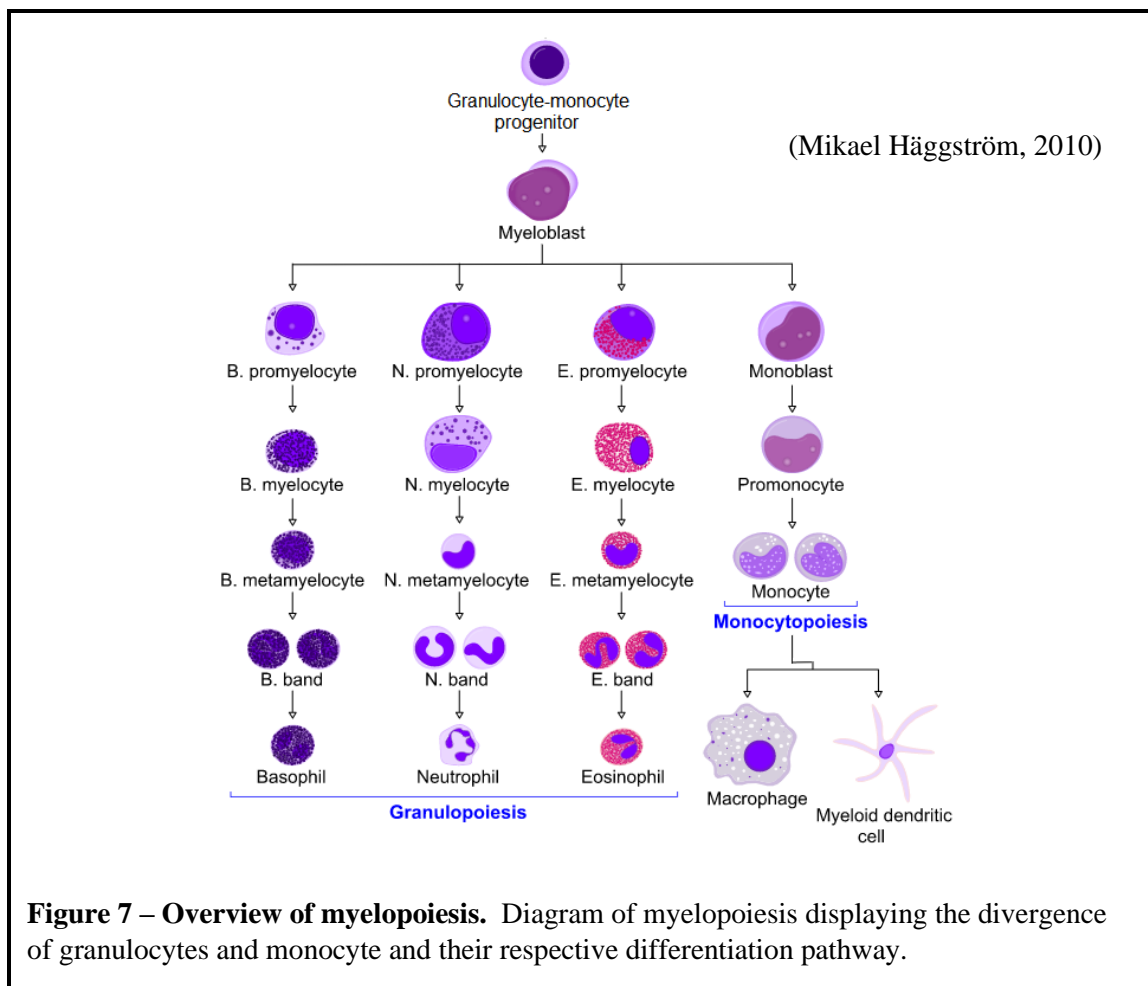


**Figure 7 – Overview of myelopoiesis.** Diagram of myelopoiesis displaying the divergence of granulocytes and monocyte and their respective differentiation pathway.

## 1.2 Myeloproliferative Neoplasms (MPN)

Myeloproliferative neoplasms (MPN) are a group of hematologic malignancies characterized by excessive production of one or more myeloid lineage cells that include erythroid, granulocytes, megakaryocytes, and monocytes/macrophages. MPNs are subclassified based on the disease phenotype as defined by World Health Organization (WHO)<sup>81</sup>. For brevity, the commonly referenced pathologies are Philadelphia chromosome-positive (Ph+) MPN, chronic myeloid/myelogenous leukemia (CML), and Ph- MPNs (classical MPN), which includes polycythemia vera (PV), essential thrombocythemia (ET), and myelofibrosis (MF). Ph+ MPN, or CML, is defined by the presence of a translocation between chromosomes 9 and 22, t(9:22), which produces an oncogenic BCR-ABL1 fusion gene<sup>82</sup>. CML has an annual incidence of 2 cases per 100,000 adults<sup>83</sup>. The absence of this translocation, Ph-, produces the remaining pathologies, PV, ET, and MF. PV and MF are the primary focus of this research.

2016 WHO classification of MPN
Chronic myeloid leukemia (CML), BCR-ABL1+
Polycythemia vera (PV)
Essential thrombocythemia (ET)
Myelofibrosis (MF) <ul style="list-style-type: none"><li>↳ Prefibrotic/Early stage</li><li>↳ Overt fibrotic stage</li></ul>
Chronic neutrophilic leukemia (CNL)
Chronic eosinophilic leukemia, not otherwise specified (NOS)
MPN, unclassifiable
Mastocytosis

**Table 1 – World Health Organization (WHO) MPN classification.**

## **Polycythemia vera (PV)**

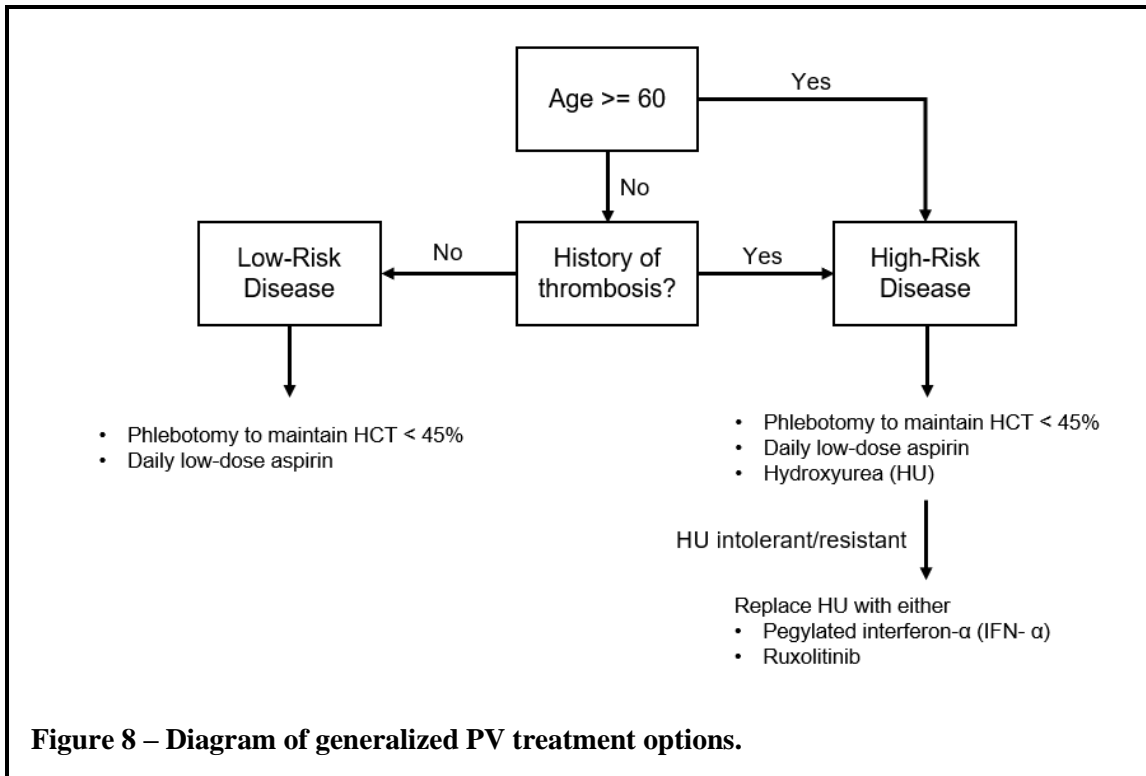
First described in 1882 by Henri Vaquez and then detailed later in 1903 by William Osler<sup>84,85</sup>, polycythemia vera (PV) is characterized by the expansion of RBC, hemoglobin (Hb), and hematocrit (HCT) due to excessive erythropoiesis. By WHO standards, the patient's diagnostic affirmation of PV is by a combination of peripheral blood smears, bone marrow (BM) biopsies, and molecular genetic testing<sup>86</sup>. The annual incidence rates of PV can range between 0.02 to 2.8 per 100,000 people with a total prevalence of 22.43 per 100,000 people<sup>87</sup>. With a median age of ~70 years old, the disease prevalence is skewed in the older population with a prevalence upward of 237.57 people per 100,000 in this age group. The median survival of PV patients after diagnosis is 14 years, which can be up to 24 years in a patient younger than 60 years old<sup>88</sup>. Additional risk factors that adversely affect patients' overall survival in PV include the following criterion: age >61 years, leukocytosis, thrombocytosis, and additional karyotype abnormalities<sup>89,90</sup>. A major driver in the pathogenesis of PV is the JAK2 mutation which exists in ~99% of patients and 97% of that mutation is JAK2V617F with the remaining 3% harboring a mutation elsewhere on the gene<sup>91</sup>. While the disease itself is quite moderate in severity, it is the progression to MF or AML that can be very detrimental to the patient's quality of life and survival.

<b>WHO Diagnostic Criteria for PV</b>	
1.	One of the following blood parameters > Hemoglobin Male > 16.5 g/dl Female > 16.0 g/dl > Hematocrit Male > 49% Female > 48% > Increased red blood cell mass
2.	Bone Marrow Biopsy Observation > Prominent erythroid, granulocytic, and megakaryocytic proliferation with pleomorphic mature megakaryocytes.
3.	Presence of a JAK2 mutation > JAK2V617F > JAK2 exon 12 mutation
Minor criterion (can be substituted for missing one of the above) > Subnormal serum erythropoietin	
<b>Table 2 – WHO criteria for PV diagnosis.</b>	

Treatment options for polycythemia vera (PV) are stratified by the patient's risks. Patients who are less than 60 years of age and have no history of thrombosis events are stratified as low-risk. Low-risk patients' treatment options consisted of phlebotomy to maintain less than 45% hematocrit with daily use of low-dose aspirins to mitigate the risk of cardiovascular complications, especially against thrombotic events as it accounts for 33% of patient morbidity<sup>92</sup>. If patients have any of the aforementioned risks, it is stratified as a high-risk disease, and are prescribed hydroxyurea (HU) in addition to the low-dose aspirin. HU inhibits the formation of deoxyribonucleotides by inhibiting ribonucleotide reductase, which in turn induces cell arrest and prevents further expansion of RBC, WBC, and platelets<sup>93</sup>. Furthermore, preventative treatments, such as additional

aspirin or anticoagulants, are supplemented for patients with a high risk of thrombosis<sup>94,95</sup>.

The hesitant use of HU is due to the drug-inducing cell cycle arrest and subsequent immunosuppression with the potential risk of anemia and leukopenia (low WBC) in addition to neurological and gastric side effects. Another concern for HU use stemmed from the risk of leukemic transformation, fibrosis progression, and secondary malignancies<sup>96-98</sup>. However, recent observations have refuted these risks<sup>89,99</sup>. At the same time, patients can also develop HU resistance or intolerance, about 11% and 13%, respectively, which results in higher leukemic transformation and morbidity risk<sup>100</sup>. In the situation when patients develop HU-resistant/intolerant or severe disease progression (eg. marked splenomegaly), interferon- $\alpha$  (IFN- $\alpha$ ) or ruxolitinib (a JAK inhibitor) is used to control the disease<sup>95</sup>. IFN- $\alpha$  treatment has shown efficacy in repressing erythrocytosis and thrombocytosis through activation of its receptors and JAK1/TYK2 downstream signaling<sup>101,102</sup>. While ruxolitinib (RUX) showed far greater splenomegaly reduction, hematocrit control, and reduced risk of thrombotic events than HU. However, it has significant adverse effects, like anemia, that can be quite intolerable for many patients. Patients on ruxolitinib also have significant risks of opportunistic infection and basal-cell and squamous-cell carcinoma<sup>103</sup>. Outside of bone marrow transplantation, which carries its own drawback, there is currently no curative treatment for PV<sup>94</sup>.



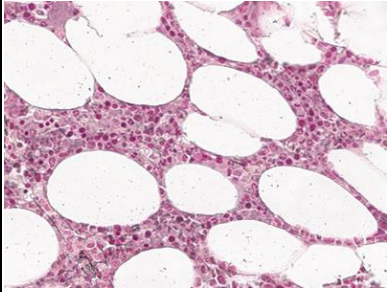
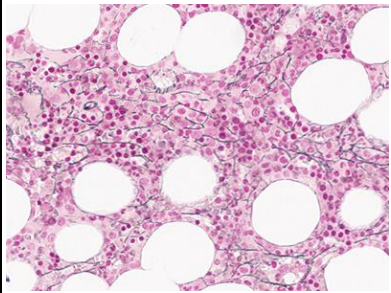
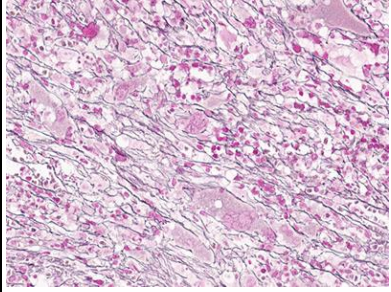
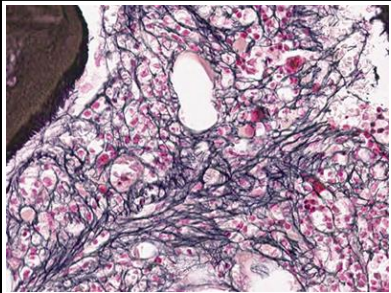
## Myelofibrosis (MF)

First described by Dr. G. Heuck in 1879, myelofibrosis (MF) is the scarring (fibrosis) of the hematopoietic tissues including bone marrow and spleen<sup>104</sup>. The disease is characterized by significant deposition of fibrosis, anemia, megakaryocyte proliferation, splenomegaly, and constitutional symptoms, such as weight loss, night sweats, and fever<sup>94</sup>. The main causes for these symptoms are due to inadequate erythropoiesis and extramedullary hematopoiesis (EMH), or hematopoiesis process occurring outside the bone marrow, in the spleen and liver. MF is subclassified into primary MF (PMF), post-PV MF, or post-ET MF based on the condition it was diagnosed. MF also has stage distinction which WHO has defined as, pre-PMF, an early

stage of PMF, and overt-PMF<sup>81</sup>. The primary criterion for the distinction between pre-PMF and over-PMF is the grade of fibrosis observed in BM biopsies<sup>105</sup>.

As part of WHO's major criteria for myelofibrosis, JAK2, CALR, and MPL are the primary driver mutations in the disease. JAK2, CALR, and MPL mutation are identified in approximately 50-60%, 20-25%, and 3-8% of MF cases<sup>106,107</sup>. Other concomitant mutations (TET2, DNMT3A, EZH2, U2AF1, and SRSF2) and cytogenetic abnormalities (deletion of chromosome 13q or 20q) also play a significant role in the disease progression and patient's prognosis<sup>108,109</sup>.

<b>WHO Diagnostic Criteria for Myelofibrosis (MF)</b>	
<b>Pre-PMF</b>	<b>Overt-PMF</b>
<b>Major Criteria</b>	
1. Megakaryocytes proliferation with Grade 0-1 reticulin/collagen fibrosis	1. Megakaryocytes proliferation with Grade 2-3 reticulin/collagen fibrosis
2. Presence of JAK2, CALR, or MPL mutation or other clonal markers	2. Presence of JAK2, CALR, or MPL mutation or other clonal markers
3. Does not meet WHO other MPN criteria	3. Does not meet WHO other MPN criteria
<b>Minor Criteria</b>	
1. Unexplained anemia	1. Unexplained anemia
2. Leukocytosis	2. Leukocytosis
3. Significant splenomegaly	3. Significant splenomegaly
	4. Leukoerythroblastic blood smear
<b>Table 3 – WHO criteria for the distinction of primary MF.</b>	

<b>Myelofibrosis Grade</b>	
<p>MF-0</p> <p>Scattered linear reticulin with no intersections corresponding to normal BM</p>	
<p>MF-1</p> <p>Loose network of reticulin with many intersections, especially in perivascular area</p>	
<p>MF-2</p> <p>Diffuse and dense increase in reticulin with extensive intersections, occasionally with focal bundles of thick fibers mostly consistent with collagen and/or focal osteosclerosis</p>	
<p>MF-3</p> <p>Diffuse and dense increase in reticulin with extensive intersections and coarse bundles of thick fibers mostly consistent with collagen, usually associated with osteosclerosis</p>	
<p><b>Table 4 – Myelofibrosis grading score with corresponding human BM reticulin-stained images.</b></p>	

(Salama, 2021)



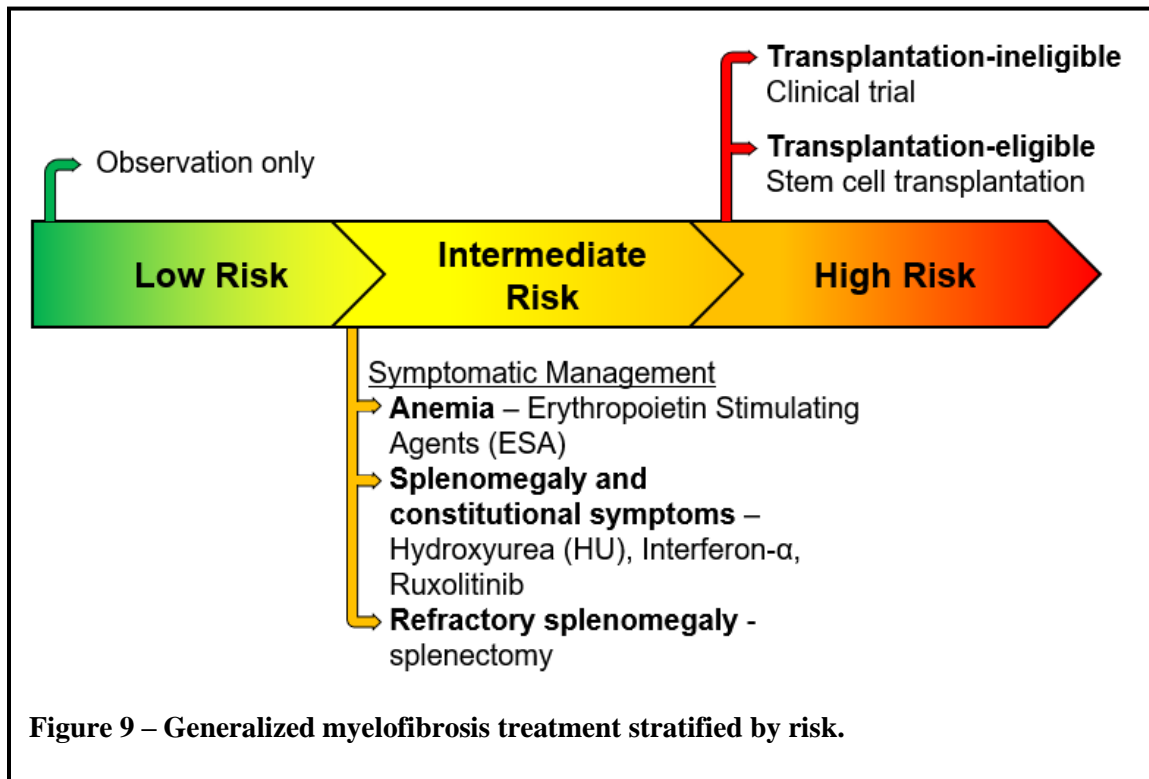
Myelofibrosis treatment options are also risk stratified. The original proposal in 2009 by the International Working Group for Myelofibrosis Research and Treatment (IWG-MRT) established the International Prognostic Scoring System (IPSS) for assessing the risk imposed by the disease and the treatment options necessary. The IPSS scoring is based on factors like age, hemoglobin, leukocyte count, peripheral blast percentage, and constitutional symptoms<sup>110</sup>. The IPSS score limitation is that it is only assessed at diagnosis. As such, refinement to the scoring system was made to increase the accuracy due to disease progression, which is called Dynamic IPSS (DIPSS)<sup>111</sup>. This was then improved upon the following year to DIPSS-plus<sup>112</sup>. In the context of post-ET/PV MF, a comparison between IPSS, DIPSS, and DIPSS-plus, showed greater accuracy in DIPSS-plus<sup>113</sup>. Even so, additional improvement is still needed as years of MF research since the advent of these scoring systems has created a new layer of depth in genetic aberrations that are quite consequential to the patient's prognosis. The new system introduced in 2018 is called Mutation-enhanced IPSS or MIPSS70, which itself was also improved upon to produce MIPSS70-plus and MIPSS70-plus v2<sup>114,115</sup>. In addition, another scoring system, Genetically-inspired IPSS (GIPSS), was made to simplify the scoring system for clinician<sup>116</sup>. Irrespective of the scoring system, the score tally will stratify the patient's risk in MF from very low risk to very high risk, with elevated risk resulting in significantly poorer survival. In general, low-risk patients show > 8 years median survival, 4-8 years for intermediate, and <4 years for high-risk<sup>107</sup>.

Scoring System	Assessment Time	Risk and Median Survival (years)		
		Low	Intermediate	High
IPSS	At Diagnosis	0 pts 11.2	1 - 2 pts 4 - 7.9	3+ pts 2.2
DIPSS	At anytime	0 pts 14.6	1 - 4 pts 4 - 7.4	5+ pts 2.3
DIPSS-Plus	At anytime	0 pts 15.4	1 - 3 pts 2.9 - 6.5	4+ pts 1.3
MIPSS70	At anytime	0 - 1 pts 27.7	2 - 4 pts 7.1	5+ pts 2.3
MIPSS70-Plus	At anytime	0 - 2 pts 20	3 pts 6.3	4+ pts 1.7 - 3.9
MIPSS70-Plus Version 2.0	At anytime	1 - 2 pts 16.4	3 - 4 pts 7.7	5+ pts 1.8 - 4.1
GIPSS	At anytime	0 - 1 pts 8 - 26.4		2+ pts 2 - 4.2

**Table 5 – Myelofibrosis scoring systems with associated risk strata and patient’s median survival.**

Treatment options for MF are based on the patient’s risk status. Low and very low-risk patients are typically just monitored by observation for presenting symptoms and disease progression. Therapeutic options for intermediate-risk patients are symptom-based approaches to improve the patient’s quality of life. Commonly presented symptoms are anemia, splenomegaly, and constitutional symptoms<sup>117</sup>. Symptoms of anemia are typically managed with blood transfusion in addition to drugs to stimulate erythropoiesis, or erythropoiesis-stimulating agents (ESA), especially in cases with low EPO levels. For splenomegaly and constitutional symptoms, patients can be treated with hydroxyurea, interferon- $\alpha$ , or ruxolitinib. In the situation of refractory splenomegaly, splenectomy could be an option to alleviate the burden<sup>118</sup>. If the patients are high risk, stem cell transplantation can be an option; however, few patients are eligible for the

transplantation due to a combination of advanced age, donor availability, and other medical conditions. Even if carried out, the additional risk of opportunistic infection and graft versus host disease can produce life-threatening conditions for patients<sup>119</sup>. In such transplantation-ineligible cases, the best approach now may be enrollment in ongoing clinical trials<sup>107</sup>. Similar to PV, aside from transplantation, there are no curative options. Treatments are provided for the patient's palliative benefits.



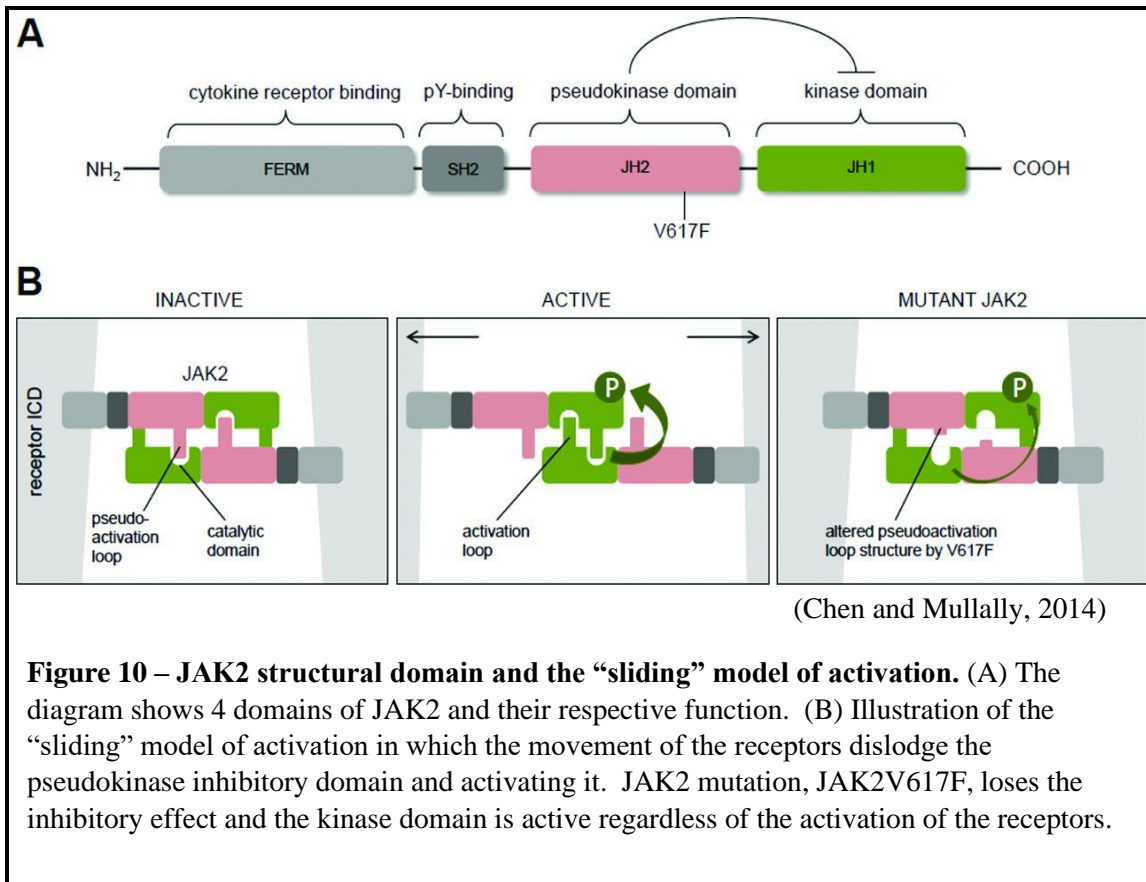
### 1.3 – JAK2-STAT Signaling

#### Janus Kinase 2 (JAK2)

JAK2 was discovered in 1989 by screening for protein-tyrosine kinases (PTK)-related sequencing in cDNA derived from a mouse cell line<sup>120</sup>. Since this was at a time when numerous other PTKs were identified, it was originally coined “Just Another Kinase” or JAK. However, after further understanding the kinase, it was given the name “Janus Kinase”, as a reference to the two-headed Roman god, Janus, to describe the presence of two adjacent kinase domains<sup>121</sup>. JAK2 is a member of a family of four non-receptor tyrosine kinases, JAK1, JAK2, JAK3, and TYK2. Structurally, JAK2 is composed of an N-terminal FERM (4.1 protein, Ezrin, Radixin, and Moesin) domain, SH2-domain, pseudokinase domain (JH2), and kinase domain (JH1). The FERM domain non-covalently binds JAK2 to the cytoplasmic region of a receptor<sup>122</sup>. The SH2 domain (Src homology 2) mediates the association of JAK2 with its signaling partners, signal transducer and activator of transcriptions (STATs)<sup>123</sup>. While the JH1 kinase domain is straightforward, the pseudokinase domain, JH2, is devoid of enzymatic activities and serves more of an inhibitory role toward the kinase domain<sup>124</sup>. The receptors that JAK2 binds to are subclassified into type 1 and type 2 cytokine receptors. The major distinction is the presence of an extracellular amino acid motif WSXWS (W=Tryptophan, S=Serine, and X=any amino acids), which is absent in type 2 receptors. Of the two, type 1 receptors are more associated with hematopoietic signaling which encompasses EPOR, MPL, granulocyte-macrophage colony-stimulating factor (GM-CSF), and most interleukins<sup>125</sup>.

As a non-receptor tyrosine kinase, JAK2 is activated by the conformational changes of the associating membrane's receptors binding to a ligand. The canonical model of receptor activation is through the binding of the ligand to its receptor to initiate dimerization that brings the kinases to proximity for activation<sup>126</sup>. However, later studies revealed that many of these receptors, including EPOR and MPL, mainly existed in a dimerized state before ligand binding and the dimerization already occurred in the endoplasmic reticulum (ER)<sup>127-129</sup>. If the receptor is already pre-dimerized, proximity activation of JAK2 needs reevaluation and further clarification. Structural and biophysical measurements have shown that the activation of the dimerized receptor by ligand binding induced conformational changes in the receptors that also shift the position of dimerized JAK2. Established as the "sliding model", this shift dislodges the pseudokinase, inhibitory, domain from the kinase domain and activates it<sup>130</sup>.

Upon activation, the kinase phosphorylates itself and the receptors to recruit STATs. STATs are phosphorylated by JAK2 then unbound from the receptors to dimerize and be transported to the nucleus to drive transcription<sup>131</sup>. In addition to STATs signaling, JAK2 activation also activates the MAPK pathway (RAS-RAF-MEK-ERK) and phosphoinositide 3-kinase (PI3K) / AKT pathway<sup>132</sup>. The importance of the JAK2-mediated signaling is displayed when the genetic deletion of JAK2 in mice results in embryonic lethality<sup>133</sup>. Furthermore, conditional deletion of JAK2 in adult mice exhibits rapid BM failure and death. This highlights the critical role of JAK2 in the hematopoiesis process<sup>134</sup>.



### Signal Transducers and Activators of Transcription (STATs)

The STATs family consists of 7 members including, STAT1, STAT2, STAT3, STAT4, STAT5A, STAT5B, and STAT6. Of the 7 STAT members, STAT1, STAT3, and STAT5A/B play a significant role in myeloid cell development and malignancies. STAT5 is robustly expressed in the hematopoietic tissues and plays a significant role in the development and proliferation of many hematopoietic cells<sup>135</sup>. In erythroid lineages, it is directly activated by EPOR-JAK2 signaling to enhance differentiation and proliferation<sup>136</sup>. The importance of STAT5 on erythropoiesis is demonstrated when whole-body deletion of the STAT5 mice induces anemia in mice<sup>137</sup>; while conditional

knockout of STAT5 in mice can ablate JAK2V617F-induced disease phenotype including leukocytosis, erythrocytosis, and splenomegaly<sup>138</sup>. In stem cells, STAT5 is activated by stem cell factor (SCF) and TPO, which enhances HSC renewal and proliferation<sup>139,140</sup>. The ablation of STAT5 also impairs the development of lymphoid as well<sup>141</sup>. Interestingly, myelopoiesis is normal in STAT5 deletion but is unresponsive to granulocyte-macrophage colony-stimulating factor (GM-CSF)<sup>142</sup>.

STAT3 is one of the most studied members of the STATs family due to its extensive role in many cancers beyond leukemia (>32,000 publications between 2000-2023, [pubmed.gov]). The activity STAT3 in cancer is crucial in its formation, metastasis, and resistance<sup>143</sup>. Its hyperactivation is detrimental to the patient's prognosis<sup>144</sup>. This aberrant role of STAT3 signaling is generally associated with the IL6 signaling axis; however, STAT3 activation can be induced by GM-CSF, SCF, and IL3 as well<sup>145</sup>. STAT3 is critical in the body and deletion is embryonically lethal<sup>146</sup>. Selective deletion of STAT3 resulted in differentiation defect and reduced proliferation in B-cells<sup>147</sup>. Hematopoietic stem cells exhibit defective function, shorten lifespan, and increase reactive oxygen species (ROS) in absence of STAT3<sup>148</sup>. Interestingly, when examining the properties of hyperactivity of STAT3 in mice using mutated gp130 (IL6ST), IL6 receptor  $\beta$ -subunit, thrombocytosis and splenomegaly were observed<sup>149</sup>. This phenotype was ablated when STAT3 signaling was reduced by heterozygous deletion of STAT3. In addition to modulating hematopoiesis, IL6 signaling via STAT3 plays a pivotal role in inflammation. STAT3 interacts with the NF $\kappa$ B pathway at multiple levels in modulating inflammation<sup>150</sup>. On one level, NF $\kappa$ B signaling increases IL6 expression, which directly increases STAT3 activities<sup>151</sup>. On another, STAT3

directly interacts with EP300 in the nucleus, which is required for EP300 to acetylate RELA, a subunit of NFκB. The acetylation of RELA increases nuclear retention by interfering with nuclear export and causes prolonged activation of NFκB<sup>152</sup>.

Unlike its detrimental family member, STAT3, STAT1 roles appear more tumor suppressor and can directly antagonize STAT3 activities. The accumulation of STAT1 in the nucleus promotes cell arrest and apoptosis<sup>153</sup>. This is supported by the fact that patients with higher expression of STAT1 have a better clinical outcome; while the loss of STAT1 results in poor prognosis<sup>154</sup>. In terms of myeloid hematopoiesis and malignancies, STAT1 plays a significant role in the myeloid differentiation decision. Signaling through STAT1 promotes megakaryopoiesis and is important for the maturation process of megakaryocytes<sup>155</sup>. On the other hand, the loss of STAT1 in the context of the JAK2V617F mutation favors erythropoiesis while reducing megakaryopoiesis. Examining JAK2V617F-positive patients-derived erythroid, higher phosphorylation of STAT1 was detected in ET patients over PV, while phosphorylation of STAT5 was similar. The downregulation of STAT1 activities in ET progenitor cells resulted in differentiation favoring erythroid over megakaryocytes<sup>156</sup>.

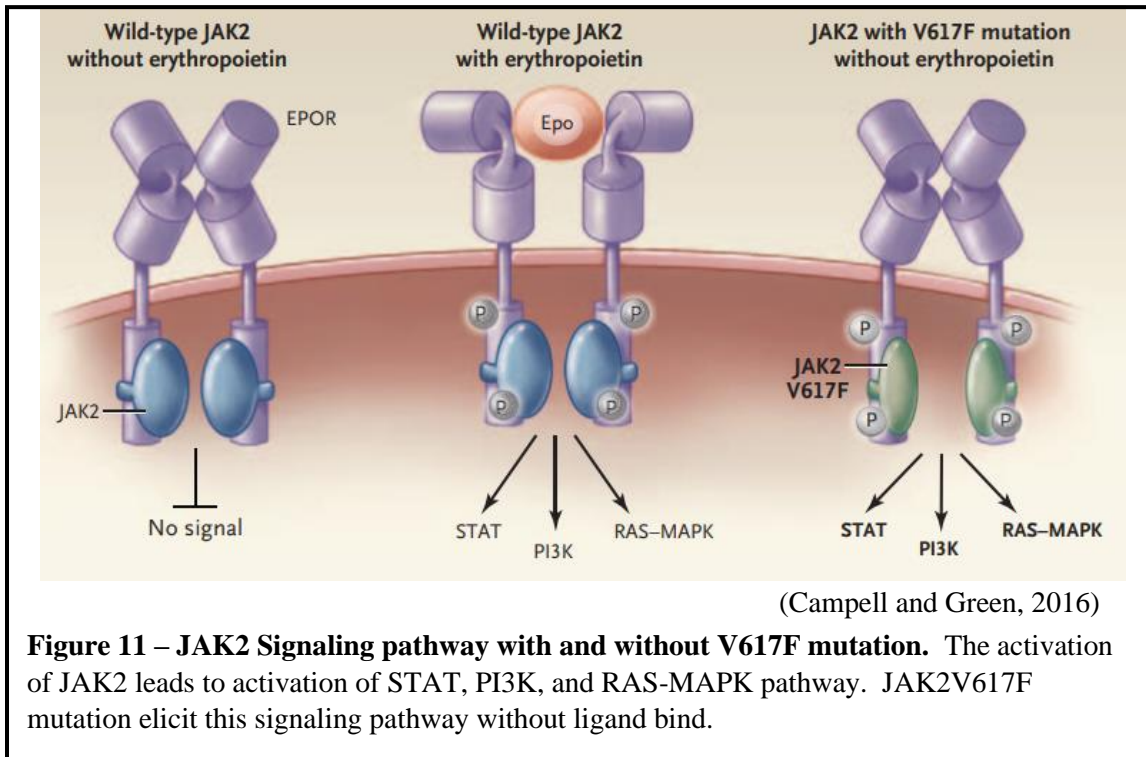
### **JAK2V617F Mutation**

In early 2005, multiple groups around the world published the identification of a significant mutation in JAK2 that was prevalent in a majority of MPN patients<sup>157–161</sup>. A single nucleotide mutation (G to T) at position 1849 on exon 12 of JAK2 led to a missense protein that substituted valine (V) with phenylalanine (F) at the amino acid position of 617, termed JAK2V617F. The resulting mutation in the pseudokinase domain



of JAK2 prevents the inhibitory properties of the kinase leading to constitutive activation. As such, all the signaling pathways downstream of JAK2 signaling, STATs, ERK/MAPK, and PI3K/AKT, are hyperactivated. Furthermore, JAK2V617F mutation can produce growth factor independence growth in cells, such as Ba/F3 and mouse erythroid colonies, as the consequence of being downstream of growth factor receptors signaling<sup>162,163</sup>.

Following the identification of the JAK2V617F mutation, murine model studies were performed using transgenic expression of JAK2V617F<sup>164-166</sup>. The transgenic model utilizes bone marrow transplantation (BMT) of virally-infected donor cells with a JAK2V617F expression vector. The recipient mice exhibited PV-like phenotype with significant erythrocytosis and modest leukocytosis and thrombocytosis. While the transgenic model provided good insight into the disease, it has major drawbacks that could not be overlooked. Transgenic model expression of a virally delivered gene is randomly integrated into the host genome, variation in the number of copies of the gene of interest, and the expression is driven by a non-native promoter<sup>167</sup>. This problem was addressed with the development of the JAK2V617F knock-in model mouse which allows the native control of the gene and its endogenous promoter without the random integration<sup>163,168,169</sup>. The knock-in mice also exhibited PV-like erythrocytosis and splenomegaly. Though the JAK2V617F mutation is quite prevalent, the distinct role it has between MPNs (PV, ET, and MF) and the progression to fibrosis remained poorly understood.

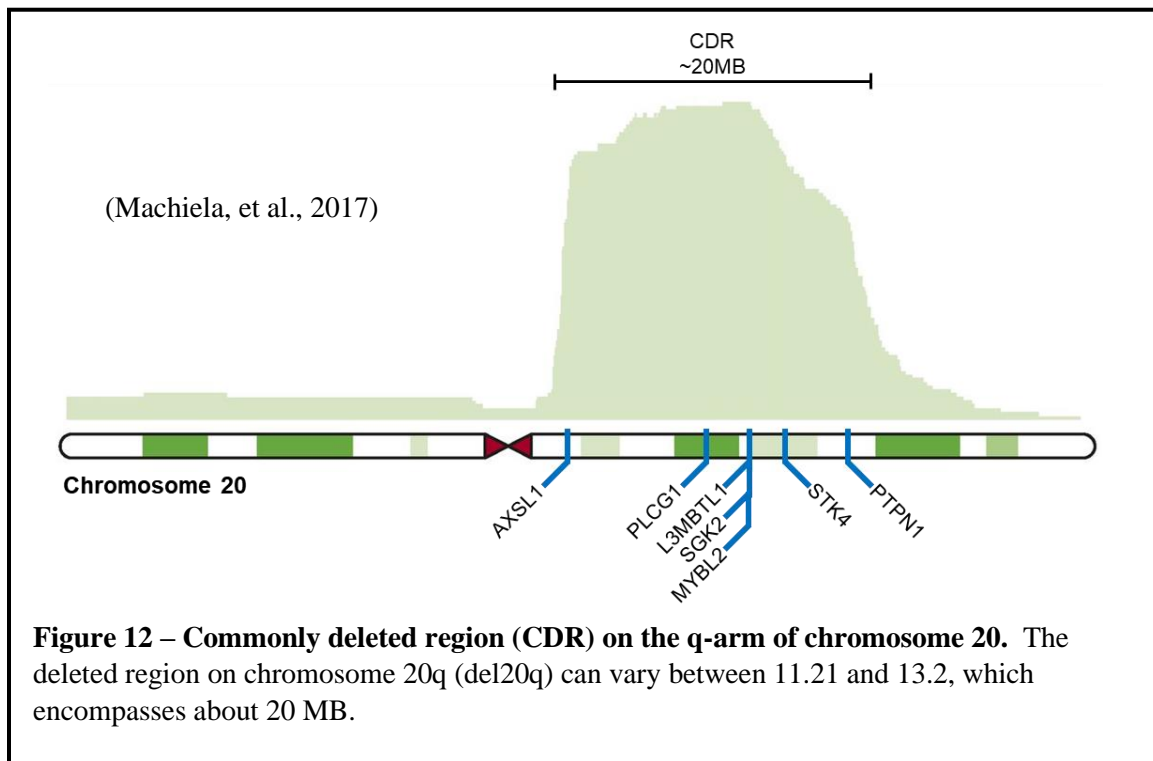


#### 1.4 – Deletion of Chromosome 20q (del20q)

Deletion of the q-arm of chromosome 20 (del20q) was first described in a cytogenetic study in 1964<sup>170</sup>. At the time, it was categorized as part of the F-group chromosome. The deleted region can vary between individuals but is commonly between q11.21-q13.2. This karyotypic abnormality is reported in cases of acute granulocytic leukemia<sup>171</sup>, polycythemia vera (PV)<sup>172</sup>, and secondary myelofibrosis (MF) following PV<sup>173</sup>. Subsequently, multiple studies were able to establish a strong prevalence of del20q in cases of PV and MF<sup>174-176</sup>. Even though del20q is more common in myeloproliferative neoplasms (MPN) (~15%), it is also observed in myelodysplastic syndrome (MDS) (~10%), acute myeloid leukemia (~5%), and MPN/MDS overlapping disease (~5%). However, it is rarely observed in lymphoid malignancies<sup>177</sup>. Even when

observed in lymphoid pathologies, del20q mostly resides in the myeloid lineages with the added potential for the development of myeloid disorders<sup>178</sup>. It is unclear what factor(s) give rise to del20q. While cytotoxic therapies have been implicated, it does not account for most cases, as the general population can give rise to del20q with no known causation factor<sup>179</sup>.

The acquisition of del20q without myeloid malignancies is about 1 in 1000 or 0.1% over the age of 55<sup>180</sup>. Studies of healthy individuals with del20q determined that, in isolation, del20q does not lead to myeloid malignancies progression. Though, if del20q is accompany by a mutation like, JAK2, DNMT3A, CBL, TET2, PTPN11, ASXL1, etc., ~39% of the patients progressed to myeloid malignancies<sup>181</sup>. It is also interesting to note that the chromosome 20q amplification, due to increase copy number, is also frequently



observed in multiple cancers including, breast, prostate, ovarian, colorectal, pancreatic, and bladder. This 20q gain is in about 12-40% of primary breast cancer<sup>182</sup>.

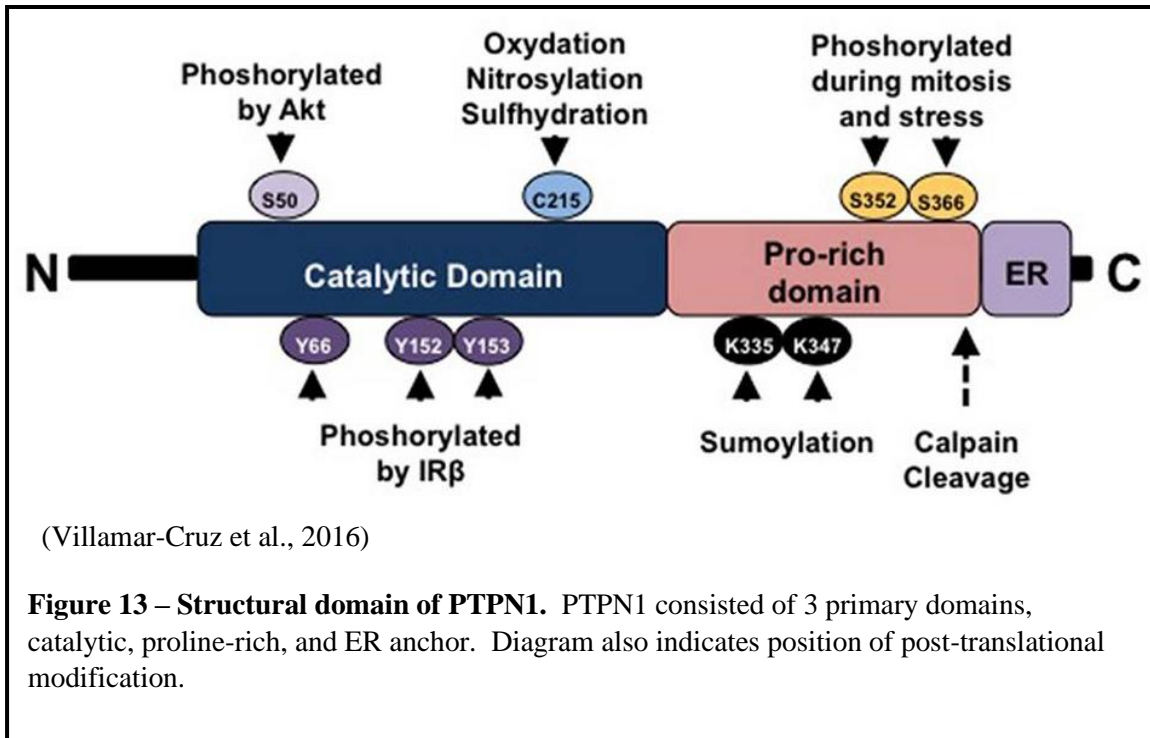
The consequences of del20q in myeloid malignancies have a great deal of ambiguity. MDS patients with sole del20q are seen as having favorable prognoses with improved survival and decreased risk of leukemic transformation<sup>183,184</sup>. In MPN, however, multiple studies find that patients with sole karyotype abnormality were displaying a range of prognosis from inferior to no substantial differences in survival with the majority of those abnormalities being del(20q) followed by del(13q)<sup>185</sup>. PV patients, on the other hand, were deemed intermediate-risk with del20q as they displayed a higher frequency of disease progression and inferior survival overall<sup>186</sup>. The variability of deletion likely plays a role in this ambiguity. If patients acquire an additional karyotype abnormality, in addition to del(20q), the prognosis is consensually very poor.

While we have some insight into how del20q impacts patients, there is a lack of understanding of the causal factor for myeloid malignancies-bias. This bias suggests the loss of tumor suppressor gene(s) within the deleted region. Several genes have been proposed. ASXL1 deletion can induce MDS-like disease with impaired HSC repopulation and favoring granulocytic lineages, but heterozygous deletion only exhibited mild phenotype<sup>187</sup>. However, as a common mutation gene, if one copy is deleted and another copy is mutated (ASXL<sup>Mut/-</sup>), the results can be very detrimental in patients<sup>188</sup>. PLCG1 reduction in expression is associated with inferior survival in MDS<sup>189</sup>. Loss of L3MBTL1 promotes erythroid differentiation and in combination with SGK2 can promote megakaryocytic proliferation as well<sup>190,191</sup>. MYBL2 deficiency leads to the

development of MDS-like phenotype in aged mice population<sup>192</sup>. The loss of PTPN1 leads to a protracted development of MPN-like phenotype in mice<sup>193</sup>. As sole del20q displayed little impact in the development of myeloid neoplasms, del20q role in combination with another mutation or karyotypic abnormality needs to be explored. With the elevated risk of disease progression in PV to myelofibrosis in the presence of del20q, there is an urgent need to understand the pathological process and gene(s) involved in the disease progression. Of these genes, PTPN1 plays a significant role in modulating the activity of JAK/STAT signaling and is a promising candidate in JAK2V617F-induced pathogenesis.

### **1.5 – Protein Tyrosine Phosphatase Non-Receptor Type 1 (PTPN1/PTP1B)**

PTPN1, also referenced as PTP1B, is a ubiquitously expressed classical non-receptor tyrosine phosphatase. The gene is located on chromosome 20q13.1 and translated to a 435 amino acid protein that consisted of an N-terminal catalytic domain, two proline-rich domains, and a 35 amino acid C-terminal tail, which anchors the phosphatase to the endoplasmic reticulum (ER)<sup>194</sup>. PTPN1's two proline-rich domains mediate its interaction with the protein-containing Src-homology 3 (SH3) domain, such as GRB2, SRC, and BCAR1 (p130Cas)<sup>195–197</sup>. PTPN1 has also been known to direct target, insulin receptor (IR), JAK2, and tyrosine kinase 2 (TYK2)<sup>198,199</sup>. A study of crystallography of PTPN1 and its interaction with IR reveals a phosphatase preference for the sequence E/D-pY-pY-R/K (E=Glutamic acid, D=Aspartic acid, pY=phosphor-



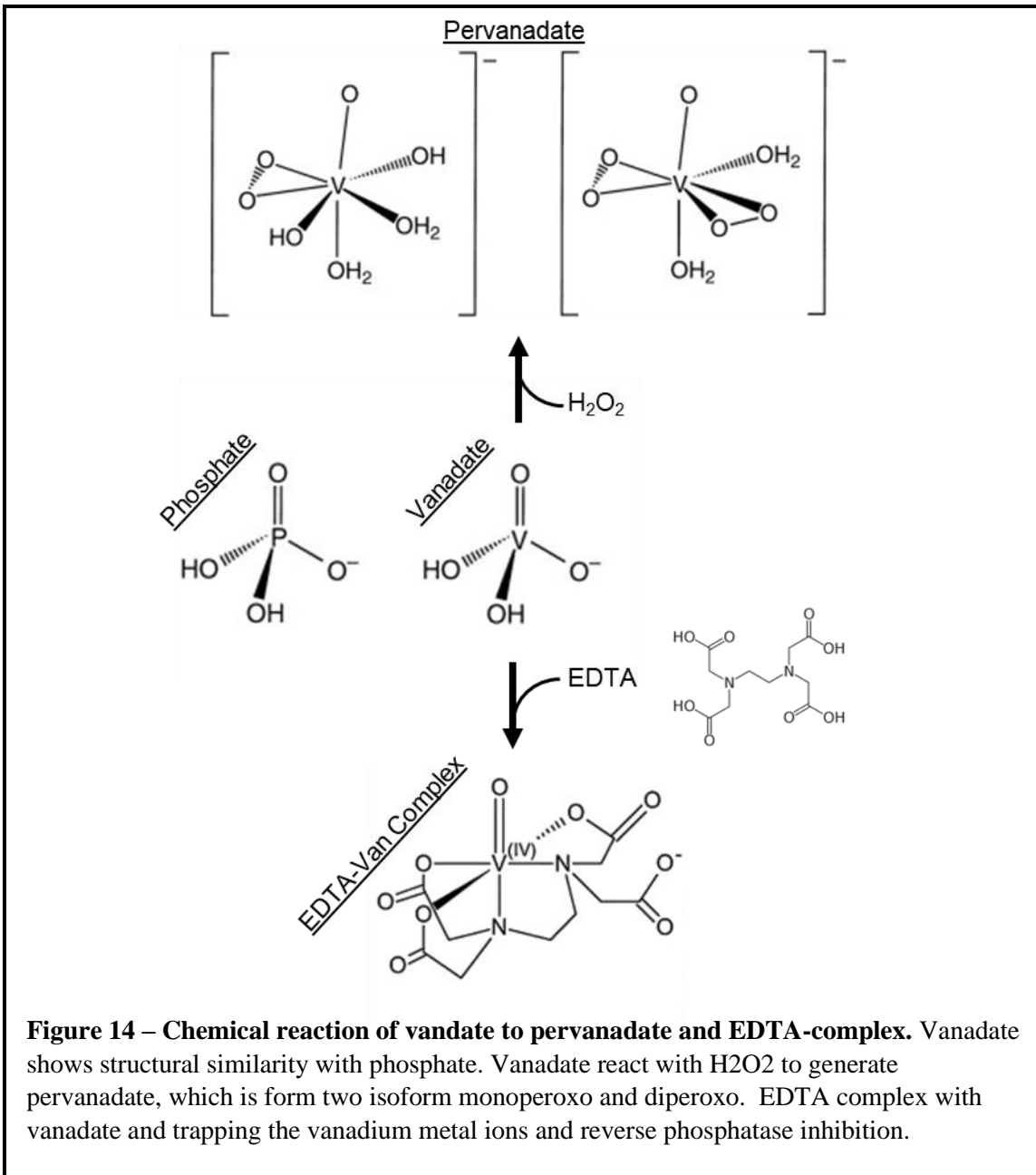
tyrosine, R=Arginine, K=Lysine); though PTPN1 has a higher affinity for this phospho-signal sequence, it is not required for PTPN1 targeting<sup>200</sup>.

### Regulation of PTPN1

The structural studies of PTPN1 reveal an important cysteine residue on amino acid position 215 of the catalytic domain to be an essential amino acid for its catalytic activity<sup>201</sup>. Mutation of cysteine to serine (C215S) or alanine (C215A) will result in a catalytically dead phosphatase<sup>201</sup>. In addition to the mutagenesis of the site, other contributing modifications to this cysteine include oxidation<sup>202</sup>, nitrosylation<sup>203</sup>, and sulfhydrylation<sup>204</sup>, all of which inhibit the activity of PTPN1. All these modifications are reversible. Oxidation, nitrosylation, and sulfhydrylation are induced by reactive oxygen species (ROS), nitric oxide (NO), and hydrogen sulfide (H<sub>2</sub>S), respectively. Of the three, oxidation of PTPN1 has greater influence as it is a more prevalent physiological stimulus,

such as inflammation and stress. This oxidation is reversible by antioxidants, glutathione and glutaredoxin<sup>205</sup>. Another interesting mutagenesis study revealed the mutation of aspartic acid (D) to alanine (A) at position 181 resulted in a substrate-trapping mutant of PTPN1 which serves as a powerful tool to identify the substrate of PTPN1<sup>206</sup>. While not phosphatase dead, PTPN1-D181A has severely limited phosphatase activity, but yields 5-fold higher binding affinity to substrates<sup>207</sup>.

The study of cell signaling often utilizes a pan phosphatase inhibitor, sodium orthovanadate (or vanadate) [Na<sub>3</sub>VO<sub>4</sub>] to preserve phosphorylated signals<sup>208</sup>. The absence of phosphatase inhibitors can devoid an entire lysate of tyrosine phosphorylation within minutes of lysis. Mechanistically, vanadate is a structural analog of phosphate and so it is targeted by phosphatase and gets structurally locked. This reaction is reversible when ethylenediaminetetraacetic acid (EDTA) is added, as vanadate has a higher affinity for EDTA and forms a complex with it<sup>209</sup>. However, a reaction with hydrogen peroxide converts vanadate to a peroxide form, pervanadate. Unlike vanadate, when pervanadate interacts with phosphatase, it triply oxidizes the 215-cysteine, which creates an irreversibly inhibited phosphatase<sup>210</sup>. It is interesting to note that while EDTA inhibits vanadate, both are typically added both to a standard lysis buffer. This is dictated by the importance of metal chelators in protecting proteins from damage due to metal-dependent enzyme activities. To overcome this, most researchers just use vanadate in excess to circumvent the EDTA inhibition.





Two lysines (K) amino acids (335 and 347) on the proline-rich motif are sites for the sumoylation of PTPN1, which reduces its catalytic activity<sup>211</sup>. Interestingly, sumoylated PTPN1 is typically found in the inner nuclear membrane (INM) instead of the ER<sup>212</sup>. This indicated a potential role for PTPN1 interaction with nuclear exporters, transcription, and RNA splicing. PTPN1 can also be tyrosine phosphorylated at amino acid positions 66, 152, and 153 by kinases, like IR, to increase their interaction and PTPN1 phosphatase activities<sup>213</sup>. Serine phosphorylation of PTPN1 at position 50 by AKT can inhibit phosphatase activity<sup>214</sup>. Lastly, the ER-anchored region of PTPN1 can be cleaved by calpain, which creates a cytoplasmic PTPN1<sup>215</sup>. Many would imagine this would great a different variant of PTPN1 that serves a different purpose, but studies of the role of PTPN1 and Calpain revealed its mostly induces PTPN1 degradation<sup>216,217</sup>. In term of gene expression regulation, the PTPN1 promoter is extremely GC-rich<sup>218</sup>, which pose a potential epigenetic regulation. Additionally, it has been identified to be targeted by multiple miRNAs, such as miR-135a, miR-206, miR-146-b, etc<sup>219-221</sup>. These multilevel regulations of PTPN1 demonstrate the complexity of its role in the physiological state.

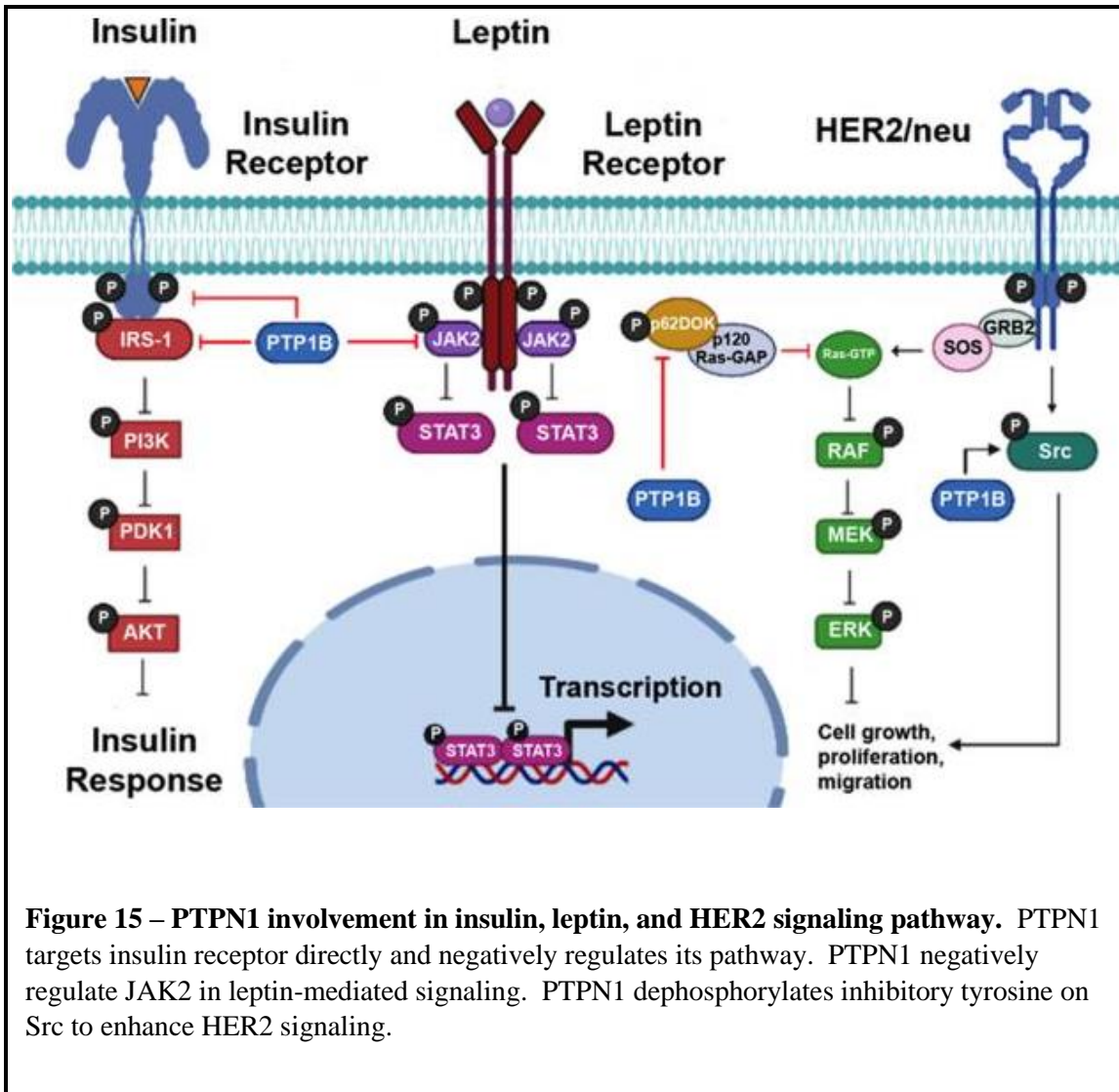


**Figure 15 – PTPN1 involvement in insulin, leptin, and HER2 signaling pathway.** PTPN1 targets insulin receptor directly and negatively regulates its pathway. PTPN1 negatively regulate JAK2 in leptin-mediated signaling. PTPN1 dephosphorylates inhibitory tyrosine on Src to enhance HER2 signaling.

## **The role of PTPN1 in metabolism**

As previously mentioned, PTPN1 is a negative regulator of IR signaling. Mouse in vivo study revealed that PTPN1 knockout mouse exhibit obesity-resistant and increased insulin sensitivity in comparison to wild-type (WT) mice<sup>222</sup>. In addition to insulin signaling, PTPN1 also negatively regulates leptin signaling by modulating JAK2 activity<sup>223</sup>. Leptin signaling is a critical signaling pathway that regulates metabolic homeostasis. The impairment of this signaling pathway is a key factor in metabolic diseases like obesity, diabetes, cardiovascular disease, and so on<sup>224</sup>. This places a great emphasis on PTPN1's role in metabolic health and a major endeavor to identify potential therapeutic targets against PTPN1 activity.

## **The role of PTPN1 role in non-hematological malignancies**

Both oncogenic and tumor suppressor functions of PTPN1 have been suggested in several malignancies. The oncogenic properties of PTPN1 are displayed in breast cancer, as it is commonly overexpressed in association with ERBB2 (HER2) overexpression<sup>225</sup>. This correlation is also observed in ovarian cancer. The importance of PTPN1 is supported when mice lacking PTPN1 with HER2 overexpression would show delay or absence of tumorigenesis<sup>226</sup>. This oncogenic property of PTPN1 is due to its dephosphorylation of inhibitory pTyr530 on SRC, thus activating it. This oncogenic activation is also exhibited in non-small cell lung cancer (NSCLC), as the expression of PTPN1 is higher here than in benign lung diseases<sup>227</sup>. Recently, this SRC activation is also been shown to promote melanoma disease progression as well<sup>228</sup>. The fact that chromosome 20q amplification is often observed in these cancers, as previously

mentioned<sup>182</sup>, it would not be surprising to see this translated to the observed Ptpn1 overexpression. The tumor suppressor property of PTPN1 is also observed in cases such as chronic myeloid leukemia (CML), where PTPN1 directly targets and antagonizes p210 BCR-ABL oncoprotein<sup>229</sup>. In colon and thyroid cancer, a splice variant of PTPN1 with exon 6 deletion results in loss of phosphatase activity but induces oncogenic transformation<sup>230</sup>.

PTPN1 has played a diverse role in the oncogenicity of the cells. It has demonstrated its capabilities in regulating multiple signaling pathways, especially that of JAK/STAT. With the prevalence of JAK2V617F mutation in myeloid malignancies and the resulting aberrant signaling, the role of PTPN1 in regulating the JAK/STAT pathway is put into question. What are the role it serves in the pathogenesis of MPN and the effects of its deletion as a consequence of del20q? As such, it is important to understand the role of PTPN1 in clonal expansion and progression of JAK2V617F-induced MPN.

## 1.6 – References

1. Sender, R., Fuchs, S. & Milo, R. Are We Really Vastly Outnumbered? Revisiting the Ratio of Bacterial to Host Cells in Humans. *Cell* **164**, 337–340 (2016).
2. Sender, R. & Milo, R. The distribution of cellular turnover in the human body. *Nat. Med.* **27**, 45–48 (2021).
3. Shenghui, H., Nakada, D. & Morrison, S. J. Mechanisms of Stem Cell Self-Renewal. *Annu. Rev. Cell Dev. Biol.* **25**, 377–406 (2009).
4. Galloway, J. L. & Zon, L. I. Ontogeny of hematopoiesis: Examining the emergence of hematopoietic cells in the vertebrate embryo. in *Current Topics in Developmental Biology* 139–158 (Current Topics in Developmental Biology, 2003). doi:10.1016/S0070-2153(03)53004-6.
5. Palis, J. & Yoder, M. C. Yolk-sac hematopoiesis. *Exp. Hematol.* **29**, 927–936 (2001).
6. Jagannathan-Bogdan, M. & Zon, L. I. Hematopoiesis. *Development* **140**, 2463–2467 (2013).
7. Tavian, M., Biasch, K., Sinka, L., Vallet, J. & Peault, B. Embryonic origin of human hematopoiesis. *Int. J. Dev. Biol.* **54**, 1061–1065 (2010).
8. Lorenz, E., Congdon, C. & Uphoff, D. Modification of Acute Irradiation Injury in Mice and Guinea-Pigs by Bone Marrow Injections. *Radiology* **58**, 863–877 (1952).
9. FORD, C. E., HAMERTON, J. L., BARNES, D. W. H. & LOUITIT, J. F. Cytological Identification of Radiation-Chimæras. *Nature* **177**, 452–454 (1956).
10. Jacobson, L. O., Marks, E. K., Gaston, E. O., Robson, M. & Zirkle, R. E. The Role of the Spleen in Radiation Injury. *Exp. Biol. Med.* **70**, 740–742 (1949).
11. Till, J. E. & McCulloch, E. A. A Direct Measurement of the Radiation Sensitivity of Normal Mouse Bone Marrow Cells. *Radiat. Res.* **14**, 213 (1961).
12. BECKER, A. J., McCULLOCH, E. A. & TILL, J. E. Cytological Demonstration of the Clonal Nature of Spleen Colonies Derived from Transplanted Mouse Marrow Cells. *Nature* **197**, 452–454 (1963).
13. Siminovitch, L., McCulloch, E. A. & Till, J. E. The distribution of colony-forming cells among spleen colonies. *J. Cell. Comp. Physiol.* **62**, 327–336 (1963).
14. Morstyn, G., Nicola, N. & Metcalf, D. Purification of hemopoietic progenitor cells from human marrow using a fucose-binding lectin and cell sorting. *Blood* **56**, 798–805 (1980).
15. Krause, D. S., DeLelys, M. E. & Preffer, F. I. Flow Cytometry for Hematopoietic Cells. in *Bone Marrow and Stem Cell Transplantation* (ed. Beksac, M.) 23–46 (Humana Press, 2014). doi:10.1007/978-1-4614-9437-9\_2.

16. Hoy, T. G. 7 Flow cytometry: clinical applications in haematology. *Baillieres. Clin. Haematol.* **3**, 977–998 (1990).
17. Orfao, A. *et al.* Flow cytometry: its applications in hematology. *Haematologica* **80**, 69–81 (1995).
18. Ikuta, K. & Weissman, I. L. Evidence that hematopoietic stem cells express mouse c-kit but do not depend on steel factor for their generation. *Proc. Natl. Acad. Sci.* **89**, 1502–1506 (1992).
19. Osawa, M., Hanada, K., Hamada, H. & Nakauchi, H. Long-Term Lymphohematopoietic Reconstitution by a Single CD34-Low/Negative Hematopoietic Stem Cell. *Science (80-. )*. **273**, 242–245 (1996).
20. Adolfsson, J. *et al.* Upregulation of Flt3 Expression within the Bone Marrow Lin–Sca1+c-kit+ Stem Cell Compartment Is Accompanied by Loss of Self-Renewal Capacity. *Immunity* **15**, 659–669 (2001).
21. Morrison, S. J., Wandycz, A. M., Hemmati, H. D., Wright, D. E. & Weissman, I. L. Identification of a lineage of multipotent hematopoietic progenitors. *Development* **124**, 1929–1939 (1997).
22. Reya, T., Morrison, S. J., Clarke, M. F. & Weissman, I. L. Stem cells, cancer, and cancer stem cells. *Nature* **414**, 105–111 (2001).
23. Adolfsson, J. *et al.* Identification of Flt3+ Lympho-Myeloid Stem Cells Lacking Erythro-Megakaryocytic Potential. *Cell* **121**, 295–306 (2005).
24. Paul, F. *et al.* Transcriptional Heterogeneity and Lineage Commitment in Myeloid Progenitors. *Cell* **163**, 1663–1677 (2015).
25. Qin, P. *et al.* Integrated decoding hematopoiesis and leukemogenesis using single-cell sequencing and its medical implication. *Cell Discov.* **7**, 2 (2021).
26. Savino, W., Smaniotto, S. & Dardenne, M. Hematopoiesis. in *The Growth Hormone/Insulin-Like Growth Factor Axis During Development* 167–185 (Springer-Verlag, 2005). doi:10.1007/0-387-26274-1\_7.
27. Shivdasani, R. & Orkin, S. The transcriptional control of hematopoiesis [see comments]. *Blood* **87**, 4025–4039 (1996).
28. Kuhn, V. *et al.* Red Blood Cell Function and Dysfunction: Redox Regulation, Nitric Oxide Metabolism, Anemia. *Antioxid. Redox Signal.* **26**, 718–742 (2017).
29. Axelrad, A., McLeod, D., Shreeve, M. & Heath, D. Properties of cells that produce erythrocytic colonies in vitro. in *Hemopoiesis in Culture* (ed. Robinson, W. A.) 226 (National Institutes of Health, 1974).
30. Gregory, C. J., McCulloch, E. A. & Till, J. K. Erythropoietic progenitors capable of colony formation in culture: State of differentiation. *J. Cell. Physiol.* **81**, 411–420 (1973).

31. Moras, M., Lefevre, S. D. & Ostuni, M. A. From Erythroblasts to Mature Red Blood Cells: Organelle Clearance in Mammals. *Front. Physiol.* **8**, 1076 (2017).
32. Dzierzak, E. & Philipsen, S. Erythropoiesis: Development and Differentiation. *Cold Spring Harb. Perspect. Med.* **3**, a011601–a011601 (2013).
33. Nandakumar, S. K., Ulirsch, J. C. & Sankaran, V. G. Advances in understanding erythropoiesis: evolving perspectives. *Br. J. Haematol.* **173**, 206–218 (2016).
34. Carnot, P. & Deflandre, C.-C. Sur l'activite hematopoietique du serum au cours de la regeneration du sang. in *Comptes Rendus Hebdomadaires des Seances de l'Acad des Sci.* vol. 143 384–386 (1906).
35. Miyake, T., Kung, C. K. & Goldwasser, E. Purification of human erythropoietin. *J. Biol. Chem.* **252**, 5558–5564 (1977).
36. Jacobs, K. *et al.* Isolation and characterization of genomic and cDNA clones of human erythropoietin. *Nature* **313**, 806–810 (1985).
37. Rizzo, J. D. *et al.* American Society of Hematology/American Society of Clinical Oncology clinical practice guideline update on the use of epoetin and darbepoetin in adult patients with cancer. *Blood* **116**, 4045–4059 (2010).
38. REISSMANN, K. R. STUDIES ON THE MECHANISM OF ERYTHROPOIETIC STIMULATION IN PARABIOTIC RATS DURING HYPOXIA. *Blood* **5**, 372–380 (1950).
39. D'Andrea, A. D., Lodish, H. F. & Wong, G. G. Expression cloning of the murine erythropoietin receptor. *Cell* **57**, 277–285 (1989).
40. Watowich, S. S. *et al.* Homodimerization and constitutive activation of the erythropoietin receptor. *Proc. Natl. Acad. Sci.* **89**, 2140–2144 (1992).
41. Witthuhn, B. A. *et al.* JAK2 associates with the erythropoietin receptor and is tyrosine phosphorylated and activated following stimulation with erythropoietin. *Cell* **74**, 227–236 (1993).
42. Laki, K. OUR ANCIENT HERITAGE IN BLOOD CLOTTING AND SOME OF ITS CONSEQUENCES. *Ann. N. Y. Acad. Sci.* **202**, 297–307 (1972).
43. Golebiewska, E. M. & Poole, A. W. Platelet secretion: From haemostasis to wound healing and beyond. *Blood Rev.* **29**, 153–162 (2015).
44. Yu, M. & Cantor, A. B. Megakaryopoiesis and thrombopoiesis: An update on cytokines and lineage surface markers. in *Methods in Molecular Biology* vol. 788 291–303 (2012).
45. Lu, Y.-C. *et al.* The Molecular Signature of Megakaryocyte-Erythroid Progenitors Reveals a Role for the Cell Cycle in Fate Specification. *Cell Rep.* **25**, 2083–2093.e4 (2018).
46. Ichikawa, M. *et al.* AML-1 is required for megakaryocytic maturation and

- lymphocytic differentiation, but not for maintenance of hematopoietic stem cells in adult hematopoiesis. *Nat. Med.* **10**, 299–304 (2004).
47. Chang, A. N. *et al.* GATA-factor dependence of the multitype zinc-finger protein FOG-1 for its essential role in megakaryopoiesis. *Proc. Natl. Acad. Sci.* **99**, 9237–9242 (2002).
  48. Elagib, K. E. *et al.* RUNX1 and GATA-1 coexpression and cooperation in megakaryocytic differentiation. *Blood* **101**, 4333–4341 (2003).
  49. Huang, H. *et al.* Differentiation-Dependent Interactions between RUNX-1 and FLI-1 during Megakaryocyte Development. *Mol. Cell. Biol.* **29**, 4103–4115 (2009).
  50. Hart, A. *et al.* Fli-1 Is Required for Murine Vascular and Megakaryocytic Development and Is Hemizygotously Deleted in Patients with Thrombocytopenia. *Immunity* **13**, 167–177 (2000).
  51. Tsang, A. P., Fujiwara, Y., Hom, D. B. & Orkin, S. H. Failure of megakaryopoiesis and arrested erythropoiesis in mice lacking the GATA-1 transcriptional cofactor FOG. *Genes Dev.* **12**, 1176–1188 (1998).
  52. Nakorn, T. N., Miyamoto, T. & Weissman, I. L. Characterization of mouse clonogenic megakaryocyte progenitors. *Proc. Natl. Acad. Sci.* **100**, 205–210 (2003).
  53. Sanjuan-Pla, A. *et al.* Platelet-biased stem cells reside at the apex of the haematopoietic stem-cell hierarchy. *Nature* **502**, 232–236 (2013).
  54. Sun, L., Hwang, W. Y. K. & Aw, S. E. Biological characteristics of megakaryocytes: Specific lineage commitment and associated disorders. *Int. J. Biochem. Cell Biol.* **38**, 1821–1826 (2006).
  55. Vitrat, N. *et al.* Endomitosis of human megakaryocytes are due to abortive mitosis. *Blood* **91**, 3711–23 (1998).
  56. Ravid, K., Lu, J., Zimmet, J. M. & Jones, M. R. Roads to polyploidy: The megakaryocyte example. *J. Cell. Physiol.* **190**, 7–20 (2002).
  57. Geddis, A. E., Fox, N. E., Tkachenko, E. & Kaushansky, K. Endomitotic Megakaryocytes that Form a Bipolar Spindle Exhibit Cleavage Furrow Ingression Followed by Furrow Regression. *Cell Cycle* **6**, 455–460 (2007).
  58. Qiao, X. *et al.* Immunocytochemistry and flow cytometry evaluation of human megakaryocytes in fresh samples and cultures of CD34+ cells. *Cytometry* **23**, 250–259 (1996).
  59. Eckly, A. *et al.* Biogenesis of the demarcation membrane system (DMS) in megakaryocytes. *Blood* **123**, 921–930 (2014).
  60. NAKAO, K. & ANGRIST, A. A. Membrane Surface Specialization of Blood
-



- Platelet and Megakaryocyte. *Nature* **217**, 960–961 (1968).
61. Schulze, H. *et al.* Characterization of the megakaryocyte demarcation membrane system and its role in thrombopoiesis. *Blood* **107**, 3868–3875 (2006).
  62. Italiano, J. E., Lecine, P., Shivdasani, R. A. & Hartwig, J. H. Blood Platelets Are Assembled Principally at the Ends of Proplatelet Processes Produced by Differentiated Megakaryocytes. *J. Cell Biol.* **147**, 1299–1312 (1999).
  63. Radley, J. M. & Haller, C. J. Fate of senescent megakaryocytes in the bone marrow. *Br. J. Haematol.* **53**, 277–287 (2008).
  64. Kelemen, E., Cserhádi, I. & Tanos, B. Demonstration and Some Properties of Human Thrombopoietin in Thrombocythaemic Sera. *Acta Haematol.* **20**, 350–355 (1958).
  65. Bartley, T. Identification and cloning of a megakaryocyte growth and development factor that is a ligand for the cytokine receptor Mpl. *Cell* **77**, 1117–1124 (1994).
  66. Souyri, M. *et al.* A putative truncated cytokine receptor gene transduced by the myeloproliferative leukemia virus immortalizes hematopoietic progenitors. *Cell* **63**, 1137–47 (1990).
  67. Methia, N., Louache, F., Vainchenker, W. & Wendling, F. Oligodeoxynucleotides antisense to the proto-oncogene c-mpl specifically inhibit in vitro megakaryocytopoiesis. *Blood* **82**, 1395–401 (1993).
  68. Emmons, R. V *et al.* Human thrombopoietin levels are high when thrombocytopenia is due to megakaryocyte deficiency and low when due to increased platelet destruction. *Blood* **87**, 4068–71 (1996).
  69. Sungaran, R., Markovic, B. & Chong, B. H. Localization and regulation of thrombopoietin mRNA expression in human kidney, liver, bone marrow, and spleen using in situ hybridization. *Blood* **89**, 101–7 (1997).
  70. Fielder, P. J. *et al.* Regulation of thrombopoietin levels by c-mpl-mediated binding to platelets. *Blood* **87**, 2154–61 (1996).
  71. Fielder, P. J. *et al.* Human platelets as a model for the binding and degradation of thrombopoietin. *Blood* **89**, 2782–8 (1997).
  72. Kaushansky, K. & Drachman, J. G. The molecular and cellular biology of thrombopoietin: the primary regulator of platelet production. *Oncogene* **21**, 3359–3367 (2002).
  73. Sitnicka, E. *et al.* The effect of thrombopoietin on the proliferation and differentiation of murine hematopoietic stem cells. *Blood* **87**, 4998–5005 (1996).
  74. Actor, J. K. Cells and Organs of the Immune System. in *Elsevier's Integrated Review Immunology and Microbiology* 7–16 (Elsevier, 2012). doi:10.1016/B978-0-323-07447-6.00002-8.
-

75. Hidalgo, A., Chilvers, E. R., Summers, C. & Koenderman, L. The Neutrophil Life Cycle. *Trends Immunol.* **40**, 584–597 (2019).
76. Hettlinger, J. *et al.* Origin of monocytes and macrophages in a committed progenitor. *Nat. Immunol.* **14**, 821–830 (2013).
77. Rose, S., Misharin, A. & Perlman, H. A novel Ly6C/Ly6G-based strategy to analyze the mouse splenic myeloid compartment. *Cytom. A* **81A**, 343–350 (2012).
78. McFarland, H. I., Nahill, S. R., Maciaszek, J. W. & Welsh, R. M. CD11b (Mac-1): a marker for CD8+ cytotoxic T cell activation and memory in virus infection. *J. Immunol.* **149**, 1326–33 (1992).
79. Mildner, A., Marinkovic, G. & Jung, S. Murine Monocytes: Origins, Subsets, Fates, and Functions. *Microbiol. Spectr.* **4**, (2016).
80. Lin, H.-H., Stacey, M., Stein-Streilein, J. & Gordon, S. F4/80: The Macrophage-Specific Adhesion-GPCR and its Role in Immunoregulation. in 149–156 (2010). doi:10.1007/978-1-4419-7913-1\_13.
81. Arber, D. A. *et al.* The 2016 revision to the World Health Organization classification of myeloid neoplasms and acute leukemia. *Blood* **127**, 2391–2405 (2016).
82. Kurzrock, R., Kantarjian, H. M., Druker, B. J. & Talpaz, M. Philadelphia Chromosome-Positive Leukemias: From Basic Mechanisms to Molecular Therapeutics. *Ann. Intern. Med.* **138**, 819 (2003).
83. Jabbour, E. & Kantarjian, H. Chronic myeloid leukemia: 2018 update on diagnosis, therapy and monitoring. *Am. J. Hematol.* **93**, 442–459 (2018).
84. Vaquez, H. Sur une forme speciale de cyanose s’accompagnant d’hyperglobulie excessive et peristente. *CR Soc Biol* **44**, 384–388 (1892).
85. Osler, W. CHRONIC CYANOSIS, WITH POLYCYTHAEMIA AND ENLARGED SPLEEN: A NEW CLINICAL ENTITY. *Am. J. Med. Sci.* **126**, 187 (1903).
86. Tefferi, A., Thiele, J., Vannucchi, A. M. & Barbui, T. An overview on CALR and CSF3R mutations and a proposal for revision of WHO diagnostic criteria for myeloproliferative neoplasms. *Leukemia* **28**, 1407–1413 (2014).
87. Ma, X., Vanasse, G., Cartmel, B., Wang, Y. & Selinger, H. A. Prevalence of polycythemia vera and essential thrombocythemia. *Am. J. Hematol.* **83**, 359–362 (2008).
88. Tefferi, A. *et al.* Long-term survival and blast transformation in molecularly annotated essential thrombocythemia, polycythemia vera, and myelofibrosis. *Blood* **124**, 2507–2513 (2014).
89. Tefferi, A. *et al.* Survival and prognosis among 1545 patients with contemporary

- polycythemia vera: an international study. *Leukemia* **27**, 1874–1881 (2013).
90. Bonicelli, G. *et al.* Leucocytosis and thrombosis at diagnosis are associated with poor survival in polycythaemia vera: a population-based study of 327 patients. *Br. J. Haematol.* **160**, 251–254 (2013).
  91. Tefferi, A. Somatic JAK2 mutations and their tumor phenotypes. *Blood* **128**, 748–749 (2016).
  92. Stein, B. L. *et al.* Mortality and Causes of Death of Patients with Polycythemia Vera: Analysis of the Reveal Prospective, Observational Study. *Blood* **136**, 36–37 (2020).
  93. Koç, A., Wheeler, L. J., Mathews, C. K. & Merrill, G. F. Hydroxyurea Arrests DNA Replication by a Mechanism That Preserves Basal dNTP Pools. *J. Biol. Chem.* **279**, 223–230 (2004).
  94. Spivak, J. L. Myeloproliferative Neoplasms. *N. Engl. J. Med.* **376**, 2168–2181 (2017).
  95. Tefferi, A. & Barbui, T. Polycythemia vera and essential thrombocythemia: 2019 update on diagnosis, risk-stratification and management. *Am. J. Hematol.* **94**, 133–143 (2019).
  96. Bristol-Myers Squibb. *Hydrea (hydroxyurea capsules, USP) prescribing information*. [https://packageinserts.bms.com/pi/pi\\_hydrea.pdf](https://packageinserts.bms.com/pi/pi_hydrea.pdf) (2001).
  97. Kiladjian, J.-J., Chevret, S., Dosquet, C., Chomienne, C. & Rain, J.-D. Treatment of Polycythemia Vera With Hydroxyurea and Pipobroman: Final Results of a Randomized Trial Initiated in 1980. *J. Clin. Oncol.* **29**, 3907–3913 (2011).
  98. Najean, Y. & Rain, J.-D. Treatment of Polycythemia Vera: The Use of Hydroxyurea and Pipobroman in 292 Patients Under the Age of 65 Years. *Blood* **90**, 3370–3377 (1997).
  99. Barbui, T. *et al.* A reappraisal of the benefit-risk profile of hydroxyurea in polycythemia vera: A propensity-matched study. *Am. J. Hematol.* **92**, 1131–1136 (2017).
  100. Alvarez-Larrán, A. *et al.* Assessment and prognostic value of the European LeukemiaNet criteria for clinicohematologic response, resistance, and intolerance to hydroxyurea in polycythemia vera. *Blood* **119**, 1363–1369 (2012).
  101. Abu-Zeinah, G. *et al.* Interferon-alpha for treating polycythemia vera yields improved myelofibrosis-free and overall survival. *Leukemia* **35**, 2592–2601 (2021).
  102. Nguyen, V.-A. & Gao, B. Expression of interferon alfa signaling components in human alcoholic liver disease. *Hepatology* **35**, 425–432 (2002).
  103. Vannucchi, A. M. *et al.* Ruxolitinib versus Standard Therapy for the Treatment of
-

- Polycythemia Vera. *N. Engl. J. Med.* **372**, 426–435 (2015).
104. Mesa, R. A. *et al.* Primary myelofibrosis (PMF), post polycythemia vera myelofibrosis (post-PV MF), post essential thrombocythemia myelofibrosis (post-ET MF), blast phase PMF (PMF-BP): Consensus on terminology by the international working group for myelofibrosis research and. *Leuk. Res.* **31**, 737–740 (2007).
  105. Salama, M. E. Important Pathologic Considerations for Establishing the Diagnosis of Myelofibrosis. *Hematol. Oncol. Clin. North Am.* **35**, 267–278 (2021).
  106. Tefferi, A. & Vannucchi, A. M. Genetic Risk Assessment in Myeloproliferative Neoplasms. *Mayo Clin. Proc.* **92**, 1283–1290 (2017).
  107. Gangat, N. & Tefferi, A. Myelofibrosis biology and contemporary management. *Br. J. Haematol.* **191**, 152–170 (2020).
  108. Vainchenker, W. & Kralovics, R. Genetic basis and molecular pathophysiology of classical myeloproliferative neoplasms. *Blood* **129**, 667–679 (2017).
  109. Andrieux, J. *et al.* Karyotypic abnormalities in myelofibrosis following polycythemia vera. *Cancer Genet. Cytogenet.* **140**, 118–123 (2003).
  110. Cervantes, F. *et al.* New prognostic scoring system for primary myelofibrosis based on a study of the International Working Group for Myelofibrosis Research and Treatment. *Blood* **113**, 2895–2901 (2009).
  111. Passamonti, F. *et al.* A dynamic prognostic model to predict survival in primary myelofibrosis: a study by the IWG-MRT (International Working Group for Myeloproliferative Neoplasms Research and Treatment). *Blood* **115**, 1703–1708 (2010).
  112. Gangat, N. *et al.* DIPSS Plus: A Refined Dynamic International Prognostic Scoring System for Primary Myelofibrosis That Incorporates Prognostic Information From Karyotype, Platelet Count, and Transfusion Status. *J. Clin. Oncol.* **29**, 392–397 (2011).
  113. Tefferi, A. *et al.* Application of current prognostic models for primary myelofibrosis in the setting of post-polycythemia vera or post-essential thrombocythemia myelofibrosis. *Leukemia* **31**, 2851–2852 (2017).
  114. Guglielmelli, P. *et al.* MIPSS70: Mutation-Enhanced International Prognostic Score System for Transplantation-Age Patients With Primary Myelofibrosis. *J. Clin. Oncol.* **36**, 310–318 (2018).
  115. Tefferi, A. *et al.* MIPSS70+ Version 2.0: Mutation and Karyotype-Enhanced International Prognostic Scoring System for Primary Myelofibrosis. *J. Clin. Oncol.* **36**, 1769–1770 (2018).
  116. Tefferi, A. *et al.* GIPSS: genetically inspired prognostic scoring system for primary myelofibrosis. *Leukemia* **32**, 1631–1642 (2018).
-

117. Tefferi, A. How I treat myelofibrosis. *Blood* **117**, 3494–3504 (2011).
118. Malato, A., Rossi, E., Tiribelli, M., Mendicino, F. & Pugliese, N. Splenectomy in Myelofibrosis: Indications, Efficacy, and Complications. *Clin. Lymphoma Myeloma Leuk.* **20**, 588–595 (2020).
119. McLornan, D. P. *et al.* State-of-the-art review: allogeneic stem cell transplantation for myelofibrosis in 2019. *Haematologica* **104**, 659–668 (2019).
120. Wilks, A. F. Two putative protein-tyrosine kinases identified by application of the polymerase chain reaction. *Proc. Natl. Acad. Sci.* **86**, 1603–1607 (1989).
121. Wilks, A. F. *et al.* Two novel protein-tyrosine kinases, each with a second phosphotransferase-related catalytic domain, define a new class of protein kinase. *Mol. Cell. Biol.* **11**, 2057–2065 (1991).
122. Ferrao, R. & Lupardus, P. J. The Janus Kinase (JAK) FERM and SH2 Domains: Bringing Specificity to JAK–Receptor Interactions. *Front. Endocrinol. (Lausanne)*. **8**, (2017).
123. Gupta, S. *et al.* The SH2 domains of Stat1 and Stat2 mediate multiple interactions in the transduction of IFN-alpha signals. *EMBO J.* **15**, 1075–84 (1996).
124. Feener, E. P., Rosario, F., Dunn, S. L., Stancheva, Z. & Myers, M. G. Tyrosine Phosphorylation of Jak2 in the JH2 Domain Inhibits Cytokine Signaling. *Mol. Cell. Biol.* **24**, 4968–4978 (2004).
125. Schwartz, D. M., Bonelli, M., Gadina, M. & O’Shea, J. J. Type I/II cytokines, JAKs, and new strategies for treating autoimmune diseases. *Nat. Rev. Rheumatol.* **12**, 25–36 (2016).
126. Wells, J. A. Binding in the growth hormone receptor complex. *Proc. Natl. Acad. Sci.* **93**, 1–6 (1996).
127. Gent, J., van Kerkhof, P., Roza, M., Bu, G. & Strous, G. J. Ligand-independent growth hormone receptor dimerization occurs in the endoplasmic reticulum and is required for ubiquitin system-dependent endocytosis. *Proc. Natl. Acad. Sci.* **99**, 9858–9863 (2002).
128. Kubatzky, K. F. *et al.* Self assembly of the transmembrane domain promotes signal transduction through the erythropoietin receptor. *Curr. Biol.* **11**, 110–115 (2001).
129. Matthews, E. E. *et al.* Thrombopoietin receptor activation: transmembrane helix dimerization, rotation, and allosteric modulation. *FASEB J.* **25**, 2234–2244 (2011).
130. Brooks, A. J. *et al.* Mechanism of Activation of Protein Kinase JAK2 by the Growth Hormone Receptor. *Science (80-. )*. **344**, (2014).
131. Chen, E. & Mullally, A. How does JAK2V617F contribute to the pathogenesis of myeloproliferative neoplasms? *Hematology* **2014**, 268–276 (2014).
132. Gou, P., Zhang, W. & Giraudier, S. Insights into the Potential Mechanisms of

- JAK2V617F Somatic Mutation Contributing Distinct Phenotypes in Myeloproliferative Neoplasms. *Int. J. Mol. Sci.* **23**, 1013 (2022).
133. Neubauer, H. *et al.* Jak2 Deficiency Defines an Essential Developmental Checkpoint in Definitive Hematopoiesis. *Cell* **93**, 397–409 (1998).
  134. Akada, H. *et al.* Critical Role of Jak2 in the Maintenance and Function of Adult Hematopoietic Stem Cells. *Stem Cells* **32**, 1878–1889 (2014).
  135. Hennighausen, L. & Robinson, G. W. Interpretation of cytokine signaling through the transcription factors STAT5A and STAT5B. *Genes Dev.* **22**, 711–721 (2008).
  136. Pallard, C. *et al.* Interleukin-3, Erythropoietin, and Prolactin Activate a STAT5-like Factor in Lymphoid Cells. *J. Biol. Chem.* **270**, 15942–15945 (1995).
  137. Socolovsky, M. *et al.* Ineffective erythropoiesis in Stat5a<sup>-/-</sup>5b<sup>-/-</sup> mice due to decreased survival of early erythroblasts. *Blood* **98**, 3261–3273 (2001).
  138. Yan, D., Hutchison, R. E. & Mohi, G. Critical requirement for Stat5 in a mouse model of polycythemia vera. *Blood* **119**, 3539–3549 (2012).
  139. Pallard, C. *et al.* Thrombopoietin activates a STAT5-like factor in hematopoietic cells. *EMBO J.* **14**, 2847–2856 (1995).
  140. Ryan, J. J. *et al.* Stem cell factor activates STAT-5 DNA binding in IL-3-derived bone marrow mast cells. *Exp. Hematol.* **25**, 357–62 (1997).
  141. Hoelbl, A. *et al.* Clarifying the role of Stat5 in lymphoid development and Abelson-induced transformation. *Blood* **107**, 4898–4906 (2006).
  142. Kimura, A. *et al.* The transcription factors STAT5A/B regulate GM-CSF-mediated granulopoiesis. *Blood* **114**, 4721–4728 (2009).
  143. Zou, S. *et al.* Targeting STAT3 in Cancer Immunotherapy. *Mol. Cancer* **19**, 145 (2020).
  144. Johnson, D. E., O’Keefe, R. A. & Grandis, J. R. Targeting the IL-6/JAK/STAT3 signalling axis in cancer. *Nat. Rev. Clin. Oncol.* **15**, 234–248 (2018).
  145. Duarte, R. F. & Frank, D. A. SCF and G-CSF lead to the synergistic induction of proliferation and gene expression through complementary signaling pathways. *Blood* **96**, 3422–3430 (2000).
  146. Takeda, K. *et al.* Targeted disruption of the mouse Stat3 gene leads to early embryonic lethality. *Proc. Natl. Acad. Sci.* **94**, 3801–3804 (1997).
  147. Fornek, J. L. *et al.* Critical role for Stat3 in T-dependent terminal differentiation of IgG B cells. *Blood* **107**, 1085–1091 (2006).
  148. Mantel, C. *et al.* Mouse hematopoietic cell-targeted STAT3 deletion: stem/progenitor cell defects, mitochondrial dysfunction, ROS overproduction, and a rapid aging-like phenotype. *Blood* **120**, 2589–2599 (2012).
-

149. Jenkins, B. J., Roberts, A. W., Najdovska, M., Grail, D. & Ernst, M. The threshold of gp130-dependent STAT3 signaling is critical for normal regulation of hematopoiesis. *Blood* **105**, 3512–3520 (2005).
150. Yu, H., Pardoll, D. & Jove, R. STATs in cancer inflammation and immunity: a leading role for STAT3. *Nat. Rev. Cancer* **9**, 798–809 (2009).
151. McFarland, B. C. *et al.* NF- $\kappa$ B-Induced IL-6 Ensures STAT3 Activation and Tumor Aggressiveness in Glioblastoma. *PLoS One* **8**, e78728 (2013).
152. Lee, H. *et al.* Persistently Activated Stat3 Maintains Constitutive NF- $\kappa$ B Activity in Tumors. *Cancer Cell* **15**, 283–293 (2009).
153. Chin, Y. E. *et al.* Cell Growth Arrest and Induction of Cyclin-Dependent Kinase Inhibitor p21 WAF1/CIP1 Mediated by STAT1. *Science (80-. )*. **272**, 719–722 (1996).
154. Zhang, Y. & Liu, Z. STAT1 in cancer: friend or foe? *Discov. Med.* **24**, 19–29 (2017).
155. Huang, Z. *et al.* STAT1 promotes megakaryopoiesis downstream of GATA-1 in mice. *J. Clin. Invest.* **117**, 3890–3899 (2007).
156. Chen, E. *et al.* Distinct Clinical Phenotypes Associated with JAK2V617F Reflect Differential STAT1 Signaling. *Cancer Cell* **18**, 524–535 (2010).
157. Levine, R. L. *et al.* Activating mutation in the tyrosine kinase JAK2 in polycythemia vera, essential thrombocythemia, and myeloid metaplasia with myelofibrosis. *Cancer Cell* **7**, 387–397 (2005).
158. Baxter, E. J. *et al.* Acquired mutation of the tyrosine kinase JAK2 in human myeloproliferative disorders. *Lancet* **365**, 1054–1061 (2005).
159. James, C. *et al.* A unique clonal JAK2 mutation leading to constitutive signalling causes polycythaemia vera. *Nature* **434**, 1144–1148 (2005).
160. Kralovics, R. *et al.* A Gain-of-Function Mutation of JAK2 in Myeloproliferative Disorders. *N. Engl. J. Med.* **352**, 1779–1790 (2005).
161. Zhao, R. *et al.* Identification of an Acquired JAK2 Mutation in Polycythemia Vera. *J. Biol. Chem.* **280**, 22788–22792 (2005).
162. Lu, X. *et al.* Expression of a homodimeric type I cytokine receptor is required for JAK2V617F-mediated transformation. *Proc. Natl. Acad. Sci.* **102**, 18962–18967 (2005).
163. Akada, H. *et al.* Conditional expression of heterozygous or homozygous Jak2V617F from its endogenous promoter induces a polycythemia vera-like disease. *Blood* **115**, 3589–3597 (2010).
164. Bumm, T. G. P. *et al.* Characterization of Murine JAK2V617F-Positive Myeloproliferative Disease. *Cancer Res.* **66**, 11156–11165 (2006).

165. Wernig, G. *et al.* Expression of Jak2V617F causes a polycythemia vera–like disease with associated myelofibrosis in a murine bone marrow transplant model. *Blood* **107**, 4274–4281 (2006).
166. Zaleskas, V. M. *et al.* Molecular Pathogenesis and Therapy of Polycythemia Induced in Mice by JAK2 V617F. *PLoS One* **1**, e18 (2006).
167. Cheon, D.-J. & Orsulic, S. Mouse Models of Cancer. *Annu. Rev. Pathol. Mech. Dis.* **6**, 95–119 (2011).
168. Mullally, A. *et al.* Physiological Jak2V617F Expression Causes a Lethal Myeloproliferative Neoplasm with Differential Effects on Hematopoietic Stem and Progenitor Cells. *Cancer Cell* **17**, 584–596 (2010).
169. Marty, C. *et al.* Myeloproliferative neoplasm induced by constitutive expression of JAK2V617F in knock-in mice. *Blood* **116**, 783–787 (2010).
170. Borges, W. H., Wald, N. & Hoffman, E. Inherited cytogenetic mosaicism in man. *J. Pediatr.* **65**, 103 (1964).
171. Kiosoglou, K., Mitus, W. J. & Dameshek, W. Chromosomal Aberrations in Acute Leukemia. *Blood* **26**, 610–641 (1965).
172. Kay, H. E. M., Lawler, S. D. & Millard, R. E. The Chromosomes in Polycythaemia Vera. *Br. J. Haematol.* **12**, 507–527 (1966).
173. GOODMAN, R. M., BOURONCLE, B. A., MILLER, F. & NORTH, C. Unusual Chromosomal Findings in a Case of Myelofibrosis. *J. Hered.* **59**, 348–350 (1968).
174. Diez-Martin, J. L., Graham, D. L., Pettitt, R. M. & Dewald, G. W. Chromosome Studies in 104 Patients With Polycythemia Vera. *Mayo Clin. Proc.* **66**, 287–299 (1991).
175. Rege-Cambrin, G. *et al.* A chromosomal profile of polycythemia vera. *Cancer Genet. Cytogenet.* **25**, 233–245 (1987).
176. Demory, J. *et al.* Cytogenetic studies and their prognostic significance in agnogenic myeloid metaplasia: a report on 47 cases. *Blood* **72**, 855–859 (1988).
177. Huh, J. *et al.* Characterization of chromosome arm 20q abnormalities in myeloid malignancies using genome-wide single nucleotide polymorphism array analysis. *Genes, Chromosom. Cancer* NA-NA (2010) doi:10.1002/gcc.20748.
178. Yin, C. C. *et al.* Del(20q) in patients with chronic lymphocytic leukemia: a therapy-related abnormality involving lymphoid or myeloid cells. *Mod. Pathol.* **28**, 1130–1137 (2015).
179. Yin, C. C. *et al.* Clinical significance of newly emerged isolated del(20q) in patients following cytotoxic therapies. *Mod. Pathol.* **28**, 1014–1022 (2015).
180. Machiela, M. J. *et al.* Mosaic chromosome 20q deletions are more frequent in the aging population. *Blood Adv.* **1**, 380–385 (2017).



181. Ravindran, A. *et al.* The significance of genetic mutations and their prognostic impact on patients with incidental finding of isolated del(20q) in bone marrow without morphologic evidence of a myeloid neoplasm. *Blood Cancer J.* **10**, 7 (2020).
182. Hodgson, J. G., Chin, K., Collins, C. & Gray, J. W. Genome Amplification of Chromosome 20 in Breast Cancer. *Breast Cancer Res. Treat.* **78**, 337–345 (2003).
183. Haase, D. *et al.* New insights into the prognostic impact of the karyotype in MDS and correlation with subtypes: evidence from a core dataset of 2124 patients. *Blood* **110**, 4385–4395 (2007).
184. Braun, T. *et al.* Characteristics and outcome of myelodysplastic syndromes (MDS) with isolated 20q deletion: A report on 62 cases. *Leuk. Res.* **35**, 863–867 (2011).
185. Hussein, K., Van Dyke, D. L. & Tefferi, A. Conventional cytogenetics in myelofibrosis: literature review and discussion. *Eur. J. Haematol.* **82**, 329–338 (2009).
186. Tang, G. *et al.* Characteristics and clinical significance of cytogenetic abnormalities in polycythemia vera. *Haematologica* **102**, 1511–1518 (2017).
187. Wang, J. *et al.* Loss of Asx11 leads to myelodysplastic syndrome–like disease in mice. *Blood* **123**, 541–553 (2014).
188. Martín, I. *et al.* Myelodysplastic syndromes with 20q deletion: incidence, prognostic value and impact on response to azacitidine of ASXL1 chromosomal deletion and genetic mutations. *Br. J. Haematol.* **194**, 708–717 (2021).
189. Shiseki, M. *et al.* Reduced PLCG1 expression is associated with inferior survival for myelodysplastic syndromes. *Cancer Med.* **9**, 460–468 (2020).
190. Perna, F. *et al.* Depletion of L3MBTL1 promotes the erythroid differentiation of human hematopoietic progenitor cells: possible role in 20q– polycythemia vera. *Blood* **116**, 2812–2821 (2010).
191. Aziz, A. *et al.* Cooperativity of imprinted genes inactivated by acquired chromosome 20q deletions. *J. Clin. Invest.* **123**, 2169–2182 (2013).
192. Heinrichs, S. *et al.* MYBL2 is a sub-haploinsufficient tumor suppressor gene in myeloid malignancy. *Elife* **2**, (2013).
193. Jobe, F. *et al.* Deletion of Ptpn1 induces myeloproliferative neoplasm. *Leukemia* **31**, 1229–1234 (2017).
194. Villamar-Cruz, O., Loza-Mejía, M. A., Arias-Romero, L. E. & Camacho-Arroyo, I. Recent advances in PTP1B signaling in metabolism and cancer. *Biosci. Rep.* **41**, (2021).
195. Goldstein, B. J., Bittner-Kowalczyk, A., White, M. F. & Harbeck, M. Tyrosine Dephosphorylation and Deactivation of Insulin Receptor Substrate-1 by Protein-

- tyrosine Phosphatase 1B. *J. Biol. Chem.* **275**, 4283–4289 (2000).
196. Liu, F., Hill, D. E. & Chernoff, J. Direct Binding of the Proline-rich Region of Protein Tyrosine Phosphatase 1B to the Src Homology 3 Domain of p130Cas. *J. Biol. Chem.* **271**, 31290–31295 (1996).
  197. Bjorge, J. D., Pang, A. & Fujita, D. J. Identification of Protein-tyrosine Phosphatase 1B as the Major Tyrosine Phosphatase Activity Capable of Dephosphorylating and Activating c-Src in Several Human Breast Cancer Cell Lines. *J. Biol. Chem.* **275**, 41439–41446 (2000).
  198. Byon, J. C. H., Kusari, A. B. & Kusari, J. Protein-tyrosine phosphatase-1B acts as a negative regulator of insulin signal transduction. *Mol. Cell. Biochem.* **182**, 101–108 (1998).
  199. Myers, M. P. *et al.* TYK2 and JAK2 Are Substrates of Protein-tyrosine Phosphatase 1B. *J. Biol. Chem.* **276**, 47771–47774 (2001).
  200. Salmeen, A., Andersen, J. N., Myers, M. P., Tonks, N. K. & Barford, D. Molecular Basis for the Dephosphorylation of the Activation Segment of the Insulin Receptor by Protein Tyrosine Phosphatase 1B. *Mol. Cell* **6**, 1401–1412 (2000).
  201. Jia, Z., Barford, D., Flint, A. J. & Tonks, N. K. Structural Basis for Phosphotyrosine Peptide Recognition by Protein Tyrosine Phosphatase 1B. *Science (80- )*. **268**, 1754–1758 (1995).
  202. Meng, T.-C., Fukada, T. & Tonks, N. K. Reversible Oxidation and Inactivation of Protein Tyrosine Phosphatases In Vivo. *Mol. Cell* **9**, 387–399 (2002).
  203. Chen, Y.-Y., Huang, Y.-F., Khoo, K.-H. & Meng, T.-C. Mass spectrometry-based analyses for identifying and characterizing S-nitrosylation of protein tyrosine phosphatases. *Methods* **42**, 243–249 (2007).
  204. Krishnan, N., Fu, C., Pappin, D. J. & Tonks, N. K. H<sub>2</sub>S-Induced Sulfhydration of the Phosphatase PTP1B and Its Role in the Endoplasmic Reticulum Stress Response. *Sci. Signal.* **4**, (2011).
  205. Barrett, W. C. *et al.* Regulation of PTP1B via Glutathionylation of the Active Site Cysteine 215. *Biochemistry* **38**, 6699–6705 (1999).
  206. Flint, A. J., Tiganis, T., Barford, D. & Tonks, N. K. Development of “substrate-trapping” mutants to identify physiological substrates of protein tyrosine phosphatases. *Proc. Natl. Acad. Sci.* **94**, 1680–1685 (1997).
  207. Zhang, Y.-L. *et al.* Thermodynamic Study of Ligand Binding to Protein-tyrosine Phosphatase 1B and Its Substrate-trapping Mutants. *J. Biol. Chem.* **275**, 34205–34212 (2000).
  208. Cantley, L. C. *et al.* Vanadate is a potent (Na,K)-ATPase inhibitor found in ATP derived from muscle. *J. Biol. Chem.* **252**, 7421–7423 (1977).
-

209. Przyborowski, L., Schwarzenbach, G. & Zimmermann, T. Komplexe XXXVII. Die EDTA-Komplexe des Vanadiums(V). *Helv. Chim. Acta* **48**, 1556–1565 (1965).
210. Huyer, G. *et al.* Mechanism of Inhibition of Protein-tyrosine Phosphatases by Vanadate and Pervanadate. *J. Biol. Chem.* **272**, 843–851 (1997).
211. Dadke, S. *et al.* Regulation of protein tyrosine phosphatase 1B by sumoylation. *Nat. Cell Biol.* **9**, 80–85 (2007).
212. Yip, S.-C., Cotteret, S. & Chernoff, J. Sumoylated protein tyrosine phosphatase 1B localizes to the inner nuclear membrane and regulates the tyrosine phosphorylation of emerin. *J. Cell Sci.* **125**, 310–316 (2012).
213. Bandyopadhyay, D. *et al.* Protein-Tyrosine Phosphatase 1B Complexes with the Insulin Receptor in Vivo and Is Tyrosine-phosphorylated in the Presence of Insulin. *J. Biol. Chem.* **272**, 1639–1645 (1997).
214. Ravichandran, L. V., Chen, H., Li, Y. & Quon, M. J. Phosphorylation of PTP1B at Ser 50 by Akt Impairs Its Ability to Dephosphorylate the Insulin Receptor. *Mol. Endocrinol.* **15**, 1768–1780 (2001).
215. Frangioni, J. V., Oda, A., Smith, M., Salzman, E. W. & Neel, B. G. Calpain-catalyzed cleavage and subcellular relocation of protein phosphotyrosine phosphatase 1B (PTP-1B) in human platelets. *EMBO J.* **12**, 4843–4856 (1993).
216. Gulati, P., Markova, B., Göttlicher, M., Böhmer, F. & Herrlich, P. A. UVA inactivates protein tyrosine phosphatases by calpain-mediated degradation. *EMBO Rep.* **5**, 812–817 (2004).
217. Trümpler, A., Schlott, B., Herrlich, P., Greer, P. A. & Böhmer, F.-D. Calpain-mediated degradation of reversibly oxidized protein-tyrosine phosphatase 1B. *FEBS J.* **276**, 5622–5633 (2009).
218. Fukada, T. & Tonks, N. K. The Reciprocal Role of Egr-1 and Sp Family Proteins in Regulation of the PTP1B Promoter in Response to the p210 Bcr-Abl Oncoprotein-tyrosine Kinase. *J. Biol. Chem.* **276**, 25512–25519 (2001).
219. Wang, S., Cheng, Z., Chen, X. & Xue, H. microRNA-135a protects against myocardial ischemia-reperfusion injury in rats by targeting protein tyrosine phosphatase 1B. *J. Cell. Biochem.* **120**, 10421–10433 (2019).
220. Yang, Q., Zhang, L., Zhong, Y., Lai, L. & Li, X. miR-206 inhibits cell proliferation, invasion, and migration by down-regulating PTP1B in hepatocellular carcinoma. *Biosci. Rep.* **39**, (2019).
221. Xu, J., Zhang, Z., Chen, Q., Yang, L. & Yin, J. miR-146b Regulates Cell Proliferation and Apoptosis in Gastric Cancer by Targeting PTP1B. *Dig. Dis. Sci.* **65**, 457–463 (2020).
222. Elchebly, M. *et al.* Increased Insulin Sensitivity and Obesity Resistance in Mice

- Lacking the Protein Tyrosine Phosphatase-1B Gene. *Science* (80-. ). **283**, 1544–1548 (1999).
223. Cheng, A. *et al.* Attenuation of Leptin Action and Regulation of Obesity by Protein Tyrosine Phosphatase 1B. *Dev. Cell* **2**, 497–503 (2002).
224. Liu, J., Yang, X., Yu, S. & Zheng, R. The Leptin Signaling. in 123–144 (2018). doi:10.1007/978-981-13-1286-1\_7.
225. Wiener, J. R. *et al.* Overexpression of the Protein Tyrosine Phosphatase PTP1B in Human Breast Cancer: Association With p185c-erbB-2 Protein Expression. *JNCI J. Natl. Cancer Inst.* **86**, 372–378 (1994).
226. Bentires-Alj, M. & Neel, B. G. Protein-Tyrosine Phosphatase 1B Is Required for HER2/ Neu –Induced Breast Cancer. *Cancer Res.* **67**, 2420–2424 (2007).
227. Liu, H. *et al.* PTP1B promotes cell proliferation and metastasis through activating src and ERK1/2 in non-small cell lung cancer. *Cancer Lett.* **359**, 218–225 (2015).
228. Wang, Q., Pan, Y., Zhao, L., Qi, F. & Liu, J. Protein tyrosine phosphatase 1B(PTP1B) promotes melanoma cells progression through Src activation. *Bioengineered* **12**, 8396–8406 (2021).
229. LaMontagne, K. R., Flint, A. J., Franza, B. R., Pendergast, A. M. & Tonks, N. K. Protein Tyrosine Phosphatase 1B Antagonizes Signalling by Oncoprotein Tyrosine Kinase p210 bcr-abl In Vivo. *Mol. Cell. Biol.* **18**, 2965–2975 (1998).
230. Mei, W., Wang, K., Huang, J. & Zheng, X. Cell Transformation by PTP1B Truncated Mutants Found in Human Colon and Thyroid Tumors. *PLoS One* **11**, e0166538 (2016).

## CHAPTER II

# **PTPN1 deficiency accelerates the progression of Jak2V617F-induced myeloproliferative neoplasms**

Bao T. Le, Yue Yang, Fatoumata Jobe, & Golam Mohi

## 2.1 – Introduction

The deletion of the long arm of chromosome 20 (del20q) is a frequent karyotypic abnormality observed in myeloid malignancies including myeloproliferative neoplasms (MPN), myelodysplastic syndrome (MDS), MDS/MPN overlap disorder, and acute myeloid leukemia (AML). The del20q abnormality is more commonly observed in MPNs, particularly myelofibrosis (MF), compared to other myeloid malignancies<sup>1</sup>. Polycythemia vera (PV) and myelofibrosis (MF) are subsets of MPN. While PV is defined by excessive production of RBCs, MF is characterized by scarring of the hematopoietic tissue and frequent accompanying megakaryocytosis<sup>2</sup>. With proper management PV patients can maintain a decent quality of life; however, disease progression to myelofibrosis can adversely affect the patient's quality of life and survival<sup>3,4</sup>. Furthermore, PV patients exhibit an elevated frequency of disease progression and poorer survival in the presence of del20q<sup>5</sup>. Del20q is detected in ~20% of MF patients and it is the most frequent karyotypic aberration observed in these patients<sup>6</sup>. With the potential risks of disease progression, further investigation into the role of del20q in this context is needed. However, the identity of the tumor suppressor gene(s) associated with del20q remains elusive, as does the reason for the disproportional MPN bias.

The JAK2V617F mutation is the most common somatic mutation identified in MPN patients, with a prevalence of approximately 97% in PV and 50-60% in ET and MF<sup>7,8</sup>. Murine studies have demonstrated that heterozygous JAK2V617F mutation can induce PV-like disease<sup>9</sup>. Furthermore, an increased JAK2V617F burden is positively correlated with disease severity and progression<sup>10</sup>. In addition, perturbation of gene

expression can modulate disease severity, as seen with AXL<sup>11</sup>, GATA1<sup>12</sup>, and HMGA2<sup>13</sup>. The del20q abnormality is frequently observed in association with the JAK2V617F mutation in MF<sup>14</sup>. Clonal analysis indicates that del20q can confer a growth advantage to hematopoietic cells<sup>15</sup>.

The deleted segments in del20q can vary between patients, and the deletion can range between 20q12-q13.2<sup>16,17</sup>. The gene encoding protein tyrosine phosphatase non-receptor 1 (*PTPN1*) lies within 20q13.1. In a previous study, our lab demonstrated that genetic ablation of PTPN1 can result in a protracted development of MPN-like phenotype in mice<sup>14</sup>. The function of PTPN1 remains of great interest as it has been shown to directly modulate the JAK/STAT signaling pathway<sup>18</sup>. The effects of PTPN1 deficiency in the context of JAK2V617F mutation have not been explored, which places great emphasis on understanding how PTPN1 deficiency resulting from opportunistic loss of chromosome 20q is translated in the context of JAK2V617F-induced pathogenicity and its disease progression.

We hypothesize that the loss of PTPN1 cooperates with JAK2V617F in clonal expansion and progression of MPN. In this study, we investigated the effects of concurrent deletion of PTPN1 and expression of JAK2V617F on the disease burden in mice's hematopoietic compartment. We found that concurrent heterozygous deletion of PTPN1 and expression of heterozygous JAK2V617F mutation in mice's hematopoietic compartment resulted in significantly increased leukocyte and platelet counts in peripheral blood, expansion of hematopoietic stem/progenitor cells, granulocytes, and megakaryocytes, as well as a significantly larger spleen size compared to JAK2V617F expression or PTPN1 deletion alone. We also observed a gradual reduction of RBC

counts along with increased expression of inflammatory cytokines and accumulation of reticulin fibrosis in the bone marrow (BM) and spleens of PTPN1-deficient JAK2V617F mice. Additionally, we determined that the phenotypes observed in PTPN1-deficient JAK2V617F mice are cell-intrinsic, and that PTPN1 deficiency confers significant clonal advantages to hematopoietic stem/progenitors cells of JAK2V617F mice. Homozygous deletion of PTPN1 in the context of JAK2V617F resulted in a more severe phenotype and faster progression to myelofibrosis. Together, our results suggest that deficiency of PTPN1 synergizes with JAK2V617F mutation in clonal expansion and progression of myelofibrosis.

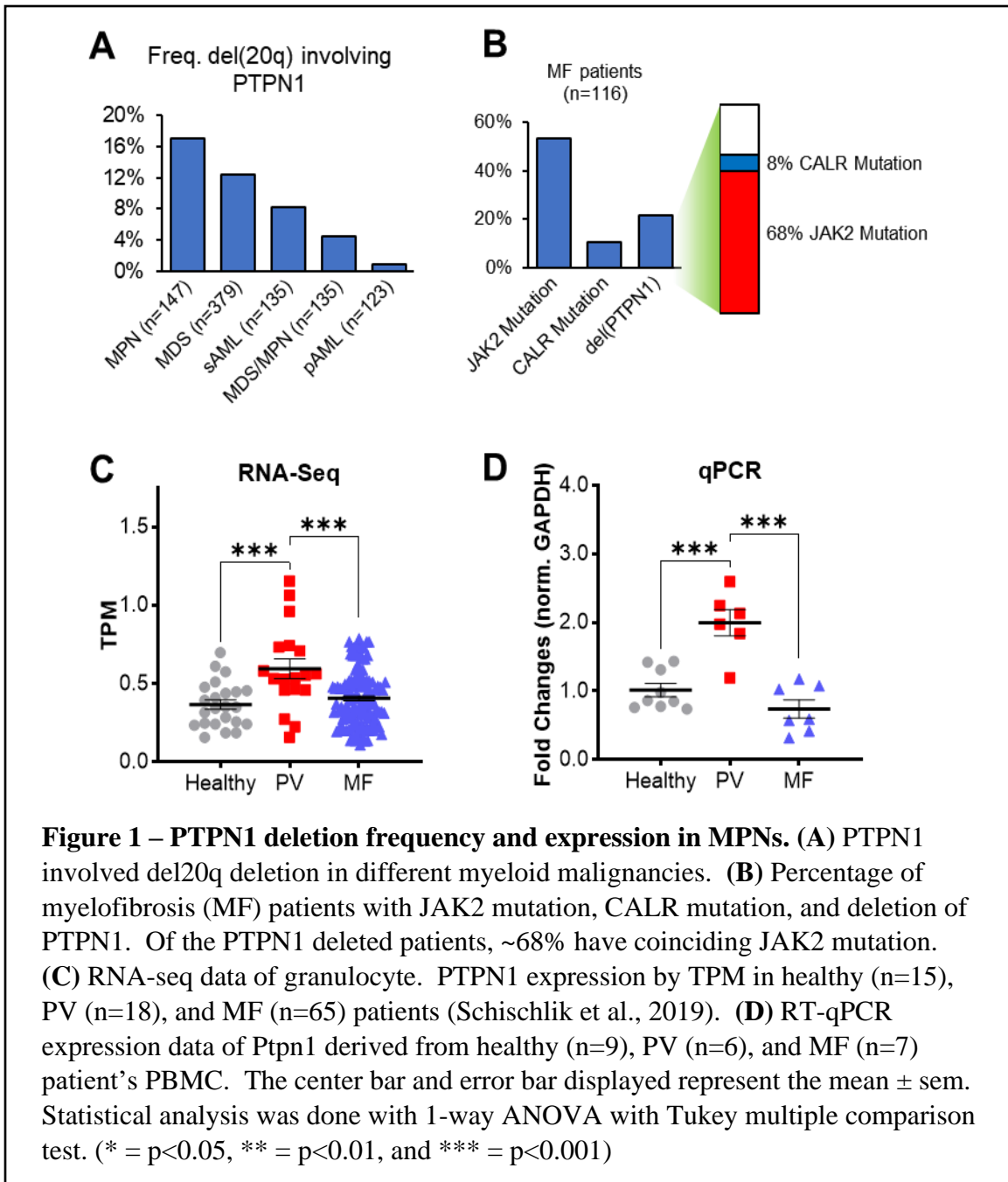


## 2.2 – Results

### **Deletion of PTPN1 in del20q is frequently observed with JAK2 mutation.**

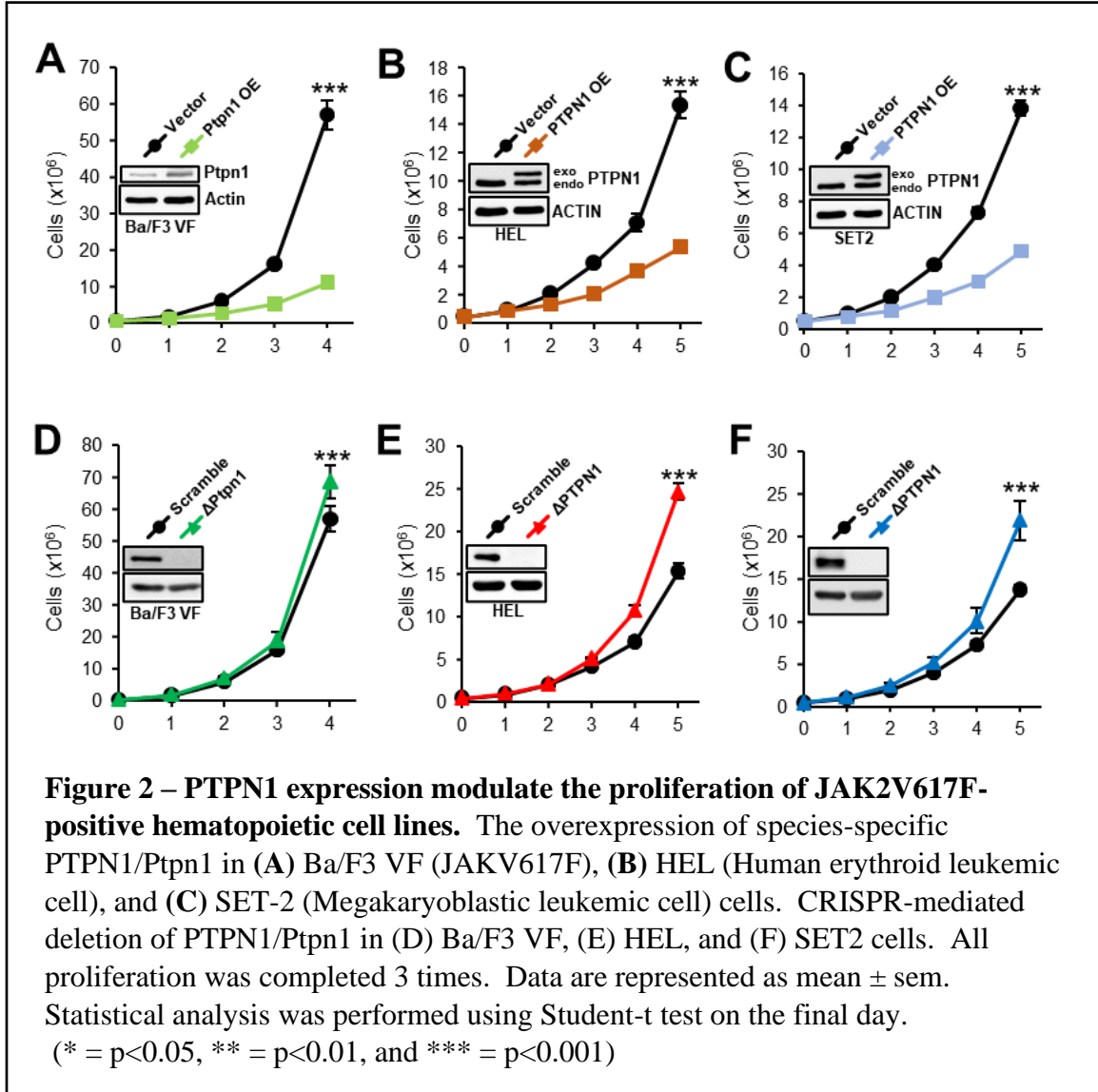
In collaboration with Mayo Clinic to ascertain clinical data<sup>14</sup>, we observed that myeloproliferative neoplasms (MPN) have the highest frequency of del20q involving PTPN1 deletion (Figure 1A). In the context of myelofibrosis (MF), JAK2 mutation, CALR mutation, and del(PTPN1) are observed at a frequency of approximately 50%, 10%, and 20%, respectively (Figure 1B). These data aligned with the current observations in other studies<sup>1,7,8</sup>. Moreover, among the ~20% of MF patients with del20q involving PTPN1 deletion, 68% also carry the JAK2V617F mutation.

We also examined the expression level of PTPN1 in MPN patients. Analysis of publicly available RNA-seq data<sup>19</sup> from 15 healthy individuals, 18 PV patients, and 65 MF patients showed a significant elevation of PTPN1 expression in PV that is drastically reduced in MF (Figure 1C). To validate this assessment, we examine the mRNA expression of PTPN1 by RT-qPCR in our small cohort of patient PBMC samples (9 healthy, 6 PV, and 7 MF) and obtained similar findings (Figure 1D). These expression data are irrespective of the presence of del20q.



**PTPN1 expression modulates the proliferation of JAK2V617F-positive hematopoietic cell lines.**

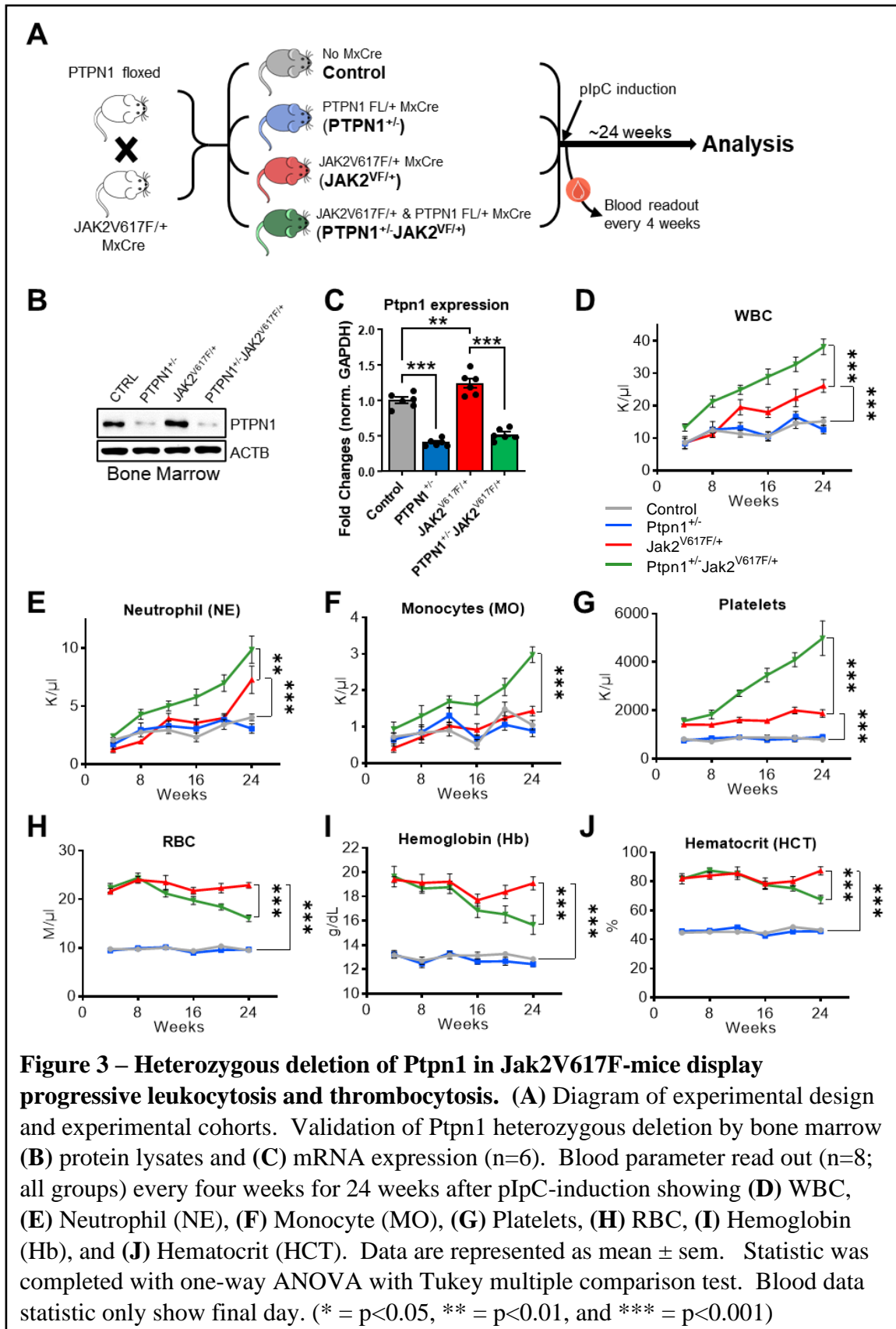
We first aimed to investigate the impact of PTPN1 expression on proliferation in JAK2V617F mutation-positive hematopoietic cells. To achieve this, we overexpressed mouse Ptpn1 in Ba/F3 VF (EpoR JAK2V617F), as well as human PTPN1 in HEL (human erythroid leukemic cell) and SET-2 (Human megakaryoblastic leukemic cells) cells. The overexpression of PTPN1 resulted in a marked reduction in the proliferation of all three hematopoietic cell lines, as shown in Figure 2A-C. To assess if the opposite effect is observed when PTPN1 expression is low, we established stable PTPN1-deleted clones of the respective cells using CRISPR/Cas9. The proliferation of all three cells - Ba/F3 VF, HEL, and SET2 - showed a significant increase in comparison to their native counterparts, as shown in Figure 2D-F. These results indicate the significant impact of PTPN1 expression on the cellular proliferation of JAK2V617F-positive hematopoietic cells.



## **Heterozygous deletion of PTPN1 in JAK2<sup>V617F</sup>-mice displays progressive leukocytosis and thrombocytosis.**

To assess the phenotypic properties of Ptpn1 deletion, we established a conditional Jak2<sup>V617F</sup> knock-in and Ptpn1 deletion mouse model. The mouse was generated by crossing Mx1-Cre mouse, Jak2<sup>V617F</sup> knock-in mouse, and Ptpn1 floxed mouse, resulting in four experimental cohorts: control (No Mx1-cre), Ptpn1<sup>+/-</sup> (induced Ptpn1<sup>FL/+</sup>; Mx1-Cre), Jak2<sup>V617F/+</sup> only (induced Jak2<sup>V617F/+</sup> knock-in; Mx1-Cre), and Ptpn1<sup>+/-</sup>Jak2<sup>VE/+</sup> (induced Jak2<sup>V617F/+</sup> knock-in; Ptpn1<sup>FL/+</sup>; Mx1-Cre). After induction, blood parameters of the experimental cohorts were assessed every four weeks for 24 weeks, and terminal analyses were performed shortly after (Figure 3A). The Ptpn1 heterozygous deletion was validated through bone marrow protein lysates and mRNA expression analysis (Figure 3B-C).

In the 24 weeks of observation, Ptpn1<sup>+/-</sup> mice did not exhibit any discernable phenotypic changes compared to the control mice. On the other hand, Ptpn1<sup>+/-</sup>Jak2<sup>V617F/+</sup> mice showed a significant increase in white blood cells (WBC) compared to Jak2<sup>V617F/+</sup> alone (Figure 3D). This increase also includes the myeloid subset of WBC, neutrophils (NE), and monocytes (MO) (Figure 3E-F). Interestingly, while Jak2<sup>V617F/+</sup> displays a static increase in platelets, Ptpn1<sup>+/-</sup> Jak2<sup>V617F/+</sup> mice show a drastic and progressive increase in platelets (Figure 3G). Jak2<sup>V617F/+</sup> mice have been previously established to exhibit PV-like disease with a marked increase of red-blood cell (RBC), hematocrit (HCT), and hemoglobin (Hb). However, when Ptpn1 is deficient, there is a progressive reduction in RBC, HCT, and Hb (Figure 3H-J).



### **Ptpn1-deficient Jak2<sup>V617F/+</sup> mice exhibit greater disease burden and poor survival.**

Following our experimental cohort for 32 weeks, it became apparent that Ptpn1<sup>+/-</sup> Jak2<sup>V617F/+</sup> mice exhibited significantly inferior survival compared to Jak2<sup>V617F/+</sup> mice alone, while Ptpn1<sup>+/-</sup> only mice showed no sign of distress or morbidity (Figure 4A). Gross examination of the mice revealed marked splenomegaly in Ptpn1<sup>+/-</sup> Jak2<sup>V617F/+</sup> mice, which was greater than Jak2<sup>V617F/+</sup> mice alone. This splenic increase was observed both in size and mass (Figure 4B-C). Analysis of the peripheral blood serum by ELISA showed an increase in proinflammatory cytokines, Il1b, Il6, and Tgfb in Jak2<sup>V617F/+</sup> mice, which was further elevated when Ptpn1 expression is reduced (Figure 4D-F). Despite the significant increase in platelet abundance observed in the peripheral blood, we assessed the serum concentration of thrombopoietin (Tpo) and observed no aberrant increase but rather an expected decrease (Figure 4G). The concentration of Tpo is inversely proportional to the abundance of platelets because it is consumed upon binding to MPL<sup>20</sup>.

Histological examination of mouse's bone marrow (BM) and spleen by reticulin staining showed a remarkable accumulation of fibrosis in Ptpn1<sup>+/-</sup> Jak2<sup>V617F/+</sup> mice, which was completely absent in the control, Ptpn1<sup>+/-</sup>, or Jak2<sup>V617F/+</sup> mice at similar age (Figure 5A). Furthermore, hematoxylin and eosin-stained (H&E) BM and spleen showed numerous megakaryocytes (MK) clusters in both tissues (Figure 5B). Taken together, these findings suggest that Ptpn1<sup>+/-</sup> Jak2<sup>V617F/+</sup> mice exhibit a significantly greater disease burden with faster progression to myelofibrosis.

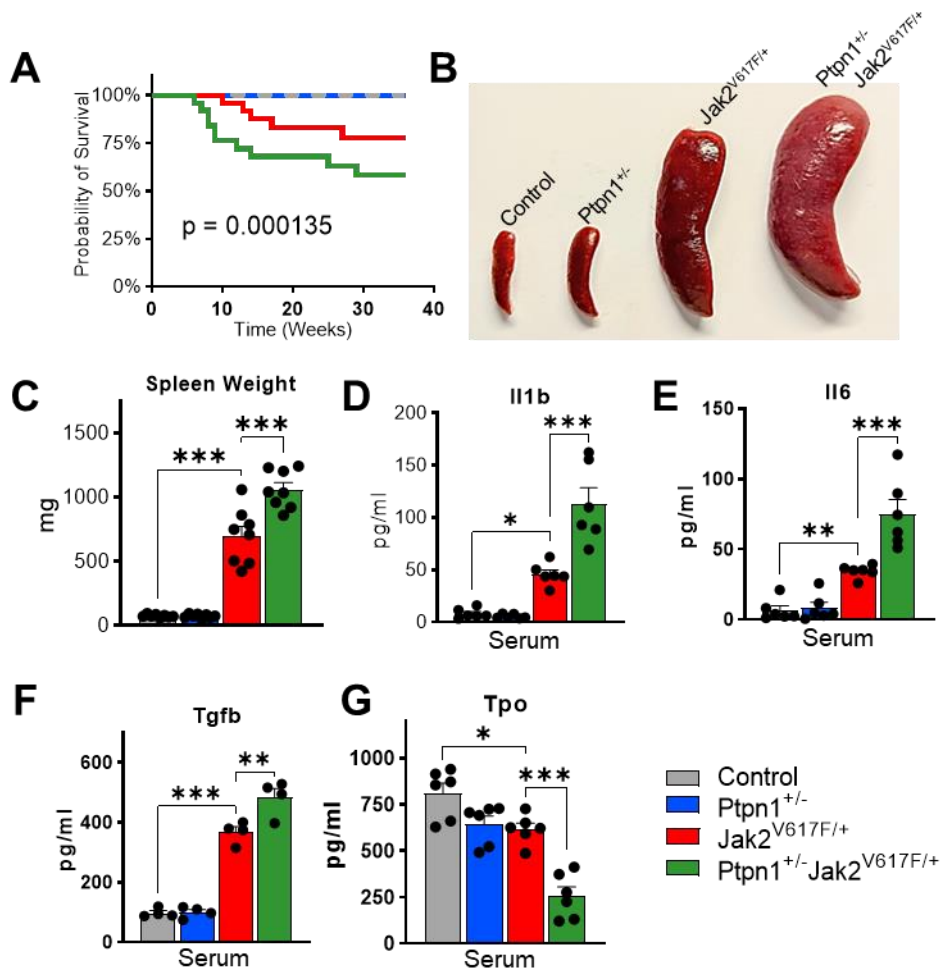


**Figure 4 - *Ptpn1*<sup>+/-</sup> *Jak2*<sup>V617E/+</sup> mice exhibit poorer survival, increase splenic burden, and elevated serum proinflammatory cytokines with reduction in thrombopoietin (Tpo).** (A) Kaplan-Meier plot (n=20+) of mice survival probability. (B) Gross examination of splenic size and (C) weight. Concentration of proinflammatory cytokines, (D) Il1b (n=6), (E) Il6 (n=6), and (F) Tgfb (n=4), measured by ELISA from PB serum. (G) Tpo (n=6) serum concentration measured by ELISA. Survival plot statistical analysis was done with Log-rank Mantel-Cox test with p-value displayed. All bar graph data are represented using mean ± sem and statistical test are done with one-way ANOVA with Tukey multiple comparison. (\* = p<0.05, \*\* = p<0.01, and \*\*\* = p<0.001)



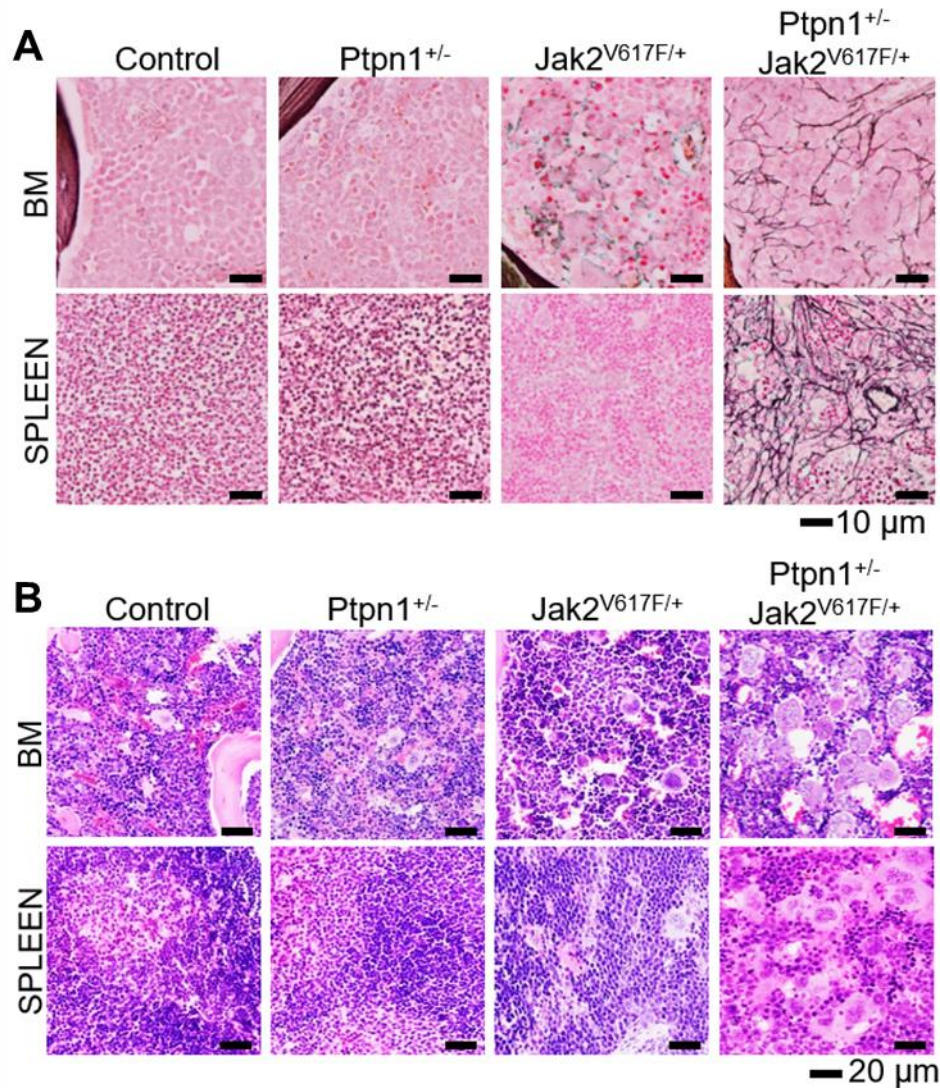


**Figure 5 – Bone marrow (BM) and spleen of Ptpn1<sup>+/-</sup> Jak2<sup>V617F/+</sup> mice showed greater deposition of fibrosis and abundance megakaryocytes (MK) clusters. (A) Reticulin stained BM and spleen of control, Ptpn1<sup>+/-</sup>, Jak2<sup>V617F/+</sup>, and Ptpn1<sup>+/-</sup> Jak2<sup>V617F/+</sup> mice. Scale bar represent 10 μm distance. (B) Hematoxylin and eosin (H&E) stained BM and spleen of same cohorts. Scale bar represent 20 μm distance.**

**Ptpn1<sup>+/-</sup>Jak2<sup>V617F/+</sup> mice exhibit increased hematopoietic stem cells with a preference for myeloid and megakaryocyte lineages cells.**

Next, we want to assess the changes in the hematopoietic compartments of the bone marrow and spleen. By using flow cytometry, we observed a remarkable increase in the hematopoietic stem cells (HSC) population, designated by the markers, lineage negative, Sca-1 positive, and c-Kit positive (LSK), in Ptpn1-deficient Jak2<sup>V617F/+</sup> mice (Figure 6A, C). This population encompasses all three subpopulations, long-term HSC (LT-HSC), short-term HSC (ST-HSC), and multipotent progenitor (MPP); all of which are increased [data not shown]. The data is the aggregate of total cellularity from both the BM and spleen. The myeloid progenitor population, which is negative for Sca-1 and designated as LK, is also significantly increased in Ptpn1<sup>+/-</sup>Jak2<sup>V617F/+</sup> mice (Figure 6B-C). Interestingly, the megakaryocytes-erythrocytes progenitor (MEP) population, a subset of LK, is the largest contributor and showed the most remarkable increase was observed in Ptpn1<sup>+/-</sup>Jak2<sup>V617F/+</sup> mice (Figure 6D).

The marked increase of MEP in Ptpn1<sup>+/-</sup>Jak2<sup>V617F/+</sup> mice is also reflected in the megakaryocyte lineage (CD41<sup>+</sup>CD61<sup>+</sup>) (Figure 6E-F), providing support for the observed expansion of platelets in the peripheral blood. Additionally, Figure 6G indicates that myeloid lineages (Gr1<sup>+</sup>Mac1<sup>+</sup>) are also significantly elevated in these mice.

Interestingly, while the erythroblast population of (CD71<sup>+</sup>Ter119<sup>+</sup>) is elevated, its precursor CFU-E (colony forming unit – erythrocytes), measured by colony assay, is significantly reduced (Figure 6H-I). It is important to note that the erythroblasts population is significantly reduced in BM but elevated in the spleen (data not shown). This may suggest an early onset of collapsing erythropoiesis and a shift toward

megakaryopoiesis in the bone marrow. Additionally, colony assays show a significant expansion of an earlier precursor, CFU-GM (colony-forming unit – granulocyte and macrophages) and common myeloid progenitor or CFU-GEMM (colony-forming unit – granulocyte, erythrocyte, monocyte, and megakaryocyte) (Figure 6J-K) in  $Ptpn1^{+/-}$   $Jak2^{V617F/+}$  mice, which further supports the observed myeloid expansions. A significant increase in CFU-Mk (colony forming unit – megakaryocytes) is also observed, which supports the robust increase in megakaryocytes (Figure 6L). Together,  $Ptpn1$ -deficient  $Jak2^{V617F/+}$  mice exhibit a significant expansion of stem and myeloid lineages along with megakaryocyte lineages.

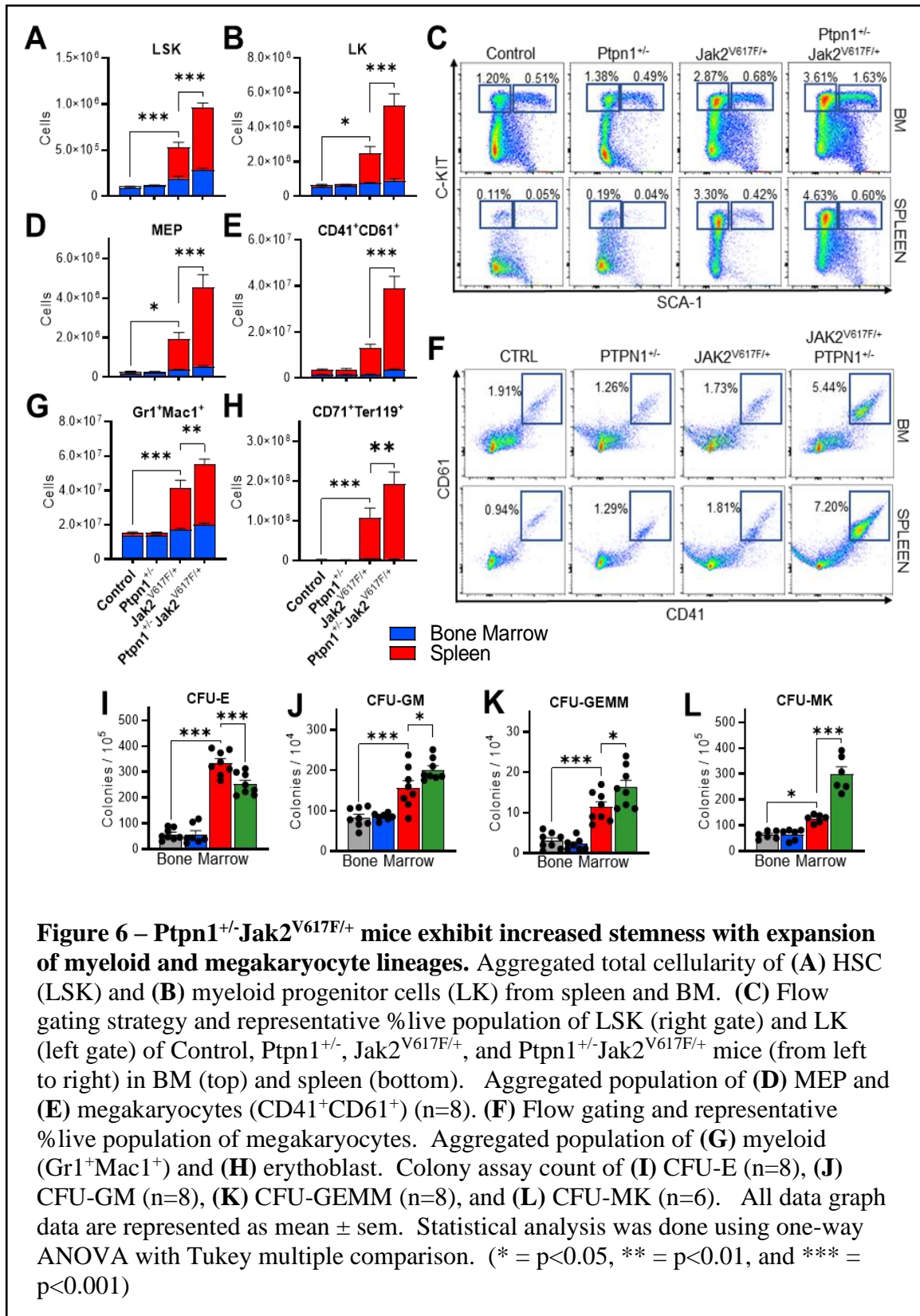
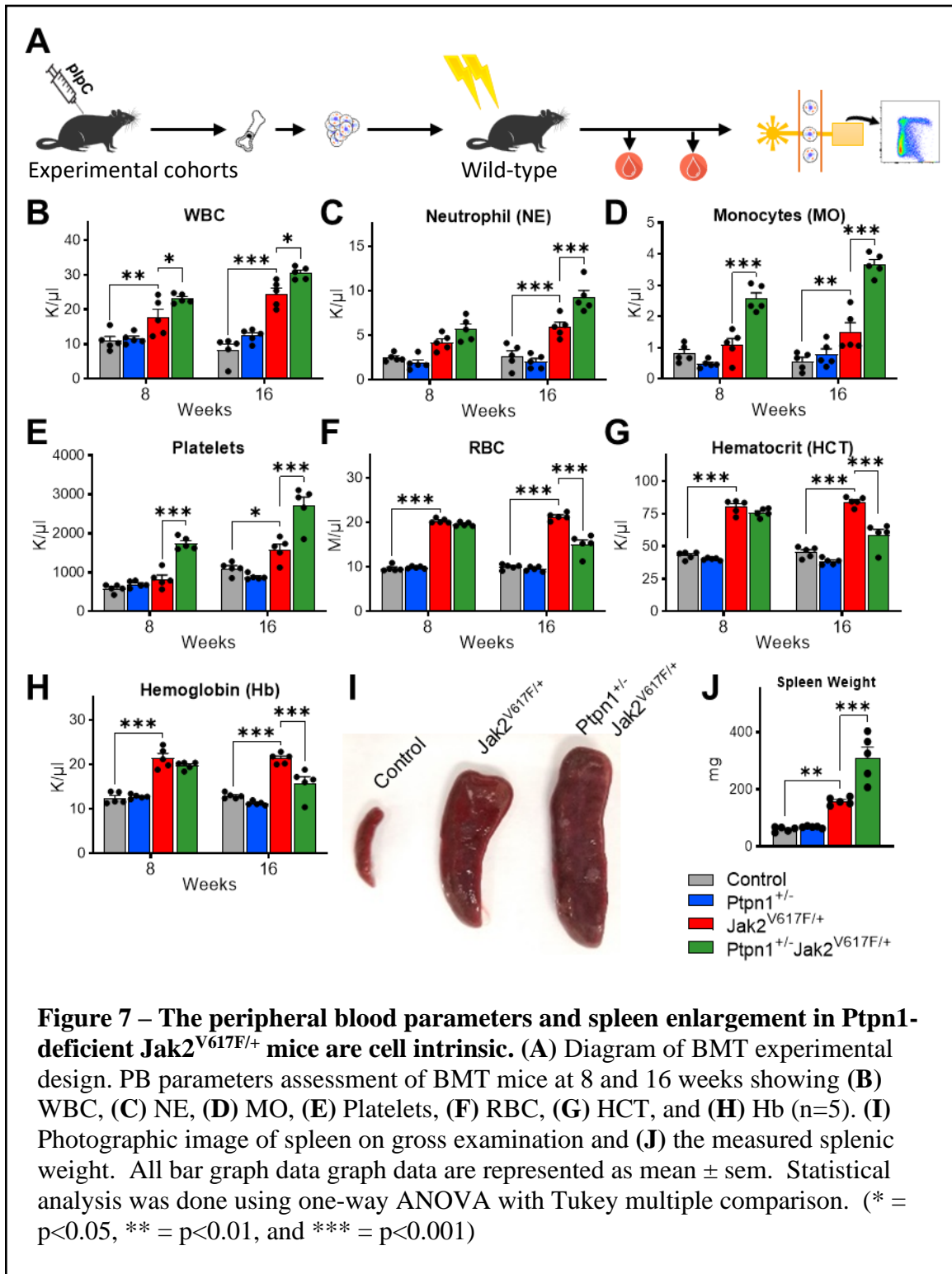


**Figure 6 – Ptpn1<sup>+/-</sup>Jak2<sup>V617F/+</sup> mice exhibit increased stemness with expansion of myeloid and megakaryocyte lineages.** Aggregated total cellularity of (A) HSC (LSK) and (B) myeloid progenitor cells (LK) from spleen and BM. (C) Flow gating strategy and representative %live population of LSK (right gate) and LK (left gate) of Control, Ptpn1<sup>+/-</sup>, Jak2<sup>V617F/+</sup>, and Ptpn1<sup>+/-</sup>Jak2<sup>V617F/+</sup> mice (from left to right) in BM (top) and spleen (bottom). Aggregated population of (D) MEP and (E) megakaryocytes (CD41<sup>+</sup>CD61<sup>+</sup>) (n=8). (F) Flow gating and representative %live population of megakaryocytes. Aggregated population of (G) myeloid (Gr1<sup>+</sup>Mac1<sup>+</sup>) and (H) erythroblast. Colony assay count of (I) CFU-E (n=8), (J) CFU-GM (n=8), (K) CFU-GEMM (n=8), and (L) CFU-MK (n=6). All data graph data are represented as mean ± sem. Statistical analysis was done using one-way ANOVA with Tukey multiple comparison. (\* = p<0.05, \*\* = p<0.01, and \*\*\* = p<0.001)

### **The phenotypic effects of Ptpn1-deficient $Jak2^{V617F/+}$ are cell intrinsic.**

Next, to determine if the exhibited phenotype is cell intrinsic, we carried out a bone marrow transplantation from our experimental cohorts to lethality irradiated wild-type mice. The experimental design is highlighted in the diagram in Figure 7A. Blood parameters were assessed every 8 weeks. Similar to the primary model,  $Ptpn1^{+/-}$  mice exhibited no discernable phenotype compared to control mice.  $Ptpn1^{+/-}$  with  $Jak2^{V617F/+}$  mice, on the other hand, showed a significant increase in WBC and both its subset population of neutrophils and monocytes (Figure 7B-D). The marked increase of platelet from the primary model was also observed (Figure 7E), as well as a significant reduction in RBC, HCT, and Hb (Figure 7F-H). Upon gross examination, the  $Ptpn1^{+/-}Jak2^{V617F/+}$  mice also displayed an increased splenic burden in both size and weight compared to  $Jak2^{V617F/+}$  alone (Figure 7I-J).

The hematopoietic compartments of the BM and spleen showed similar results to the primary model. The combined BM and spleen cellularity of  $Ptpn1^{+/-}Jak2^{V617F/+}$  mice exhibited an increase in LSK and LK population (Figure 8A-B), as well as a significant increase in MEP and its differentiated MK lineages (CD41+CD61+) (Figure 8C-D). Myeloid lineages were also elevated (Figure 8E), while erythroblasts were significantly decreased (Figure 8F). Histological examination of the bone marrow by H&E and reticulin staining revealed  $Ptpn1^{+/-}Jak2^{V617F/+}$  mice had a substantial amount of MK clusters and fibrosis accumulation (Figure 8G). Overall, these results suggest that the phenotypic effects of Ptpn1-deficient  $Jak2^{V617F/+}$  mice are cell-intrinsic.



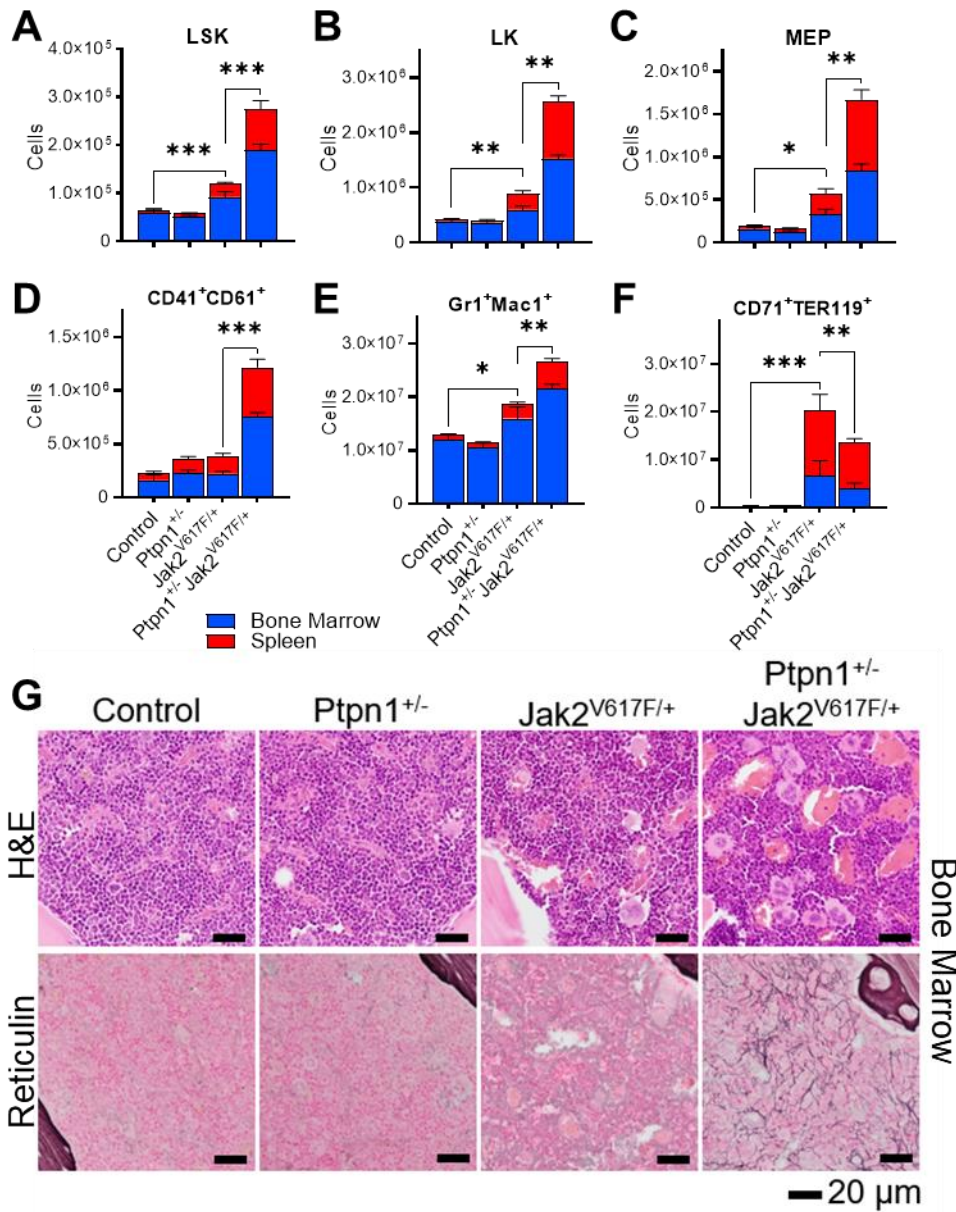


**Figure 8 – The fibrotic progression and expansion of HSC, megakaryocytes, and myeloid cells in Ptpn1-deficient Jak2<sup>V617F/+</sup> mice are cell intrinsic.**

Aggregated cellularity of (A) LSK (B) LK, (C) MEP, (D) megakaryocytes, (E) myeloid, and (F) erythroblast of BMT mice. (G) Bone marrow's H&E (top) and reticulin (bottom) stained slides of BMT experimental cohorts (n=5). All bar graph data are represented as mean ± sem. Statistical analysis was done using one-way ANOVA with Tukey multiple comparison. (\* = p<0.05, \*\* = p<0.01, and \*\*\* = p<0.001)

**JAK2<sup>V617F</sup>-positive Ptpn1-deficient cells exhibit greater clonal advantages than JAK2<sup>V617F</sup> mutation alone.**

To assess whether Ptpn1-deficient Jak2<sup>V617F/+</sup> cells have any potential clonal advantages, we performed a competitive reconstitution assay using a 1:1 mixture of experimental cells (CD45.2) and wild-type cells (CD45.1) transplanted to lethally irradiated mice and monitored for 20 weeks, as shown in the diagram in Figure 9A. Flow cytometry analysis of the peripheral blood revealed that Gr1<sup>+</sup>, B220<sup>+</sup>, and TCRB<sup>+</sup> populations of Ptpn1<sup>+/-</sup>Jak2<sup>V617F/+</sup>-derived (CD45.2<sup>+</sup>) cells demonstrated greater clonal advantages than Jak2<sup>V617F/+</sup> alone (Figure 9B-D). CD45 expression was not examined in anucleated cells (erythrocytes and platelets)<sup>21</sup>.

Examination of the bone marrow and spleen also revealed a significant clonal advantage of Ptpn1<sup>+/-</sup>Jak2<sup>V617F/+</sup>-derived cells in myeloid (Gr1<sup>+</sup>Mac1<sup>+</sup>), megakaryocyte (CD41<sup>+</sup>CD61<sup>+</sup>), hematopoietic stem cell (LSK), and myeloid progenitor (LK) population (Figure 9E-I). The clonal dominance of the Ptpn1<sup>+/-</sup>Jak2<sup>V617F/+</sup>-derived cells resulted in a significant expansion of these populations (Figure 10A-H). These data suggest that Ptpn1-deficient Jak2<sup>V617F/+</sup> promotes greater clonal advantages that significantly expand stem, myeloid progenitor, and megakaryocytes precursor.



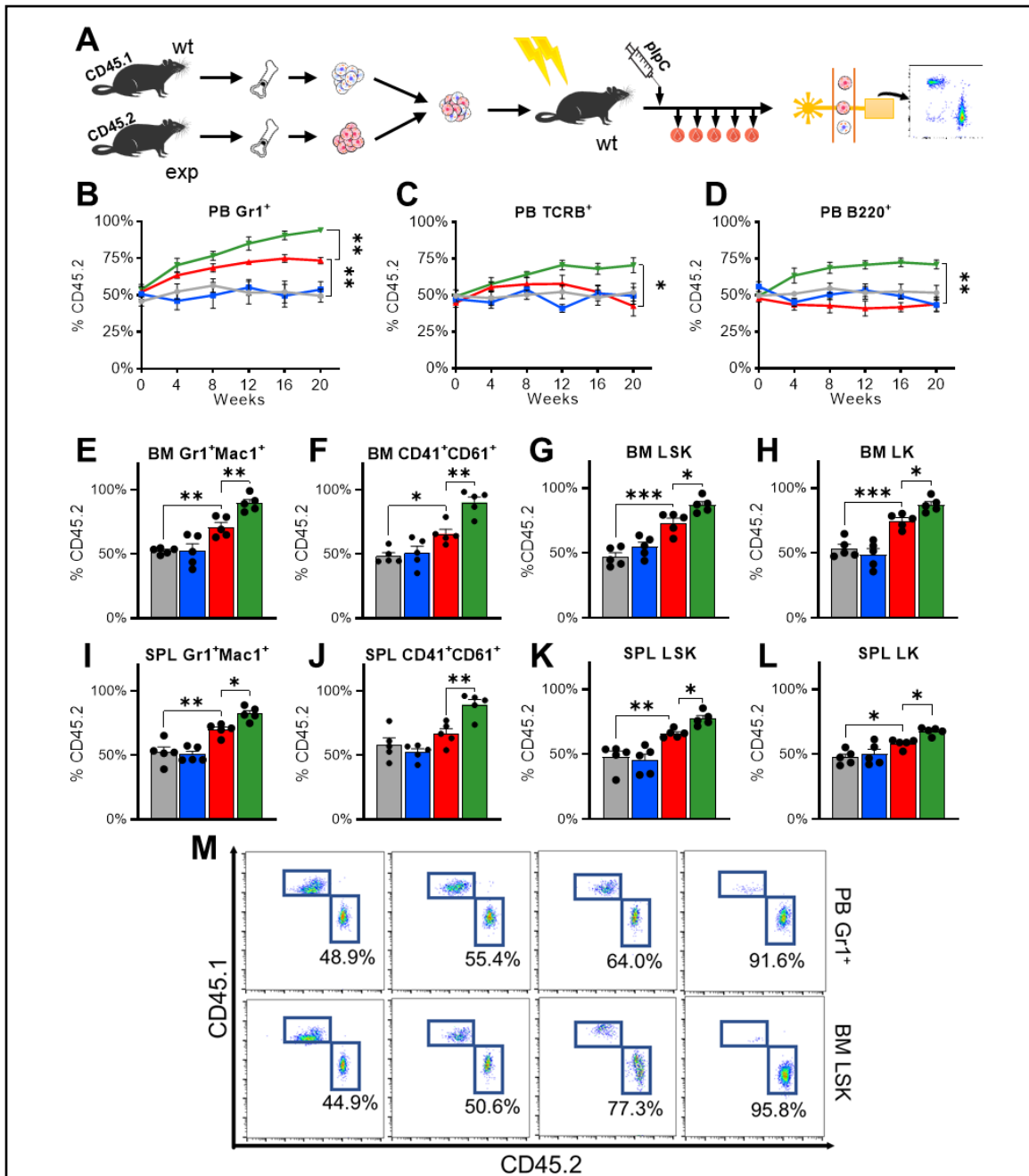
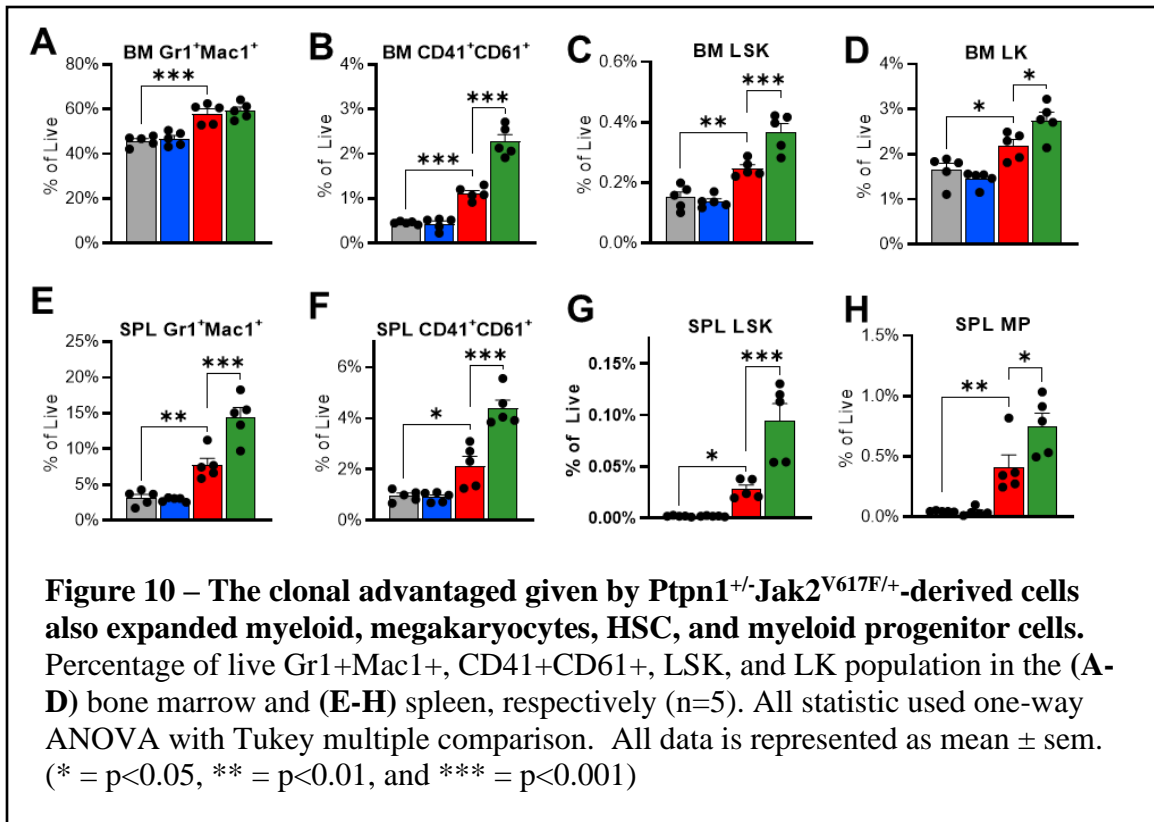


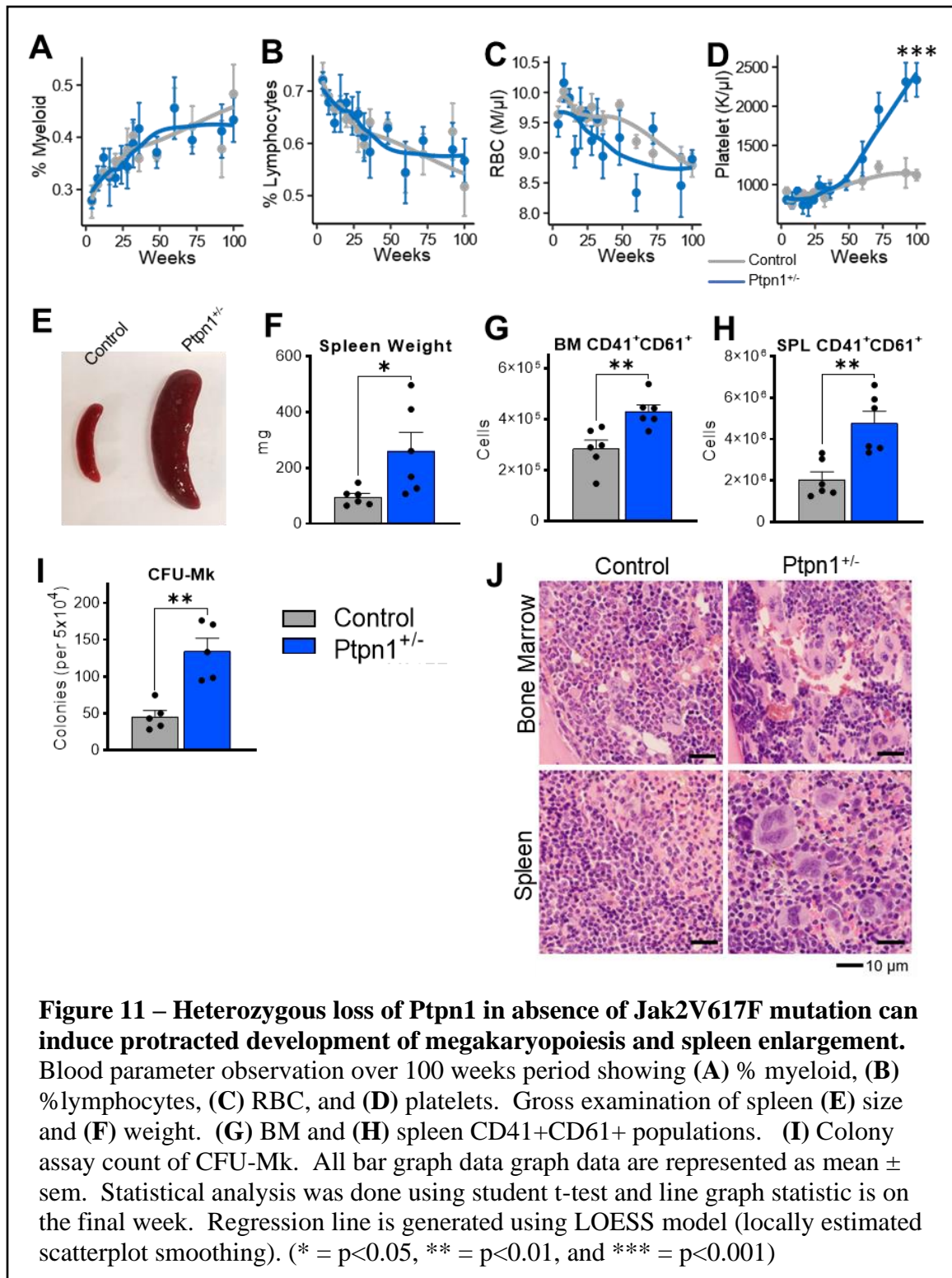
**Figure 9 –Ptpn1<sup>+/-</sup>Jak2<sup>V617E/+</sup>-derived cells exhibit greater clonal advantages than Jak2<sup>V617E/+</sup> alone.** (A) Experimental design of competitive BMT assay. Flow analysis of PB's CD45.2-positive's (B) Gr1<sup>+</sup>, (C) TCRB<sup>+</sup>, and (D) B220<sup>+</sup> population. CD45.2-positive population of Gr1<sup>+</sup>Mac1<sup>+</sup>, CD41<sup>+</sup>CD61<sup>+</sup>, LSK, and LK in the (E-H) bone marrow and (I-L) spleen, respectively (n=5). (M) Representative image of CD45.2 and CD45.1 gating in percentage of CD45.2. Line graph statistic used two-way ANOVA with Tukey multiple comparison with only the final week significant showed. Bar graph statistic used one-way ANOVA with Tukey multiple comparison. All data is represented as mean ± sem. (\* = p<0.05, \*\* = p<0.01, and \*\*\* = p<0.001)



### Heterozygous deletion of *Ptpn1* in mice exhibits splenomegaly and platelet-lineage expansion after a protracted period.

Although *Ptpn1*-deficient mice did not exhibit any discernable phenotype in the early stages of our evaluations, a prolonged observation of over 100 weeks revealed marked expansion of platelets but no significant shift in the percentage of myeloid, lymphoid, or RBC population in the peripheral blood (Figure 11A-D). Gross examination spleen showed splenic enlargement in both its size and weight (Figure 11E-F). While no significant changes in stem, progenitor, myeloid, or erythroid population were observed in the BM and spleen (data not shown), the number of CFU-MK colonies and  $CD41^{+}CD61^{+}$  megakaryocytes was significantly increased, as well as the presence of

MK clusters upon H&E staining. Taken together, our results suggest that *Ptpn1* deficiency leads to a unique MK-biased property.



## **Homozygous deletion of Ptpn1 results in faster progression to myelofibrosis in Jak2<sup>V617F</sup>-positive mice.**

To evaluate the degree to which Ptpn1 expression impacts the severity of the disease progression, we studied the effects of homozygous deletion of Ptpn1 in the context of Jak2<sup>V617F/+</sup> mutation. While we originally observed a significant increase in WBC and myeloid subsets of NE and MO, Ptpn1-deleted Jak2<sup>V617F/+</sup> mice experienced a collapse in WBC and NE at 20 weeks (Figure 12A-C). The RBC parameters, including RBC count, HCT, and Hb, declined rapidly in Ptpn1<sup>-/-</sup>Jak2<sup>V617F/+</sup> mice compared to both Jak2<sup>V617F/+</sup> alone and Ptpn1<sup>+/-</sup> Jak2<sup>V617F/+</sup> mice (Figure 12D-F). Although platelets of Ptpn1<sup>-/-</sup>Jak2<sup>V617F/+</sup> mice exhibited more robust platelet expansion than Ptpn1<sup>+/-</sup> Jak2<sup>V617F/+</sup>, they also collapsed at around 16 weeks (Figure 12G). These Jak2<sup>V617F/+</sup>-positive Ptpn1 knockout mice showed poorer survival than heterozygous deleted mice and exhibit far greater splenic burden in term of size and weight (Figure 12H-J).

Examination of the bone marrow and spleen revealed a significant expansion of the LSK, LK, and MEP populations (Figure 13A-C) as well as elevated levels of myeloid (Gr1<sup>+</sup>Mac1<sup>+</sup>) and megakaryocytes (CD41<sup>+</sup>CD61<sup>+</sup>) populations (Figure 13D-F). Reticulin-stained slides showed severe fibrosis in both the bone marrow and spleen of Ptpn1<sup>-/-</sup>Jak2<sup>V617F/+</sup> mice (Figure 13G). It is worth noting that the expansion in cellularity of Ptpn1<sup>-/-</sup>Jak2<sup>V617F/+</sup> mice is primarily attributed to splenic cells, as the bone marrow's cellularity is heavily compromised due to severe fibrosis. Overall, these findings suggest that the absence of Ptpn1 expression in Jak2<sup>V617F/+</sup> mice leads to severe disease progression and highlights the direct role of Ptpn1 expression in modulating disease severity.

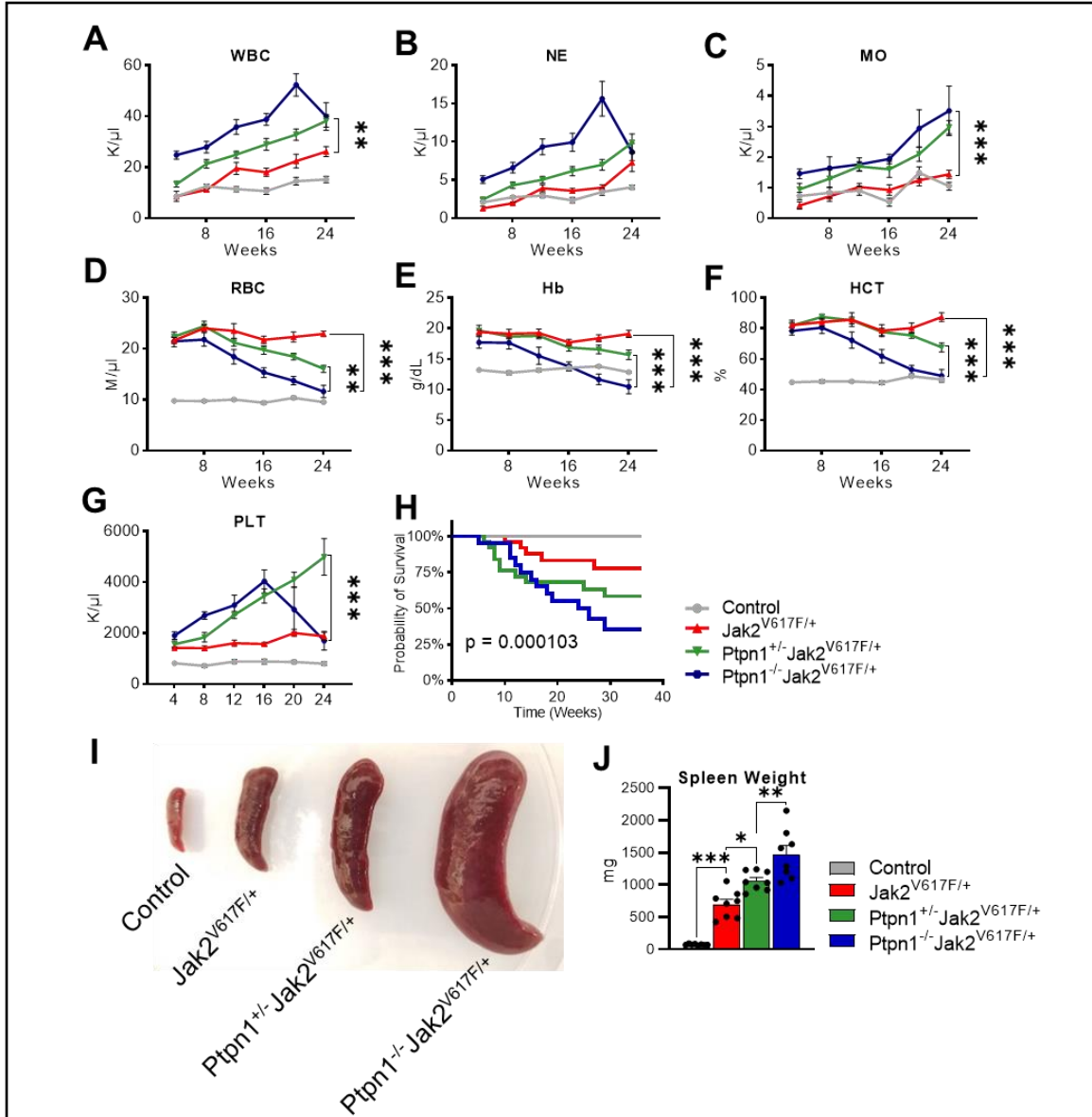
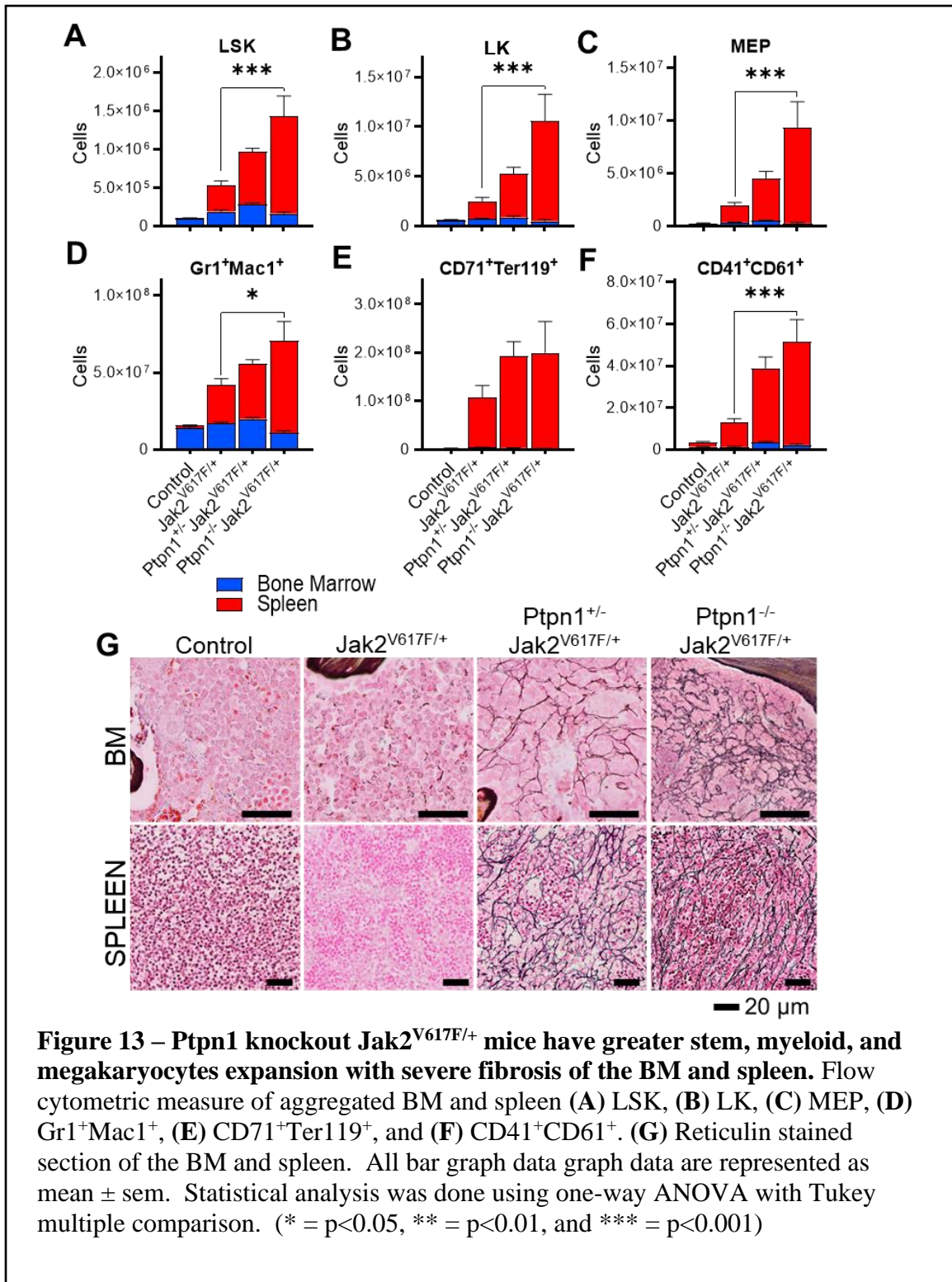


**Figure 12 – Deletion of PTPN1 in Jak2<sup>V617F/+</sup> mice results in significantly higher disease burden and morbidity.** Blood parameter of Control, Jak2<sup>V617F/+</sup>, Ptpn1<sup>+/-</sup>Jak2<sup>V617F/+</sup>, Ptpn1<sup>-/-</sup>Jak2<sup>V617F/+</sup> mice showing (A) WBC, (B) NE, (C) MO, (D) RBC, (E) Hb, (F) HCT, and (G) platelet (n=8). (I) Photographic image of spleen on gross examination and (J) the measured splenic weight. All bar graph data are represented as mean  $\pm$  sem. Statistical analysis was done using one-way ANOVA with Tukey multiple comparison. Two-way ANOVA with Tukey multiple comparison was done for multiple dates. Only final date statistic is shown. (\* = p<0.05, \*\* = p<0.01, and \*\*\* = p<0.001)



## 2.3 – Methods

### Cell culture

Murine Ba/F3 cells with stable ectopic expression of EpoR carrying the JAK2V617F mutation (Ba/F3 VF), human erythroid leukemic cells (HEL), and megakaryoblastic leukemia cells (SET-2) were cultured in RPM-1640 medium supplemented with 10% FBS and 1x Penicillin-Streptomycin (P/S) solution (Corning # 30-002-CI). HEK293T cells were used for transfection and lentiviral production and were cultured in DMEM medium supplemented with 10% FBS and 1X P/S. Ba/F3 VF cells were stably transduced with lentiviral pCDH-Puro-GFP-Flag-mPtpn1, while both HEL and SET2 cells were stably transduced with lentiviral pCDH-puro-GFP-3xFlag-huPTPN1. The cells were transduced with lentiviruses and selected in puromycin for 2-3 days. Deletion of PTPN1/Ptpn1 in Ba/F3 VF, HEL, and SET2 was mediated with CRISPR-Cas9 using the guide RNA listed in the table below, and the cells were clonally selected. Cell proliferation was assessed by manual counting daily for 4-5 days after equalizing the starting cell count.

### Mice

Conditional Ptpn1 floxed mice<sup>22</sup>, Jak2V617F knock-in<sup>9</sup>, and Mx1-Cre mice<sup>23</sup> were crossed to generate the experimental cohorts, with wild-type mice or mice without Mx1-Cre as control. Deletion and knock-in were induced by three intraperitoneal injections of polyinosine-polycytosine (pIpC). All mice used in the study were of C57BL/6 strain. Animal studies were conducted following the guidelines set by the Institutional Animal Care and Use Committee of the University of Virginia School of Medicine. Terminal analysis was performed after 24 weeks.

### **Patient samples**

Peripheral blood samples from MPN patients were acquired from the University of Virginia Cancer Center. All collected samples were obtained with informed consent, and the protocol was approved by the Institutional Review Board of the University of Virginia Health System.

### **Blood and tissue analysis**

Blood collection from mice was taken from the tail vein. Hemavet 950FS (Drew Scientific) was used to measure peripheral blood counts of mice. Peripheral blood serum was collected from terminal cardiac puncture and analyzed for IL-1 $\beta$ , IL-6, TGF $\beta$ , and mTpo using ELISA (R&D Systems), following the manufacturer's protocol. For bone marrow histology, a mouse femur was used. The femur and spleens were fixed in 10% neutral-buffered formalin, and the bones were decalcified using Decalcifying Solution (EpreDia) before paraffin embedding. Paraffin-embedded tissues were sectioned (4  $\mu$ m) and stained with hematoxylin & eosin and reticulin staining by the University of Virginia's Biorepository and Tissue Research Facility (BTRF).

### **Flow cytometry**

The bone marrow cells were flushed from one femur and two tibias and RBC lysed before staining. Splenic cells were isolated through a 70  $\mu$ m nylon mesh strainer (Fisher) and subsequently, RBC lysed and stained. Cells were stained for 60 minutes on ice using two different panels for hematopoietic stem and progenitor staining and the general population separately. The HSC panel included APC/Cy7-c-kit, PE/Cy7-Sca1, FITC-



CD34, APC-Flt3, PE-CD16/32, and a lineage negative marker of PerCP/Cy5.5-CD3, CD4, CD8, CD19, B220, Gr1, CD127, and Ter119. The general panel included PerCP/Cy5.5-Gr1, BV785-CD11b, FITC-Ter119, PE/Cy7-CD71, Alexa Fluor 700-B220, BV605-TCR $\beta$ , APC/Cy7-CD41, and PE-CD61. Flow cytometry was performed with the Aurora and North Lights (Cytex Biosciences). For the competitive assay, an adjusted panel was used to accommodate additional markers, and CD45.1 and CD45.2 were stained with BV785 and FITC, respectively.

### **Bone marrow transplantation (BMT)**

For the BMT experiment, bone marrow cells were harvested from the experimental cohort mice 6-8 weeks post-pIpC induction and transplanted retroorbitally at a cell density of  $1 \times 10^6$  cells to lethally irradiated ( $2 \times 550$  Gy) wild-type mice of similar age. For competitive reconstitution assay, the bone marrow cells of experimental cohort mice (CD45.2<sup>+</sup>) without pIpC induction were harvested along with bone marrow cells of wild-type (CD45.1<sup>+</sup>) mice (Jackson Lab). The BM cells were mixed in a 1:1 ratio and transplanted at a density of  $1 \times 10^6$  cells into lethally-irradiated wild-type mice. Mx1-Cre induction with pIpC was done 4 weeks post-transplantation. Blood analysis of CD45.1<sup>+</sup> versus CD45.2<sup>+</sup> was done using ~5-10  $\mu$ l of blood from the tail vein and RBC lysed before staining for Gr1<sup>+</sup>, B220<sup>+</sup>, and TCRB<sup>+</sup>. Analysis was done by flow cytometry.

### **Colony Assay**

Colony assays were performed using the mouse bone marrow cells. CFU-GM and CFU-GEMM were assessed by inoculating mouse bone marrow cells in MethoCult™ GF

M3434 (STEMCELL Technologies). The cells were plated in duplicates on a 3.5 cm dish and incubated for 6-8 days before counting. CFU-E was assessed using MethoCult™ M3234 (STEMCELL Technologies) without erythropoietin. The cells are plated in duplicates in a 3.5 cm dish for 48 hours and then stained with a mixture of hydrogen peroxide and benzidine for 24 hours before counting. CFU-Mk was assessed using MegaCult™ media (STEMCELL Technologies) with added collagen solution and growth factors, Tpo, mIL3, mIL6, and mIL11. The cells are incubated in chamber culture slides and incubated for 6-8 hours before dehydrating, fixing, and staining following manufacturer protocol.

### **Real-time quantitative PCR**

Total RNA extraction of Ba/F3 VF, HEL, and SET2 cells was completed with RNeasy Mini Micro Kit (QIAGEN). The RNAs were converted to cDNA using High-Capacity cDNA Reverse Transcription Kit (Applied Biosystems). Real-time PCR was performed with Quantstudio3 (Applied Biosystems). The primer sequence used in the qPCR reaction is detailed below. The readout was measured with SYBR green using the SYBR Green PCR master mix (QuantaBio). All data were normalized with HPRT1/Hprt1 or GAPDH/Gapdh and fold changes were calculated by  $\Delta\Delta C_t$ .

### **Data Analysis**

MPN dataset used is provided by Schischlik group<sup>19</sup> and is available through the European Genome-Phenome Archive (ID EGAS00001003486). The data were realigned from GRCh37 to GRCh38 using samtools and HISAT2. Gene counts were generated

from featureCounts. TPM counts, gene annotations, and selected gene expression profiling is done using R. All graphing and statistic analysis were done in GraphPad Prism.

### **Immunoblotting**

Cells were lysed with RIPA lysis buffer (50mM Tris-HCl, 150mM NaCl, 1% Triton X-100, 1% sodium deoxycholate, 0.1% SDS) with protease inhibitors (2mM Na<sub>3</sub>VO<sub>4</sub>, 5mM NaF, 10 mM  $\beta$ -glycol phosphate, 10  $\mu$ g/mL leupeptin, 10  $\mu$ l/mL aprotinin, 2  $\mu$ g/mL pepstatin A, 2  $\mu$ l/mL antipain, and 100  $\mu$ l/mL phenylmethylsulfonyl fluoride [PMSF]). Immunoblotting was performed using the antibodies mPtpn1 specific antibody (R&D system), huPTPN1 specific antibody (EMD Millipore), and  $\beta$ -Actin.

### **Statistical analysis**

For two-group analyses, a Student's t-test was used to determine statistical significance. For comparisons of more than two groups, one-way ANOVA with post-hoc Tukey-HSD test was performed to assess statistical significance. Two-way ANOVA with post-hoc Tukey-HSD test was performed for multiple time points and multiple groups comparisons. Only the final statistics are displayed. All data are expressed as mean  $\pm$  SEM.

### sgRNA Table

Name	Sequence
huPTPN1_sg_E8_FWD	GGATAAAGACTGCCCCATCA
huPTPN1_sg_E8_REV	TGATGGGGCAGTCTTTATCC
huPTPN1_sg_E9_FWD	GTTAGAAGTCGGGTCGTGGG
huPTPN1_sg_E9_REV	CCCACGACCCGACTTCTAAC
huPTPN1_sg_E4_FWD	GTGTGGGAGCAGAAAAGCAG
huPTPN1_sg_E4_REV	CTGCTTTTCTGCTCCCACAC
huPTPN1_sg_E6_FWD	TCTGTCTGGCTGATACCTGC
huPTPN1_sg_E6_REV	GCAGGTATCAGCCAGACAGA
mPtpn1_sg_E2_FWD	ATGCAAAGTCGCGAAGCTTC
mPtpn1_sg_E2_REV	GAAGCTTCGCGACTTTGCAT
mPtpn1_sg_E3_FWD	GAGGAGCTATATTCTCACCC
mPtpn1_sg_E3_REV	GGGTGAGAATATAGCTCCTC
mPtpn1_sg_E4_FWD	GCCCTTTACCAAACACATGT
mPtpn1_sg_E4_REV	ACATGTGTTTGGTAAAGGGC
mPtpn1_sg_E6_FWD	GCGCCGGCATCGGGAGGTCA
mPtpn1_sg_E6_REV	TGACCTCCCGATGCCGGCGC

### RT-qPCR Primer Table

Name	Sequence
mPtpn1_RT_294F	CGGAACAGGTACCGAGATGT
mPtpn1_RT_452R	GAAGTGCCACATGTGTTTG
huPTPN1_RT_553F	CCTGAATCACCGCCTCATT
huPTPN1_RT_697R	AGAGGCAGGTATCAGCCAGA
mGapdh_RT_Fwd	ACTCCACTCACGGCAAATTC
mGapdh_RT_Rev	TCTCCATGGTGGTGAAGACA
HuGAPDH_RT_20F	GAGTCAACGGATTTGGTCGT
HuGAPDH_RT_204R	GACAAGCTTCCCGTTCTCAG

## 2.4 – References

1. Hussein, K., Van Dyke, D. L. & Tefferi, A. Conventional cytogenetics in myelofibrosis: literature review and discussion. *Eur. J. Haematol.* **82**, 329–338 (2009).
2. Barbui, T. *et al.* The 2016 revision of WHO classification of myeloproliferative neoplasms: Clinical and molecular advances. *Blood Reviews* (2016) doi:10.1016/j.blre.2016.06.001.
3. Kiladjian, J.-J., Gardin, C., Renoux, M., Bruno, F. & Bernard, J.-F. Long-term outcomes of polycythemia vera patients treated with pipobroman as initial therapy. *Hematol. J.* **4**, 198–207 (2003).
4. Cervantes, F. *et al.* New prognostic scoring system for primary myelofibrosis based on a study of the International Working Group for Myelofibrosis Research and Treatment. *Blood* **113**, 2895–2901 (2009).
5. Tang, G. *et al.* Characteristics and clinical significance of cytogenetic abnormalities in polycythemia vera. *Haematologica* **102**, 1511–1518 (2017).
6. Wassie, E. *et al.* A compendium of cytogenetic abnormalities in myelofibrosis: molecular and phenotypic correlates in 826 patients. *Br. J. Haematol.* **169**, 71–76 (2015).
7. Vainchenker, W. & Kralovics, R. Genetic basis and molecular pathophysiology of classical myeloproliferative neoplasms. *Blood* **129**, 667–679 (2017).
8. Scott, L. M. *et al.* Acquired mutation of the tyrosine kinase JAK2 in human myeloproliferative disorders. *Lancet* **365**, 1054–1061 (2005).
9. Akada, H. *et al.* Conditional expression of heterozygous or homozygous Jak2V617F from its endogenous promoter induces a polycythemia vera–like disease. *Blood* **115**, 3589–3597 (2010).
10. Gou, P., Zhang, W. & Giraudier, S. Insights into the Potential Mechanisms of JAK2V617F Somatic Mutation Contributing Distinct Phenotypes in Myeloproliferative Neoplasms. *Int. J. Mol. Sci.* **23**, 1013 (2022).
11. Pearson, S., Blance, R., Somerville, T. C. P., Whetton, A. D. & Pierce, A. AXL Inhibition Extinguishes Primitive JAK2 Mutated Myeloproliferative Neoplasm Progenitor Cells. *HemaSphere* **3**, e233 (2019).
12. Sangiorgio, V. F. I., Nam, A., Chen, Z., Orazi, A. & Tam, W. GATA1 downregulation in prefibrotic and fibrotic stages of primary myelofibrosis and in the myelofibrotic progression of other myeloproliferative neoplasms. *Leuk. Res.* **100**, 106495 (2021).
13. Dutta, A., Hutchison, R. E. & Mohi, G. Hmga2 promotes the development of myelofibrosis in Jak2V617F knockin mice by enhancing TGF- $\beta$ 1 and Cxcl12

- pathways. *Blood* **130**, 920–932 (2017).
14. Jobe, F. *et al.* Deletion of Ptpn1 induces myeloproliferative neoplasm. *Leukemia* **31**, 1229–1234 (2017).
  15. Schaub, F. X. *et al.* Clonal analysis of deletions on chromosome 20q and JAK2-V617F in MPD suggests that del20q acts independently and is not one of the predisposing mutations for JAK2-V617F. *Blood* **113**, 2022–2027 (2009).
  16. Douet-Guilbert, N. *et al.* Chromosome 20 deletions in myelodysplastic syndromes and Philadelphia-chromosome-negative myeloproliferative disorders: characterization by molecular cytogenetics of commonly deleted and retained regions. *Ann. Hematol.* **87**, 537–544 (2008).
  17. Bacher, U. *et al.* Investigation of 305 patients with myelodysplastic syndromes and 20q deletion for associated cytogenetic and molecular genetic lesions and their prognostic impact. *Br. J. Haematol.* **164**, 822–833 (2014).
  18. Myers, M. P. *et al.* TYK2 and JAK2 Are Substrates of Protein-tyrosine Phosphatase 1B. *J. Biol. Chem.* **276**, 47771–47774 (2001).
  19. Schischlik, F. *et al.* Mutational landscape of the transcriptome offers putative targets for immunotherapy of myeloproliferative neoplasms. *Blood* **134**, 199–210 (2019).
  20. Fielder, P. J. *et al.* Human platelets as a model for the binding and degradation of thrombopoietin. *Blood* **89**, 2782–8 (1997).
  21. Gorczyca, W. *et al.* Immunophenotypic Pattern of Myeloid Populations by Flow Cytometry Analysis. in 221–266 (2011). doi:10.1016/B978-0-12-385493-3.00010-3.
  22. Bence, K. K. *et al.* Neuronal PTP1B regulates body weight, adiposity and leptin action. *Nat. Med.* **12**, 917–924 (2006).
  23. Kühn, R., Schwenk, F., Aguet, M. & Rajewsky, K. Inducible Gene Targeting in Mice. *Science* (80-. ). **269**, 1427–1429 (1995).

## **CHAPTER III**

### **The mechanistic basis for synergy between PTPN1 deficiency and JAK2V617F mutation in myeloproliferative neoplasms**

Bao T. Le, Yue Yang, Fatoumata Jobe, & Golam Mohi

### 3.1 – Introduction

The del20q abnormality involving *PTPN1* deletion has frequently been observed in association with the JAK2V617F mutation in MPN/MF. In this study, we demonstrated that heterozygous or homozygous deletion of PTPN1 enhances the severity of MPN and accelerates the progression to bone marrow fibrosis in Jak2V617F mice. The Ptpn1-deficient Jak2<sup>V617F/+</sup> mice exhibited increased leukocytosis, megakaryopoiesis, expansion of hematopoietic stem/progenitor cells, enhanced splenomegaly and accumulation of reticulin fibrosis in the bone marrow and spleens. Additionally, Ptpn1-deficient Jak2<sup>V617F/+</sup> mice's hematopoietic stem/progenitor cells exhibited greater clonal advantages compared to Jak2<sup>V617F/+</sup> mice. However, the mechanism by which PTPN1 deficiency synergizes with JAK2V617F mutation in the progression of MPN has not been elucidated.

Constitutive activation of the JAK2 signaling has been suggested to play a pivotal role in the pathogenesis of MPN. The JAK2V617F mutation has been associated with three different disease models: polycythemia vera (PV), essential thrombocythemia (ET), and myelofibrosis (MF), but how a single JAK2V617F mutation can give rise to three different MPNs is poorly understood. Research studies have identified factors such as clonal dominance of the cells, JAK2V617F allelic burden, and enhanced phosphorylation of STATs as major contributors to the phenotypic diversity and the risk of progression to myelofibrosis<sup>1-4</sup>. Although PTPN1 has been suggested to negatively regulate the JAK-STAT signaling<sup>5,6</sup>, the effects of PTPN1 deficiency on JAK2V617F-induced signaling have not been elucidated.



In this study, we demonstrated that Ptpn1 deficiency reduces Gata1 expression and enhances megakaryocytic cell proliferation in Ptpn1<sup>+/-</sup> Jak2<sup>V617F/+</sup> mice. We examined the effects of Ptpn1 deficiency on gene expression changes in Ptpn1<sup>+/-</sup> Jak2<sup>V617F/+</sup> mice HSPC and observed significant enrichment of genes related to HSC signature, Notch targets, and Wnt signaling in Ptpn1<sup>+/-</sup> Jak2<sup>V617F/+</sup> mice LSK cells. We have validated several downstream target genes, such as Gata1, Klf1, Blvrb, Notch3, Hmga2, Axl, and Colla1 that are significantly altered in Ptpn1<sup>+/-</sup> Jak2<sup>V617F/+</sup> mice LSK cells. In addition, we performed cell signaling studies using Ptpn1-deficient Jak2V617F mice bone marrow cells and PTPN1-deleted JAK2V617F-expressing hematopoietic cell lines. We showed that PTPN1 deficiency enhances phosphorylation of STAT1, STAT3, STAT5, ERK1/2 and NF-κB (p65). In an attempt to identify novel targets of PTPN1, we performed co-immunoprecipitation experiments using a PTPN1 D181A substrate-trapping mutant followed by mass spectrometry analysis. We identified several novel targets of PTPN1 in JAK2V617F mutant hematopoietic cells that are hyperphosphorylated upon PTPN1 deletion. Furthermore, we show that PTPN1 deficiency significantly reduces the sensitivity of JAK2 inhibitor, ruxolitinib, in JAK2V617F-positive hematopoietic cells, suggesting that PTPN1 deficiency may confer ruxolitinib resistance in patients with MPN.

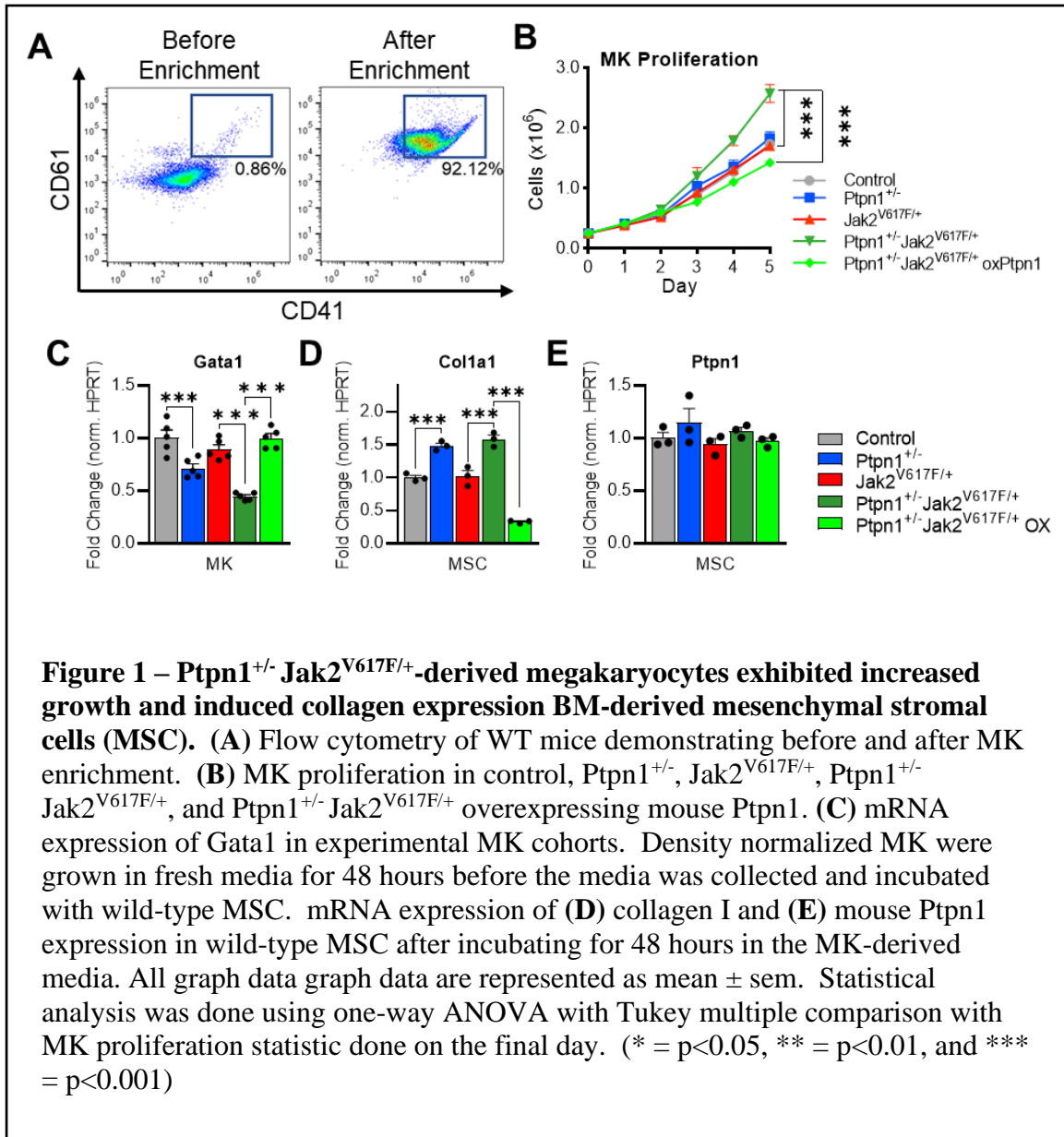
### 3.2 – Results

#### **Megakaryocytes from Ptpn1-deficient Jak2<sup>V617F</sup> mice exhibit increased proliferation and induce collagen expression in BM-derived mesenchymal stromal cells (MSC).**

We observed increased platelet counts and megakaryocytes in Ptpn1-deficient Jak2<sup>V617F/+</sup> mice. Therefore, we assessed whether Ptpn1 deficiency enhances megakaryocytic (MK) proliferation. First, we established MK cultures from control (WT), Ptpn1<sup>+/-</sup>, Jak2<sup>V617F/+</sup>, and Ptpn1<sup>+/-</sup> Jak2<sup>V617F/+</sup> mice bone marrow. Flow cytometric analysis confirmed >90% enrichment of megakaryocytes (Figure 1A). The Ptpn1<sup>+/-</sup> Jak2<sup>V617F/+</sup> MK cells showed a significant increase in proliferation compared to control, Ptpn1<sup>+/-</sup>, and Jak2<sup>V617F/+</sup> MK cells (Figure 1B). Overexpression of Ptpn1 WT in Ptpn1<sup>+/-</sup> Jak2<sup>V617F/+</sup> mice bone marrow cells ablated this proliferative advantage in MK cells (Figure 1B). Previous studies suggested a link between Gata1 deficiency and MK cell proliferation<sup>7,8</sup>. We found that Ptpn1 deficiency reduces Gata1 expression and increases MK cell proliferation, while ectopic expression of Ptpn1 WT completely rescues the Gata1 expression (Figure 1C).

Inflammation is a hallmark feature of MPN/MF, and megakaryocytes are considered major contributors to proinflammatory cytokines production<sup>9</sup>. We aimed to investigate whether soluble inflammatory mediators produced by megakaryocytes could induce collagen expression in bone marrow mesenchymal stromal cells (MSCs). To this end, we incubated culture supernatants obtained from megakaryocytes from control, Ptpn1<sup>+/-</sup>, Jak2<sup>V617F/+</sup>, and Ptpn1<sup>+/-</sup> Jak2<sup>V617F/+</sup> mice bone marrow with MSCs for 48 hours.

Our findings showed that Ptpn1-deficient megakaryocyte cell supernatant induced collagen (Col1a1) expression in BM MSCs, whereas Jak2<sup>V617F/+</sup> mutant-expressing megakaryocyte cells did not induce collagen expression (Figure 1D). Furthermore, ectopic expression of Ptpn1 WT in Ptpn1<sup>+/-</sup> Jak2<sup>V617F/+</sup> mice megakaryocyte cells repressed collagen expression in MSCs (Figure 1D). As expected, Ptpn1 expression was not affected in MSCs (Figure 1E). Taken together, these results suggest that Ptpn1 deficiency in megakaryocytes not only enhance proliferation via the downregulation of Gata1 but can also induce collagen formation in MSCs.

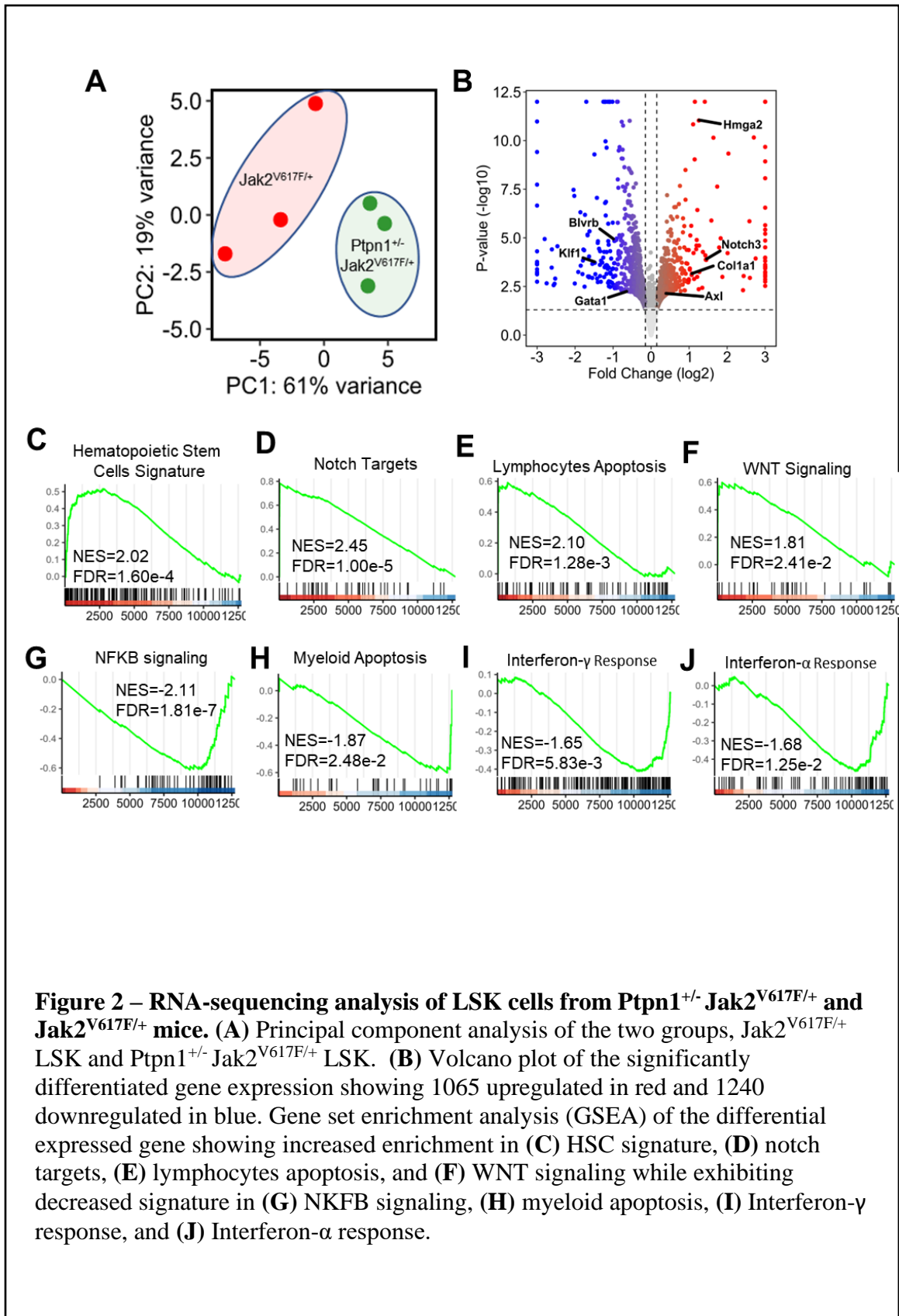


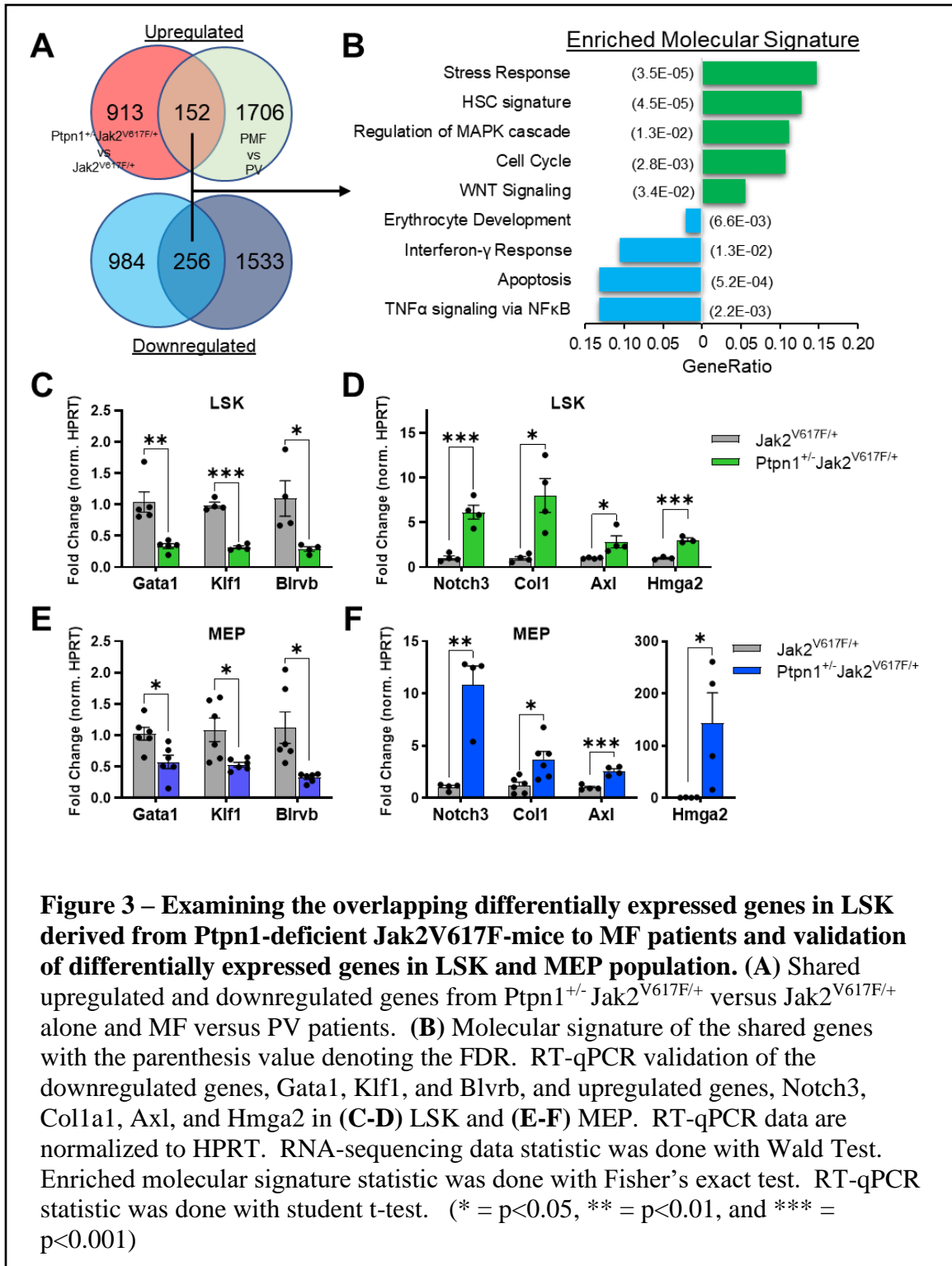
## **RNA-sequencing analysis to determine the effects of Ptpn1-deficiency on gene expression changes in Jak2<sup>V617F</sup> mice hematopoietic progenitors**

To investigate the mechanisms by which Ptpn1 deficiency contributes to the progression of MPN, we performed RNA-sequencing on sorted LSK cells from Ptpn1<sup>+/-</sup> Jak2<sup>V617F/+</sup> and Jak2<sup>V617F/+</sup> mice. The principal component analysis (PCA) showed a discernable separation between Ptpn1<sup>+/-</sup> Jak2<sup>V617F/+</sup> and Jak2<sup>V617F/+</sup> mice LSK cells (Figure 2A). The volcano plot revealed 1065 significantly upregulated genes and 1240 significantly downregulated genes when comparing Ptpn1-deficient Jak2<sup>V617F/+</sup> against Jak2<sup>V617F/+</sup> alone (Figure 2B). Gene set enrichment analysis (GSEA) showed an increased signature of HSC, notch targets, lymphocytes apoptosis, and WNT signaling (Figure 2C-F), while exhibiting a significant decrease in the enrichment of NKFB signaling, myeloid apoptosis, and interferon- $\alpha/\gamma$  signatures (Figure 2G-J).

Next, we aimed to assess the extent to which Ptpn1-deficient Jak2<sup>V617F/+</sup> LSK altered gene expression corresponds with that of MF patients versus that of PV patients. We identified 152 significantly upregulated genes and 256 downregulated genes (Figure 3A). The molecular signature of these shared upregulated genes is enriched stress responses, HSC signature, regulation of MAPK, cell cycle, and WNT signaling, while the shared downregulated genes are enriched in erythrocytes regulation, IFN- $\gamma$  responses, apoptosis, and TNF $\alpha$  signaling via NF- $\kappa$ B (Figure 3B). The reduction in IFN- $\alpha/\gamma$  response is an interesting observation as IFN- $\alpha$  is used in the treatment of ET and PV<sup>10</sup>. However, IFNs are known to be a negative regulator of HSC proliferation, and prolonged exposure can lead to a diminished response and give rise to MK-biased HSCs<sup>11-13</sup>.

Using RT-qPCR, we validated the downregulated genes *Gata1*<sup>14</sup>, *Klf1*<sup>15</sup>, and *Blvrb*<sup>16</sup>, and upregulated genes *Notch3*<sup>17</sup>, *Coll1a1*<sup>18</sup>, *Axl*<sup>19</sup>, and *Hmga2*<sup>20</sup> in LSK cells (Figure 3C-D). These genes play a significant role in enhancing HSC proliferation and megakaryopoiesis, reducing erythropoiesis, and the development of myelofibrosis. We also validated these genes in the MEP population and found similar changes (Figure 3E-F). Overall, *Ptpn1* deficiency alters gene expression in *Ptpn1*<sup>+/-</sup> *Jak2*<sup>V617F/+</sup> mice hematopoietic progenitors, which may contribute to the progression of MPN.







## **PTPN1 deficiency hyperactivates JAK-STAT signaling.**

PTPN1's effects have been observed in the direct modulation of JAK-STAT signaling through its direct targeting of JAK2<sup>5,6</sup>. We wanted to assess whether such modulation occurs in the context of JAK2V617F mutation. Using CRISPR-mediated deletion of PTPN1/Ptpn1 in Ba/F3 (mouse pro-B cells) expressing the EpoR JAK2V617F mutation, HEL (human erythroid leukemic) cells, and SET2 (human megakaryoblastic leukemic) cells, we observed systemic hyperphosphorylation of tyrosines in all three cell types (Figure 4A). Direct examination of the JAK-STAT signaling in all three cell lines showed a robust increase in phosphorylation of STAT5, STAT3, STAT1, and ERK1/2 in absence of PTPN1 (Figure 4B). Examining the bone marrow of our control, Ptpn1<sup>+/-</sup>, Jak2<sup>V617F/+</sup>, Ptpn1<sup>+/-</sup> Jak2<sup>V617F/+</sup> mice, we also observed significant phosphorylation of Stat5, Stat3, Stat1, and Erk1/2 (Figure 4C). Repeated assessment with homozygous deletion of Ptpn1 in context Jak2V617F yield a similar increase in phosphorylation (Figure 4D). Interestingly, Stat3 and Stat1 phosphorylation appears more prominent in Ptpn1 deficiency. In addition, we also observed a significant increase in the phosphorylation of NFkB. Together, these data suggest significant upregulation of the JAK/STAT signaling with greater involvement of STAT1 and STAT3 activity in PTPN1 deficiency.

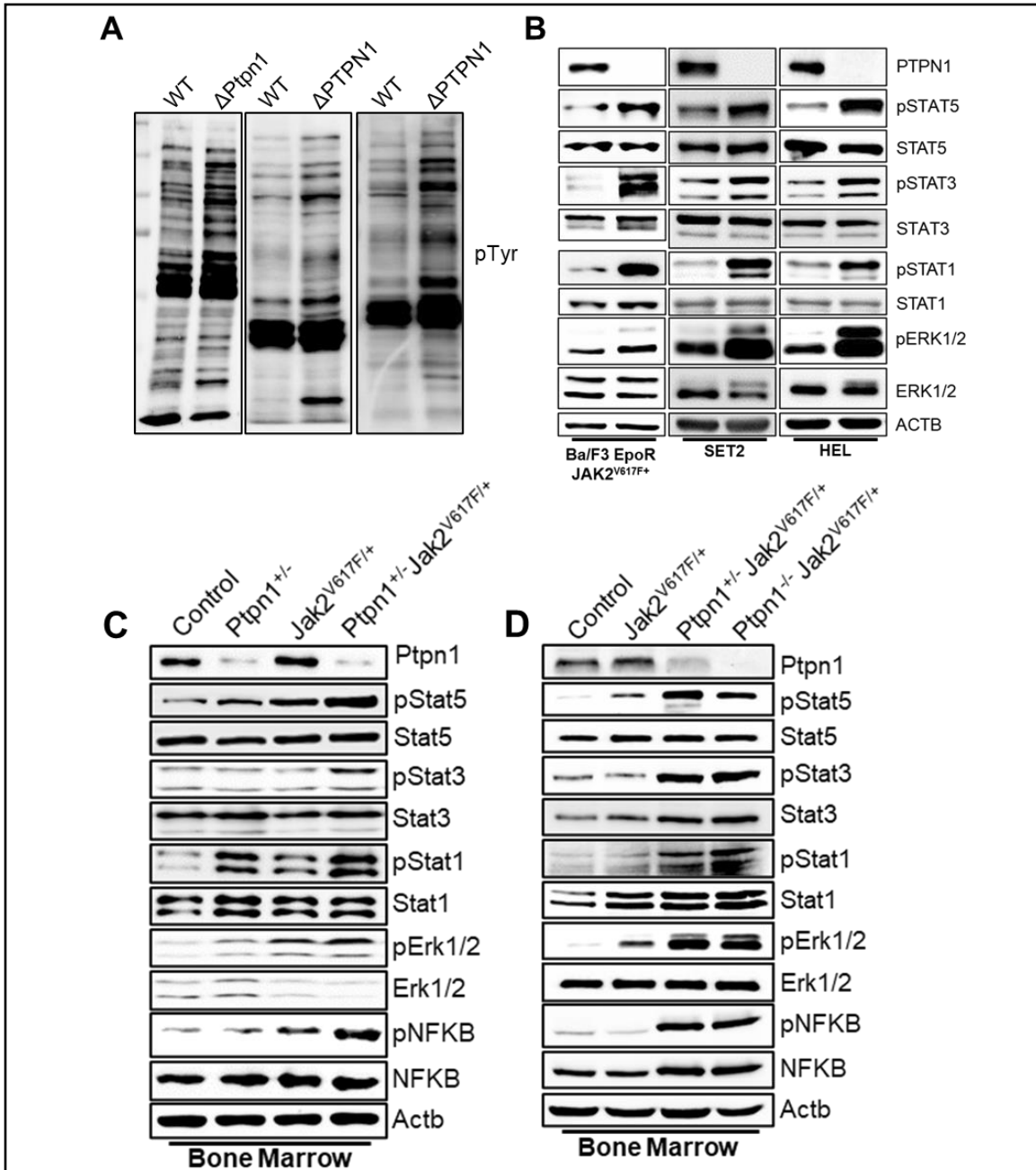


**Figure 4 – PTPN1 deficiency results in hyperphosphorylation of JAK2 signaling.** (A) Total tyrosine phosphorylation using 4G10 antibodies in Ba/F3 EpoR  $JAK2^{V617F/+}$  cells, SET2 cells, and HEL cells. (B) Hyperphosphorylation of STAT5, STAT3, STAT1, and ERK1/2 in PTPN1/Ptpn1 knocked out. (C) Phosphorylation of Stat5, Stat3, Stat1, Erk1/2, and NFKB in control, Ptpn1<sup>+/-</sup>,  $JAK2^{V617F/+}$ , and Ptpn1<sup>+/-</sup>  $JAK2^{V617F/+}$  mouse bone marrow. (D) Phosphorylation of same targets in homozygous deletion of Ptpn1.

## **Identification of novel targets of PTPN1 as a potential contributing factor to MPN progression.**

Although hyperphosphorylation of JAK-STAT signaling is a key factor in the progression of MPN, the significantly enhanced tyrosine phosphorylation seen in PTPN1-deleted JAK2<sup>V617F</sup>-positive cells suggests that other targets may also play a role in contributing to the disease phenotype. To identify these targets, we used a substrate-capturing mutant of PTPN1, PTPN1-D181A (PTPN1-DA), to perform co-immunoprecipitation (Co-IP). To maximize the potential targets, we established a two-systems approach that isolates the capture PTPN1 while separately providing it with hyperphosphorylated targets. This separate system is essential because the generation of hyperphosphorylated targets requires complete and irreversible inhibition of all phosphatases using pervanadate. The process is outlined in the diagram in Figure 5A.

To demonstrate the efficacy of this approach, we compared PTPN1-DA with PTPN1-WT and an EV negative control. Using mouse *Ptpn1*-DA and *Ptpn1*-WT, we captured hyperphosphorylated targets from Ba/F3 VF, and observed robust target capture in *Ptpn1*-DA, but little to no target in *Ptpn1*-WT (Figure 5B). To ensure the integrity of our system, we first verified that our pull-down targets were derived from the substrate (Figure 5C). We then assessed the total tyrosine phosphorylation of the substrates after incubation with the enzyme to confirm the functionality of wild-type *Ptpn1* phosphatase (Figure 5D).

We then assessed the robustness of our approach by repeating the process using hyperphosphorylated targets derived from Jak2<sup>V617F/+</sup> and wild-type BM (Figure 5E).

With the exception of greater phosphorylation in Jak2<sup>V617F/+</sup> compared to the control, the targets captured by Ptpn1-DA appear similar. We also evaluate the system in human SET-2 cells and also demonstrated similar pulldown from this approach in human cells (Figure 5F). Interestingly, although PTPN1-DA was able to isolate PTPN1's targets robustly in this system, we observed different patterns and intensities of the isolated protein between the samples of Ba/F3 VF, mouse BM, and SET2 cells. This may be attributed to differences in the expression level of the targeted protein in each substrate.

While the phosphorylation data from the western blot provided a great insight into the robust targeting of PTPN1, the identity of these targets is still unknown. To identify these targets, we used Ba/F3 VF's Co-IP targets from Ptpn1-DA for mass spectrometry. Figure 6A shows some of the identified targets. We directly probed for PLCG2 and PTK2B (also referenced as FAK2 or PYK2) and validated their interaction with PTPN1 in Ba/F3 VF, SET2, and mouse BM (Figure 6B-D). Validating PLCG2 and PTK2B from multiple sources confirms their robust involvement with PTPN1. Furthermore, we validated our process with established PTPN1 targets, including JAK2 and MET. Reverse Co-IP using PTK2B captured substrate carrying Ptpn1-DA but not WT indicating PTK2B as a direct substrate of PTP N1 (Figure 6E). Next, we assessed the phosphorylation status of these targets in our CRISPR-deleted cells and mouse BM. All three hematopoietic cells, Ba/F3 VF, HEL, and SET2, exhibited hyperphosphorylation of PLCG2 and PTK2B, as well as targets like MET and SRC (Figure 6F-G). Overall, we established a robust co-immunoprecipitation system that identified novel targets of PTPN1, such as PTK2B and PLCG2, which become hyperphosphorylated on Ptpn1 deficiency.

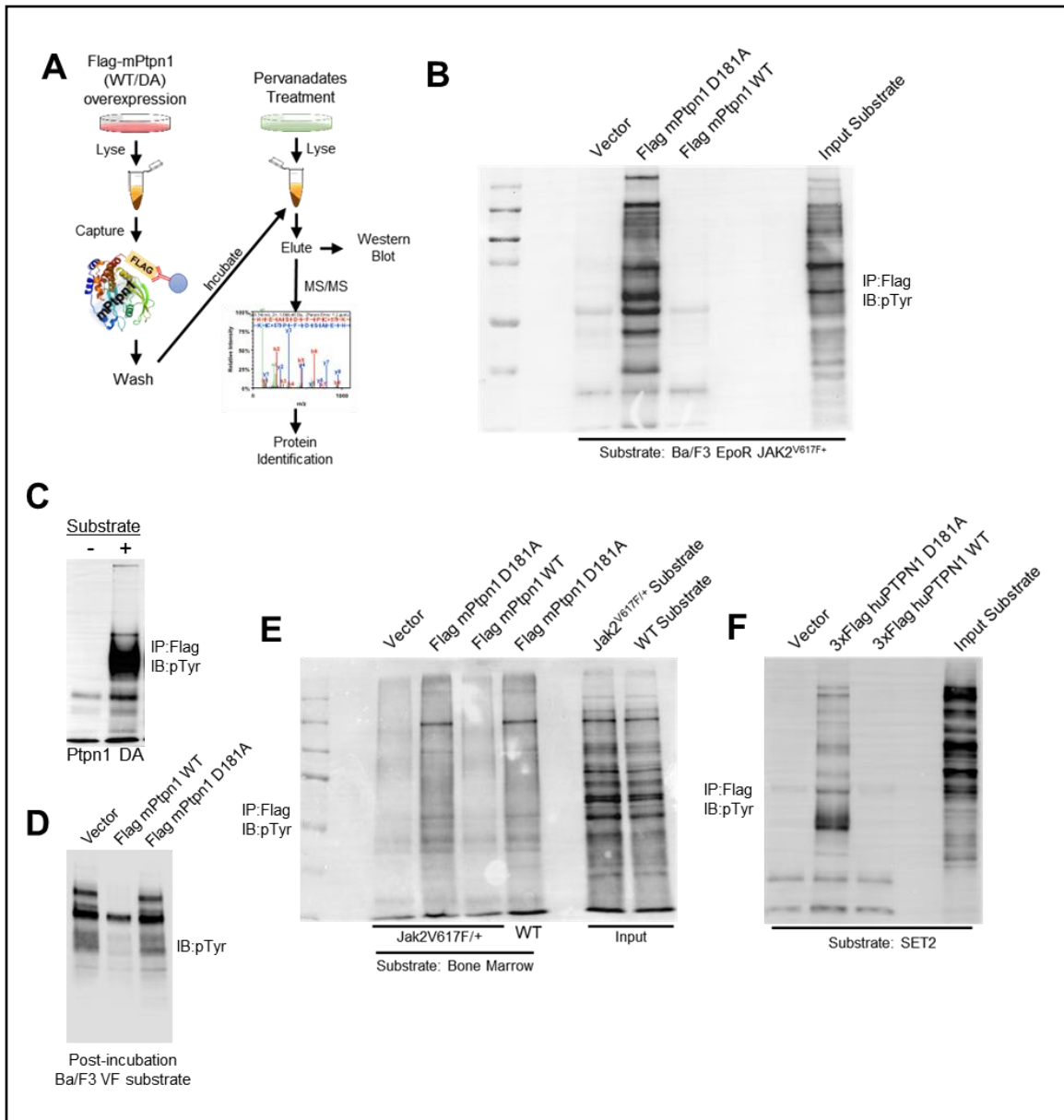


**Figure 5 – Two-system co-immunoprecipitation provides a robust method to pulldown PTPN1 substrates.** (A) Diagram of the generalized approach to the (Co-IP) process. (B) Co-IP using empty vector, mPtpn1-D181A, and mPtpn1-WT on hyperphosphorylated Ba/F3 EpoR VF substrates. (C) The absence of substrates yielded no pulldown in Ptpn1-D181A. (D) Tyrosine phosphorylation of unbound substrates after incubating with empty vector, mPtpn1-WT, and mPtpn1-D181A. (E) Co-IP using wild-type and Jak2<sup>V617F/+</sup> mouse bone marrow cells as substrates. (F) Two-system approach using human PTPN1 construct and human SET2 cells as substrates.

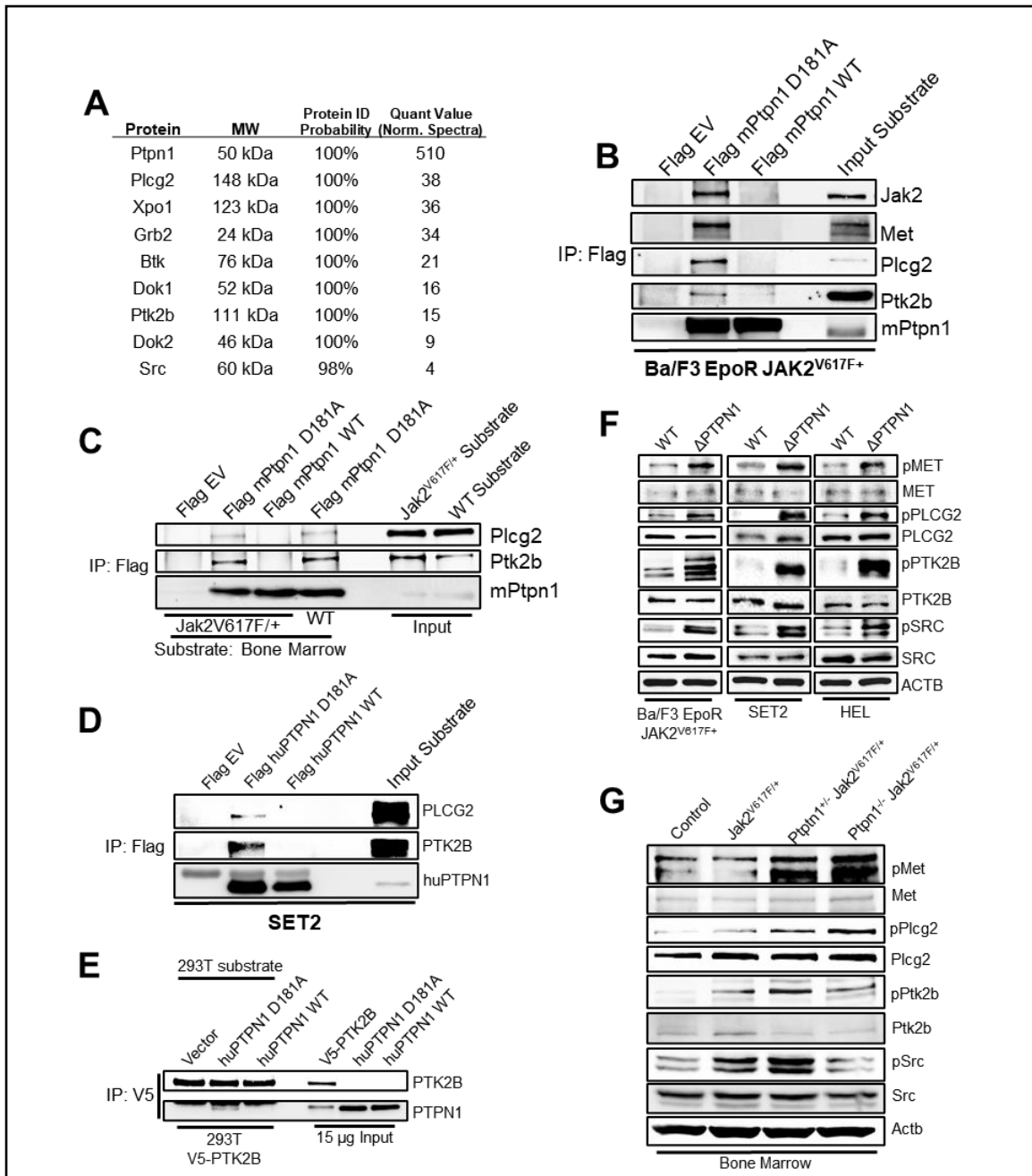


**Figure 6 – The identification of multiple targets including PTK2B as a direct substrate of PTPN1 and are robustly phosphorylated in PTPN1-deficiency.** (A) List of interesting targets of PTPN1 from mass spectrometry. (B) Validation of Plcg2 and Ptk2b as targets in Ba/F3 EpoR JAK2<sup>V617F/+</sup> substrates, in addition to the known targets, Jak2 and Met. (C) Plcg2 and Ptk2b are also directly identified in WT and Jak2<sup>V617F/+</sup> BM substrates, as well as (D) human SET2 cells. (E) Reverse capture of PTPN1-D181A using 293T cells overexpressing V5-PTK2B. Targets like Met, Plcg2, Ptk2b, and Src are hyperphosphorylated in (F) PTPN1-deleted Ba/F3 VF, SET2, and HEL cells, as well as (G) mouse bone marrow.

### **The deficiency of PTPN1 reduces sensitivity to Ruxolitinib.**

The accelerated fibrosis and hyperactivation of JAK2-mediated signaling in PTPN1 deficiency raise questions concerning the potential consequences this may have on patients' therapeutic approaches. We decided to assess the impact of PTPN1 deficiency on the sensitivity of a well-established JAK inhibitor, ruxolitinib. We treated native and PTPN1 knockout HEL and SET2 cells with a concentration gradient of ruxolitinib and fitted them with sigmoidal least square regression to calculate the IC<sub>50</sub>. PTPN1-deleted HEL exhibited a significant alteration in ruxolitinib sensitivity by shifting the IC<sub>50</sub> from 0.207 μM to 0.512 μM (Figure 7A). PTPN1-deleted SET2 cells shifted IC<sub>50</sub> from 0.147 μM to 0.470 μM (Figure 7B). This reduced sensitivity is also observed in the non-clonally selected HEL and SET2 cells as well as the PTPN1-deficient lineage-depleted bone marrow cells (Figure 7C-E).

The inhibition of JAK signaling by ruxolitinib dose-dependently abrogates the downstream phosphorylation of STAT1/3/5 and ERK1/2. PTPN1 deletion in HEL and SET2 cells shows greater preservation of phosphorylation status of STAT5, STAT3, STAT1, and ERK1/2 signaling which may explain the reduction in cell sensitivity to ruxolitinib (Figure 7C-D). Interestingly, the phosphorylation of PTK2B is minimally affected by ruxolitinib and may serve as a potential therapeutic target in combination. This significant reduction in ruxolitinib sensitivity demonstrates the importance of PTPN1 expression in MPN's therapeutic efficacy.

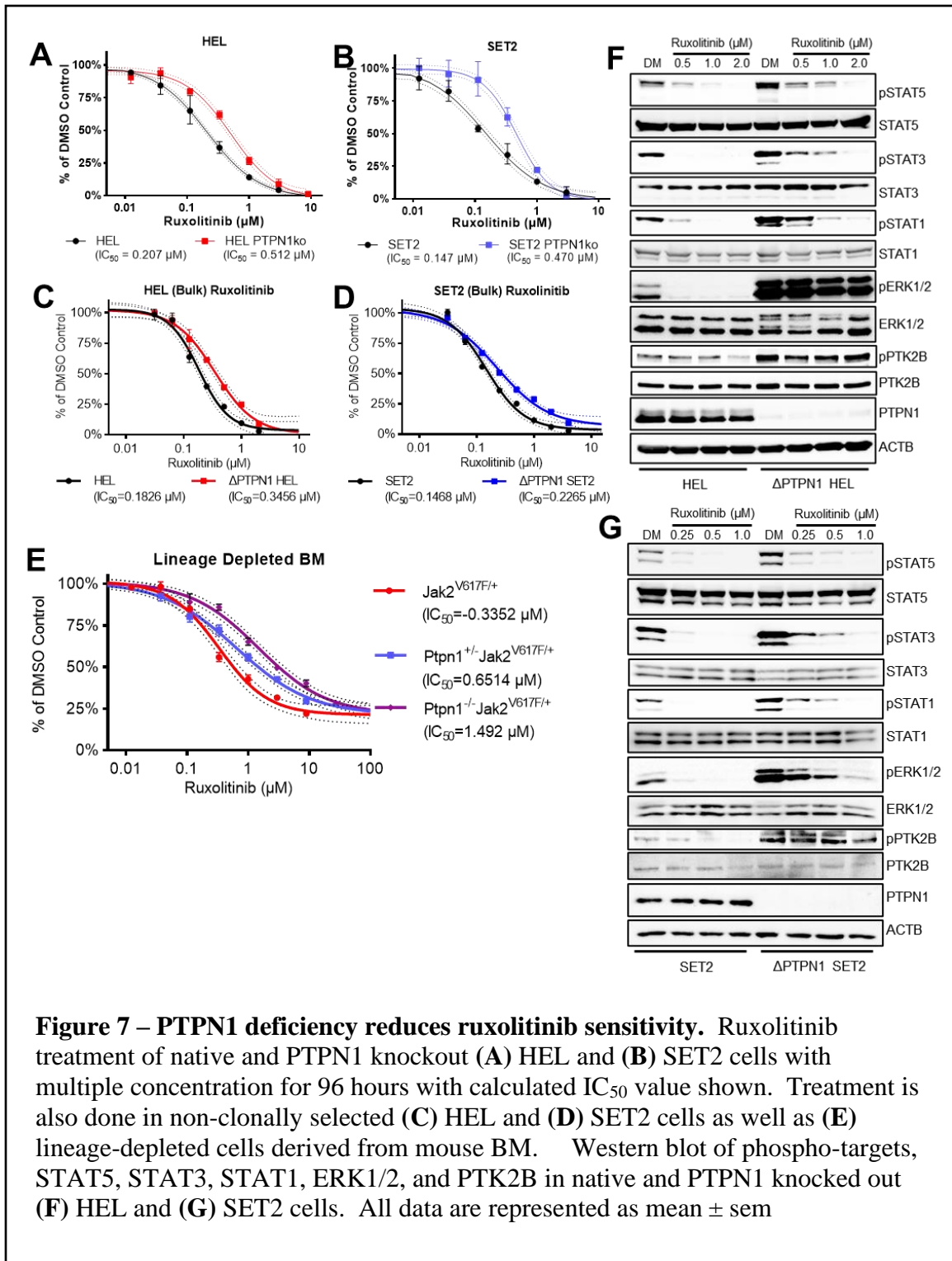
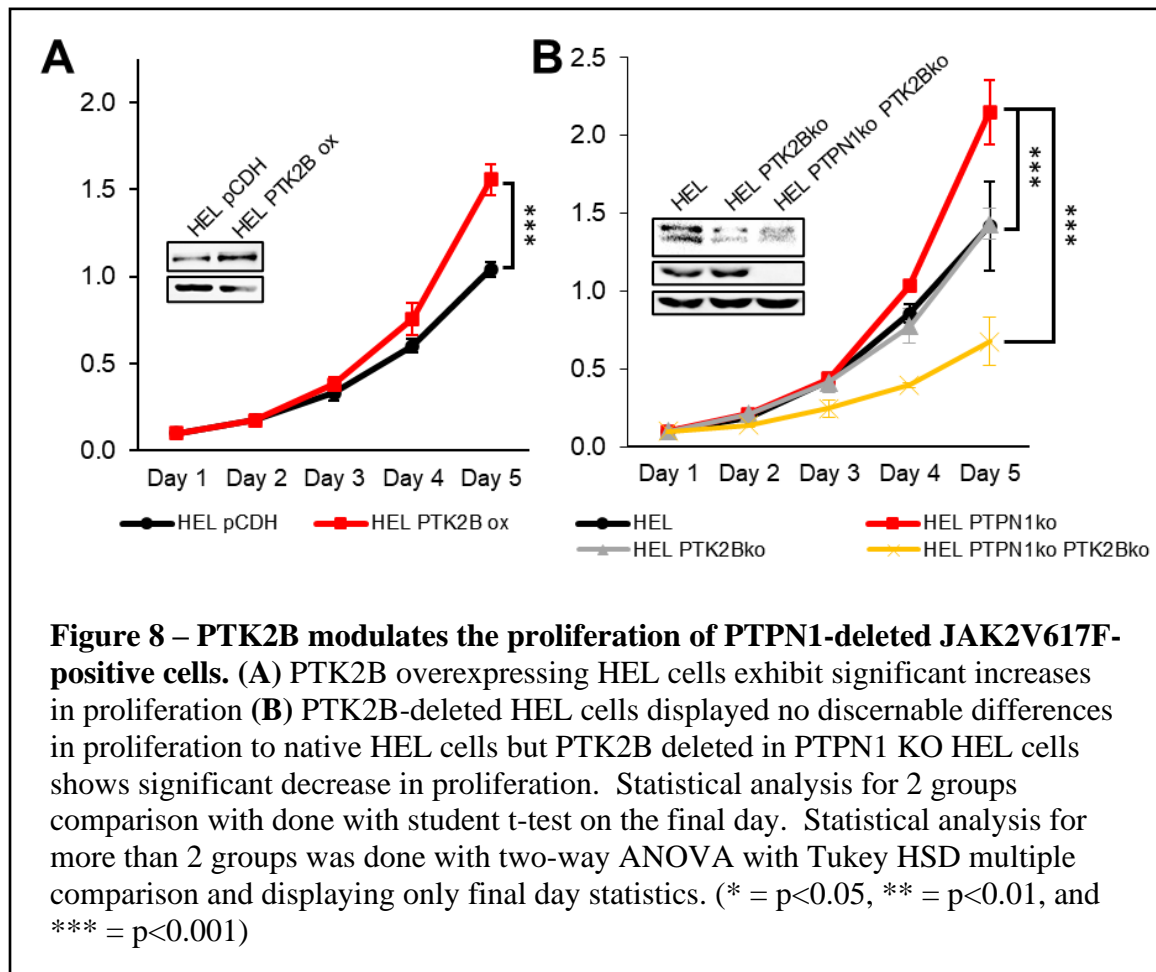


**Figure 7 – PTPN1 deficiency reduces ruxolitinib sensitivity.** Ruxolitinib treatment of native and PTPN1 knockout (A) HEL and (B) SET2 cells with multiple concentration for 96 hours with calculated  $IC_{50}$  value shown. Treatment is also done in non-clonally selected (C) HEL and (D) SET2 cells as well as (E) lineage-depleted cells derived from mouse BM. Western blot of phospho-targets, STAT5, STAT3, STAT1, ERK1/2, and PTK2B in native and PTPN1 knocked out (F) HEL and (G) SET2 cells. All data are represented as mean  $\pm$  sem



## PTK2B modulates the proliferation of PTPN1-deleted JAK2V617F-positive cells.

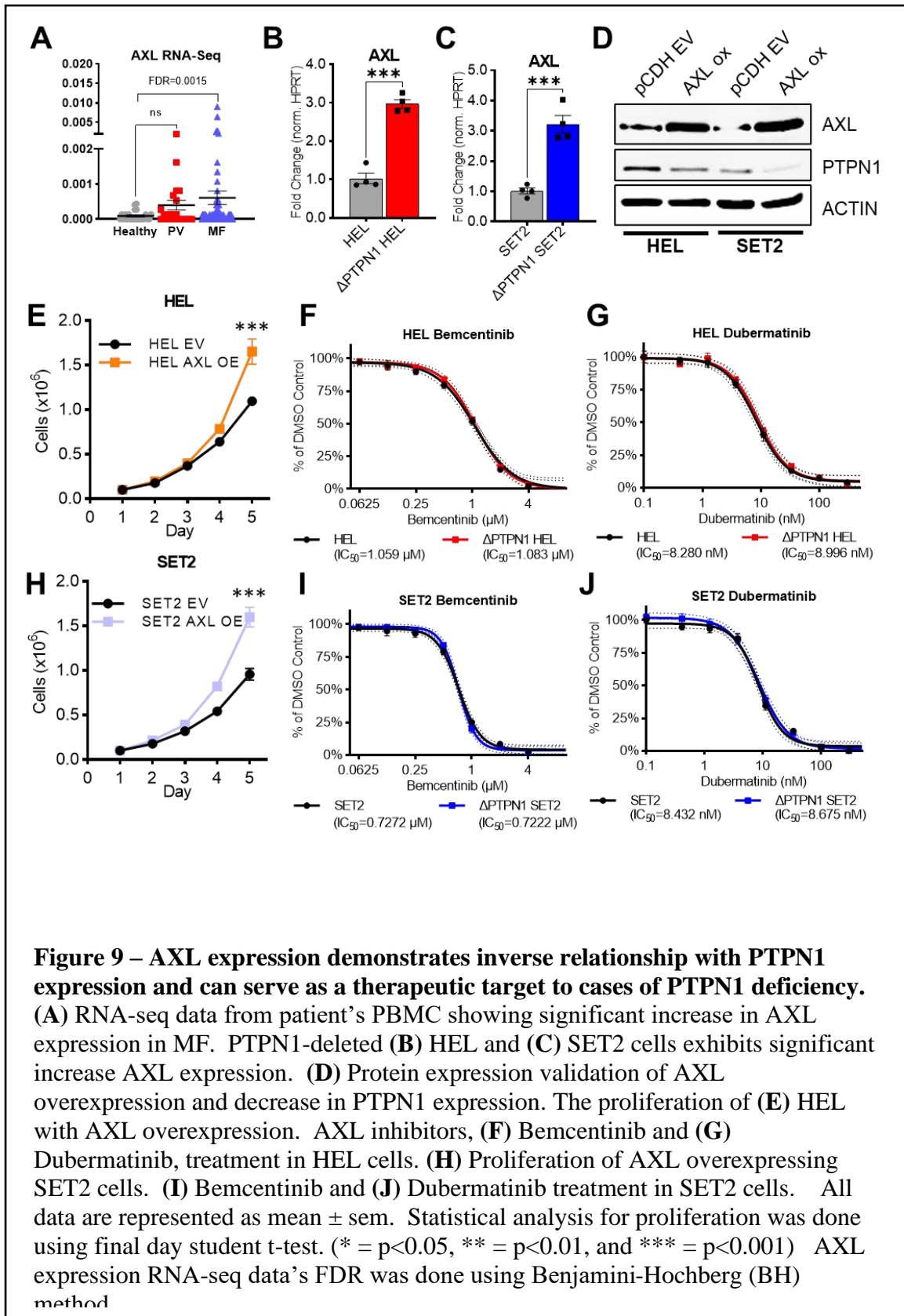
Being a direct substrate of PTPN1, we want to assess the role of PTK2B. The overexpression of PTK2B in HEL cells significantly increases proliferation (Figure 8A). However, the reduction of expression by CRISPR yields no significant changes in proliferation. On the other hand, PTK2B deficiency in PTPN1-knockout HEL cells significantly reduces proliferation (Figure 8B). This indicates the pivotal role of PTK2B in PTPN1-deficient proliferation increase.



**AXL expression demonstrates an inverse relationship with PTPN1 expression and can serve as a therapeutic target for cases of PTPN1 deficiency.**

Ptpn1-deficient Jak2<sup>V617F/+</sup> mice showed a significant increase in AXL expression in LSK and MEP populations. AXL has been observed to be increased in CD34+ cells of patients with JAK2V617F mutation<sup>19</sup>. This increased AXL expression is also observed in MF patients as well as PTPN1-deleted HEL and SET2 cells (Figure 9A-C).

Interestingly, the direct overexpression of AXL results in a reduction of PTPN1 expression in both cell types (Figure 9D). The consequences of this direct AXL overexpression also result in a significant increase in HEL cell proliferation (Figure 9E). Next, we wanted to examine the potential of targeting AXL as a therapeutic option in this PTPN1-deficient situation. Using two known inhibitors, bemcentinib and duberminib, we treated native and PTPN1-deleted HEL cells and observed indiscernible differences in the efficacy between the two cells (Figure 9F-G). This indicates the inhibition of AXL is a potential therapeutic option in the situation of PTPN1 deficiency-induced ruxolitinib insensitivity. This observation of AXL-mediated proliferation increases and indifference sensitivity to AXL inhibitors is also observed in SET2 cells (Figure 9H-J). Overall, the data suggest the inverse relationship between PTPN1 and AXL expression, and targeting AXL can be a valuable approach in the situation of ruxolitinib insensitivity.



### **3.3 – Methods**

#### **Cell culture**

Murine Ba/F3 cells with stable ectopic expression of EpoR carrying the JAK2V617F mutation, human erythroid leukemic cells (HEL), and megakaryoblastic leukemia cells (SET-2) were cultured in RPMI-1640 medium supplemented with 10% FBS and 1x Penicillin-Streptomycin (P/S) solution (Corning # 30-002-CI). HEK293T cells were used for transfection and lentiviral production and were cultured in DMEM medium supplemented with 10% FBS and 1X P/S. Cells were transduced with lentiviruses and selected in puromycin for 2-3 days. CRISPR-mediated cell lines were clonally selected. Cell proliferation was measured by manual counting daily for 4-5 days after equalizing the starting cell count.

#### **Plasmids**

PTPN1/Ptpn1 WT and DA were acquired from subcloned into pCDH vector and added C-terminal Flag tag. CRISPR sgRNAs used for PTPN1/Ptpn1 deletion are listed in the table below and were subcloned into LentiCRISPRv2-puro construct (Addgene Plasmid #98290). PTK2B plasmid was purchased from Addgene (#127233) and subcloned into pCDH. PTK2B CRISPR sgRNA used for PTK2B deletion is listed below. AXL plasmid was purchased from Addgene (#14998) and subcloned into pCDH.

### **MK/MSC cultures and MK colony assay**

BM was cultured for 21 days in DMEM medium supplemented with 10% FBS, 1X P/S, and non-essential amino acids (NEAA) to generate MSCs. For megakaryocytic culture, BM was cultured for 4 days in StemPro-34 SFM (ThermoFisher) medium supplemented with nutrient supplements, 2mM L-glutamine, Tpo (50ng/mL), and SCF (20 ng/mL) (MK media). MK proliferation was performed for 5 days in fresh MK media after establishing megakaryocytic culture. Before transferring the media to MSCs, MKs were cultured in fresh MK media for 48 hours and then incubated with MSCs for another 48 hours.

### **Real-time quantitative PCR**

Total RNA extraction of sorted LSK (Lin-Sca1+cKit+) cells, megakaryocytes, and JAK2V617F-positive hematopoietic cell lines were completed with RNeasy Mini or Micro Kit (QIAGEN). RNAs derived from LSK were prepped to cDNA using QuantiTect Reverse Transcription Kit (QIAGEN). The cell line's RNAs were converted to cDNA using High-Capacity cDNA Reverse Transcription Kit (Applied Biosystems). Real-time PCR was performed with Quantstudio3 (Applied Biosystems). The readout was measured with SYBR green using the SYBR Green PCR master mix (QuantaBio). All data were normalized with HPRT1/Hprt1 or GAPDH/Gapdh and fold changes were calculated by  $\Delta\Delta C_t$ .

### **Immunoblotting**

Cells were lysed using RIPA lysis buffer containing protease inhibitors.

Immunoprecipitation (IP) was carried out using HEK293T cells overexpressing FLAG-

tagged PTPN1/Ptpn1 WT & DA and pulled down with a FLAG antibody. The IP was allowed to incubate overnight under Triton-X lysis buffer (without EDTA and 1 mM EGTA) with protease inhibitors and sodium orthovanadate (phosphatase inhibitors). After overnight incubation, the pulldown PTPN1 WT/DA was washed 3 times and placed in Triton-X lysis buffer with 2 mM EDTA, and incubated for another 30 minutes on ice. Target cells were pre-treated with 1 mM pervanadate (a 1:1 mixture of 1M sodium orthovanadate and 1M H<sub>2</sub>O<sub>2</sub>) for 30 minutes and lysed in Triton-X lysis buffer with protease inhibitor but without sodium orthovanadate. The lysates were incubated with the pulled-down PTPN1 for 30 minutes at 4°C and then washed 3 times before adding SDS lysis buffer directly.

### **RNA-sequencing Analysis**

RNA isolation was done similarly to real-time qPCR. Sequencing RNA was collected using Poly-A selection (NEB). The library preparation process was done using NEB Ultra II Directional RNA Library Kit and carried out using manufacturer protocol. Quality assessment was made using Bioanalyzer for optimal fragment size. Samples were sent to Novogene for sequencing. Received data was given in FASTQ format and an integrity check using MD5SUM was completed. FASTQ data processing was done using fastp for trimming and QC, HISAT2 for alignment to mouse references genome GRCm38, samtools for conversation to BAM files, and Subread/FeatureCounts was used for collecting gene count data. Differential gene expression, PCAplot, volcano plot, molecular signature, and GSEA were completed in R using a combination of packages: DESeq2, Ensembl, ggplot2, enrichplot, and clusterProfiler.

## Data and Statistical Analysis

All data management and graphing were completed using a combination of EXCEL, GraphPad Prism, and R. For two-group analyses, a student's t-test was used to determine statistical significance. For comparison of more than two groups, one-way ANOVA with posthoc Tukey-HSD test was performed to assess statistical significance. Two-way ANOVA with posthoc Tukey-HSD test was performed for multiple time points and multiple groups comparison. Only the final statistics are displayed. Drug IC<sub>50</sub> was calculated after establishing sigmoidal interpolation from the provided data in GraphPad Prism. All data are expressed in mean ± SEM.

## sgRNA Primer Table

Name	Sequence
huPTPN1_sg_E8_FWD	GGATAAAGACTGCCCCATCA
huPTPN1_sg_E8_REV	TGATGGGGCAGTCTTTATCC
huPTPN1_sg_E9_FWD	GTTAGAAGTCGGGTCGTGGG
huPTPN1_sg_E9_REV	CCCACGACCCGACTTCTAAC
huPTPN1_sg_E4_FWD	GTGTGGGAGCAGAAAAGCAG
huPTPN1_sg_E4_REV	CTGCTTTTCTGCTCCCACAC
huPTPN1_sg_E6_FWD	TCTGTCTGGCTGATACCTGC
huPTPN1_sg_E6_REV	GCAGGTATCAGCCAGACAGA
mPtpn1_sg_E2_FWD	ATGCAAAGTCGCGAAGCTTC
mPtpn1_sg_E2_REV	GAAGCTTCGCGACTTTGCAT
mPtpn1_sg_E3_FWD	GAGGAGCTATATTCTCACCC
mPtpn1_sg_E3_REV	GGGTGAGAATATAGCTCCTC
mPtpn1_sg_E4_FWD	GCCCTTTACCAAACACATGT
mPtpn1_sg_E4_REV	ACATGTGTTTGGTAAAGGGC
mPtpn1_sg_E6_FWD	GCGCCGGCATCGGGAGGTCA
mPtpn1_sg_E6_REV	TGACCTCCCGATGCCGGCGC

## qPCR Primer Table

Name	Sequence
mPtpn1_RT_294F	CGGAACAGGTACCGAGATGT
mPtpn1_RT_452R	GAAGTGCCACATGTGTTTG
huPTPN1_RT_553F	CCTGAATCACCCAGCCTCATT
huPTPN1_RT_697R	AGAGGCAGGTATCAGCCAGA
mGapdh_RT_Fwd	ACTCCACTCACGGCAAATTC
mGapdh_RT_Rev	TCTCCATGGTGGTGAAGACA
HuGAPDH_RT_20F	GAGTCAACGGATTTGGTCGT
HuGAPDH_RT_204R	GACAAGCTTCCC GTTCTCAG
mCol1A_F	CCTCAGGGTATTGCTGGACAAC
mCol1A_R	CAGAAGGACCTTGTTTGCCAGG
mNotch3_RT_1123F	ACAGGCCTCTTGTCATCTG
mNotch3_RT_1315R	CACACCGACCCAAATGTTTAC
mBlvrb_561F	AGTCAGGGCTGAAATACGTGG
mBlvrb_721R	TACTCATTGGTGGTGAGGCAC
mKlf1_109F	AGCTGAGACTGTCTTACCCTCC
mKlf1_218R	GTCTGAGGAGACGCAGGATTTG
mGata1_225F	TCAGGTGTATCCACTGCTCAAC
mGata1_391R	TGTTGTTGCTCTTCCCTTCC
mHmga2_153F	ACCCAAAGGCAGCAAAAAC
mHmga2_278R	GCAGGCTTCTTCTGAACGAC
mAxl_RT_1773F	GACGTCATGGTAGATCGGCAT
mAxl_RT_1892R	CTTCACAGCGACCTTGAGGAT



### 3.4 – References

1. Kralovics, R. *et al.* A Gain-of-Function Mutation of JAK2 in Myeloproliferative Disorders. *N. Engl. J. Med.* **352**, 1779–1790 (2005).
2. Teofili, L. *et al.* Different STAT-3 and STAT-5 phosphorylation discriminates among Ph-negative chronic myeloproliferative diseases and is independent of the V617F JAK-2 mutation. *Blood* **110**, 354–359 (2007).
3. Huang, Z. *et al.* STAT1 promotes megakaryopoiesis downstream of GATA-1 in mice. *J. Clin. Invest.* **117**, 3890–3899 (2007).
4. Tiedt, R. *et al.* Ratio of mutant JAK2-V617F to wild-type Jak2 determines the MPD phenotypes in transgenic mice. *Blood* **111**, 3931–3940 (2008).
5. Jobe, F. *et al.* Deletion of Ptpn1 induces myeloproliferative neoplasm. *Leukemia* **31**, 1229–1234 (2017).
6. Myers, M. P. *et al.* TYK2 and JAK2 Are Substrates of Protein-tyrosine Phosphatase 1B. *J. Biol. Chem.* **276**, 47771–47774 (2001).
7. Shivdasani, R. A., Fujiwara, Y., McDevitt, M. A. & Orkin, S. H. A lineage-selective knockout establishes the critical role of transcription factor GATA-1 in megakaryocyte growth and platelet development. *EMBO J.* **16**, 3965–3973 (1997).
8. Shin, E. *et al.* The Gata1 murine megakaryocyte–erythroid progenitor cells expand robustly and alter differentiation potential. *Biochem. Biophys. Res. Commun.* **528**, 46–53 (2020).
9. Malara, A., Abbonante, V., Zingariello, M., Franco Migliaccio, A. R. & Balduini, A. Megakaryocyte contribution to bone marrow fibrosis: many arrows in the quiver. *Mediterr. J. Hematol. Infect. Dis.* **10**, e2018068 (2018).
10. Yacoub, A. *et al.* Pegylated interferon alfa-2a for polycythemia vera or essential thrombocythemia resistant or intolerant to hydroxyurea. *Blood* **134**, 1498–1509 (2019).
11. Yang, L. *et al.* IFN- $\gamma$  Negatively Modulates Self-Renewal of Repopulating Human Hemopoietic Stem Cells. *J. Immunol.* **174**, 752–757 (2005).
12. Qin, Y. & Zhang, C. The Regulatory Role of IFN- $\gamma$  on the Proliferation and Differentiation of Hematopoietic Stem and Progenitor Cells. *Stem Cell Rev. Reports* **13**, 705–712 (2017).
13. Rao, T. N. *et al.* JAK2 -V617F and interferon- $\alpha$  induce megakaryocyte-biased stem cells characterized by decreased long-term functionality. *Blood* **137**, 2139–2151 (2021).
14. Sangiorgio, V. F. I., Nam, A., Chen, Z., Orazi, A. & Tam, W. GATA1 downregulation in prefibrotic and fibrotic stages of primary myelofibrosis and in

- the myelofibrotic progression of other myeloproliferative neoplasms. *Leuk. Res.* **100**, 106495 (2021).
15. Barbarani, G., Fugazza, C., Strouboulis, J. & Ronchi, A. E. The Pleiotropic Effects of GATA1 and KLF1 in Physiological Erythropoiesis and in Dyserythropoietic Disorders. *Front. Physiol.* **10**, (2019).
  16. Nesbitt, N. M. *et al.* Divergent erythroid megakaryocyte fates in Blvrb-deficient mice establish non-overlapping cytoprotective functions during stress hematopoiesis. *Free Radic. Biol. Med.* **164**, 164–174 (2021).
  17. Xiu, M. *et al.* The Role of Notch3 Signaling in Cancer Stemness and Chemoresistance: Molecular Mechanisms and Targeting Strategies. *Front. Mol. Biosci.* **8**, (2021).
  18. Yao, J.-C. *et al.* TGF- $\beta$  Signaling Contributes to Myelofibrosis and Clonal Dominance of Myeloproliferative Neoplasms. *Blood* **134**, 470–470 (2019).
  19. Pearson, S., Blance, R., Somerville, T. C. P., Whetton, A. D. & Pierce, A. AXL Inhibition Extinguishes Primitive JAK2 Mutated Myeloproliferative Neoplasm Progenitor Cells. *HemaSphere* **3**, e233 (2019).
  20. Dutta, A., Hutchison, R. E. & Mohi, G. Hmga2 promotes the development of myelofibrosis in Jak2V617F knockin mice by enhancing TGF- $\beta$ 1 and Cxcl12 pathways. *Blood* **130**, 920–932 (2017).

## CHAPTER IV

### Discussion

Deletion of chromosome 20q is a karyotypic abnormality associated with myeloid malignancies, especially myeloproliferative neoplasms (MPN). However, the key tumor suppressor gene(s) involved in this pathogenesis have remained elusive. While the del20q prognosis in myelodysplastic syndrome (MDS) can range from neutral to favorable, it carries a more intermediate prognosis value in MPN. The importance of this association is more pressing when we observe an increased risk of disease progression, especially in the case of polycythemia vera (PV) when del20q is present. In this study, we have demonstrated a frequent association of PTPN1 deletion in del20q in patients and its significant overlap with JAK2V617F mutation in myelofibrosis. Using conditional knock-in of the Jak2V617F mutation and knock-out of Ptpn1 in a murine model, we observed a significant increase in leukocytosis and thrombocytosis, with a rapid decline in RBC count in the blood of Ptpn1-deficient-Jak2<sup>V617F/+</sup> mice. Furthermore, the Ptpn1-deficient Jak2<sup>V617F/+</sup> mice exhibited an increased splenic burden and accelerated progression of the disease to myelofibrosis, with significant accumulation of bone marrow and splenic fibrosis. The overall increased disease burden and poorer survival indicate the pivotal role of Ptpn1 expression in Jak2V617F mutation.

Assessment of the hematopoietic compartment showed an increase in hematopoietic stem cells (HSC) with a preference for myeloid lineage and megakaryocyte differentiation in Ptpn1-deficient Jak2<sup>V617F/+</sup> mice. The myeloid cell preferential differentiation was observed through a significant expansion in Gr1<sup>+</sup>Mac1<sup>+</sup>

population, CFU-GM, CFU-GEMM, neutrophil, and monocytes. Similarly, the MK preferential differentiation was shown by a significant expansion in megakaryocyte-erythrocyte progenitor (MEP), CFU-Mk, CD41<sup>+</sup>CD61<sup>+</sup> population, and platelets. This MK expansion was also visualized in the H&E-stained bone marrow and spleen sections, revealing extensive MK clusters. Furthermore, after a prolonged period, Ptpn1 deficiency by itself also displayed a similar MK-bias property through the expansion of CFU-Mk, CD41<sup>+</sup>CD61<sup>+</sup>, and platelets. These findings indicate a unique role of Ptpn1 in modulating megakaryopoiesis.

To ensure the phenotype we observed is cell intrinsic, we carried out a bone marrow transplantation of the experimental cohorts and recapitulated the phenotype observed in the primary model. We also demonstrated a significant clonal advantage of Ptpn1-deficient Jak2<sup>V617F/+</sup> cells over that of Jak2<sup>V617F/+</sup> alone by competitive reconstitution assay. Finally, we ascertained the role of Ptpn1 expression itself by further reducing its expression with homozygous deletion and demonstrated a more severe phenotype with greater morbidity and faster progression.

### **Thrombopoietin (TPO) in Myelofibrosis**

Previous studies have shown that excessive thrombopoietin (TPO) fuels megakaryocyte expansion, which subsequently leads to fibrosis and lethality in mice<sup>1</sup>. However, a comparative assessment of the peripheral blood serum yields no aberrant elevation of TPO in Ptpn1-deficient Jak2<sup>V617F/+</sup> mice. Instead, decreased serum TPO levels were observed. It is known that the physiological level of TPO is inversely proportional to the abundance of MK and platelets<sup>2</sup>. This is due to the consumption of

TPO in the activation of MPL (TPO receptor). This indicates to us that pathological production or accumulation of TPO is not the instigator of this observed expansion.

### **GATA1 deficiency in myelofibrosis**

Previous studies have demonstrated the role of GATA1 deficiency in megakaryocyte proliferation and the development of myelofibrosis<sup>3-6</sup>. It has also been noted that GATA1 is expressed at low levels in megakaryocytes of MF patients<sup>7</sup>. GATA1 belongs to a family of hematopoietic transcription factors known for binding the WGATAR motif and plays a significant role in hematopoietic regulation and development<sup>8,9</sup>. Our study has shown that Gata1 expression is significantly reduced in HSC, MEP, and megakaryocytes. The downregulation of GATA1 in MK coincides with a significant increase in MK proliferation. Our data from Ptpn1<sup>+/-</sup> Jak2<sup>V617F/+</sup> mice aligned with what has been observed in MF patients.

It is worth noting that in the low Gata1 mouse model, thrombocytopenia is observed along with increased MK due to a defective megakaryopoiesis process. However, the Gata1<sup>low</sup> model mouse utilizes genetic ablation of Gata1, which is an immutable process. In contrast, our Gata1 decrease is due to genetic repression by other factors and is thus much more dynamic, and unlikely to cause defective megakaryopoiesis. Furthermore, MF patients do not always exhibit thrombocytopenia<sup>10</sup>. Isolated MF CD34<sup>+</sup> cells have shown a greater propensity for MK production than CD34<sup>+</sup> cells derived from healthy or PV patients<sup>11</sup>. Typical causes of thrombocytopenia are drug-induced, such as ruxolitinib or hydroxyurea-induced cytoreduction, and severe fibrosis, which can compromise hematopoiesis. Along with fibrosis, this megakaryocyte

expansion is one of the major criteria established by the World Health Organization (WHO) for the diagnosis of myelofibrosis<sup>12</sup>.

### **Role of inflammatory in MPN progression**

Another major consequence of the increase in leukocytosis, megakaryocytes, and thrombocytosis is the elevation of pro-inflammatory cytokines secreted by them. Inflammation is an immune activation response to harmful stimuli, such as pathogens or tissue injuries<sup>13</sup>. Its activation supports the clearance and mitigation of the insults. However, dysregulation and the inability for cessation lead to chronic inflammation, which is implicated in the pathogenesis of MPN<sup>14</sup>. The inflammation process is stimulated by the secretion of pro-inflammatory cytokines, such as IL1B, TNF $\alpha$ , IFNs, IL6, and TGF $\beta$ <sup>15</sup>, many of which are elevated in the peripheral blood serum of Ptpn1-deficient Jak2<sup>V617F/+</sup> mice.

The serum level of IL1B and IL6 are significantly elevated in MPN patients, including myelofibrosis<sup>14,16</sup>. Murine model studies have demonstrated exogenous administration of IL1B accelerates the development of bone marrow fibrosis in the context of JAK2V617F mutation; while deletion of IL1 receptor ameliorates this fibrotic development and reduces disease burden<sup>17</sup>. IL1B, as well as TNF $\alpha$ , activation can increase the level of IL6 in serum<sup>18</sup>. Increased IL6 in the serum was first noted in cases of reactive thrombocytosis and was associated with increased platelet counts<sup>19</sup>. Outside of inflammation, IL6 is a major stimulator of multiple hematopoietic differentiation including T-cell, B-cell, erythrocytes, and megakaryocytes, as well as promoting HSC self-renewal<sup>20</sup>.

TGF $\beta$  is another major contributor to the development of myelofibrosis. Its native role contributes to embryonic development, tissue homeostasis, and hematopoietic cell development<sup>21</sup>. However, in malignancies, its aberrant expression and/or signaling pathways have been implicated in ET and MF. Reduced sensitivity to TGF $\beta$  inhibition has been observed in ET patients and hypothesized as a mean of ET development<sup>22</sup>. In both the excessive TPO and low GATA1 mice studies, TGF $\beta$  was significantly elevated and was associated with myelofibrosis development<sup>1,3</sup>. A study using isolated MK from MF patients showed increased production of TGF $\beta$  in the growth media compared to MK derived from healthy or PV patients<sup>11</sup>. In addition, TGF $\beta$  also contributes to collagen formation<sup>23</sup>. Our study has shown that Ptpn1<sup>+/-</sup> Jak2<sup>V617F/+</sup> mice have a significant increase in peripheral blood serum levels of TGF $\beta$ . Furthermore, using the media derived from Ptpn1<sup>+/-</sup> Jak2<sup>V617F/+</sup> MK induced wild-type MSCs to produce more collagen. While TGF $\beta$  may not be the only component in the media, it is likely to have contributed to the outcome.

TNF $\alpha$ , or tumor necrosis factor-alpha, is primarily produced by macrophages, and the signaling pathway induced by TNF $\alpha$  activates NF- $\kappa$ B<sup>24</sup>. While TNF $\alpha$  is elevated in MF patients, its pathogenesis is a bit more complex as TNF $\alpha$  can negatively regulate HSC self-renewal and expansions<sup>25</sup>. However, murine studies have demonstrated that this property only ends up facilitating increasing clonal advantages of JAK2V617F mutant clones as they have increased resistance to TNF $\alpha$  signaling<sup>26</sup>. Perhaps the elevation of TNF $\alpha$  is a self-antagonizing negative feedback loop that only ends up enriching the pathogenic cells. As such, TNF $\alpha$  inhibitors have been shown to alleviate some symptoms but have failed to control fibrosis<sup>27</sup>. Although we did not assess TNF $\alpha$

serum levels, we did detect an increase in phospho-NF- $\kappa$ B in the bone marrow of Ptpn1-deficient Jak2<sup>V617F/+</sup> mice. Our RNA-sequencing data also showed significant downregulation of the gene enrichment signature of TNF $\alpha$ -mediated signaling via NF- $\kappa$ B in LSK. This property may explain the drastic clonal advantages Ptpn1-deficient Jak2<sup>V617F/+</sup> LSK cells have over those of Jak2<sup>V617F/+</sup> alone.

Interferons (IFNs) are another set of common cytokines elevated in MPN patients. The family of IFNs consists of alpha ( $\alpha$ ), beta ( $\beta$ ), and gamma ( $\gamma$ ), although mostly alpha and gamma are associated with hematopoiesis. However, IFN- $\alpha/\gamma$  serves more of an antiproliferative and immunomodulatory role than actively driving disease progression<sup>28</sup>. IFNs inhibit human HSC colony formation *in vitro*<sup>29</sup>. In murine model, IFNs negatively affect HSC maintenance and perturb TPO-induced STAT5 signaling<sup>30</sup>. Interestingly, while negatively impacting TPO signaling, it does not impact megakaryopoiesis<sup>31</sup>. It is possible that the activation of STAT1, induced by IFN- $\gamma$ , circumvents this, as it has been shown to play a significant role in megakaryopoiesis<sup>32</sup>. IFNs also reduce erythropoiesis<sup>33</sup>. In turn, IFNs have been used for the past three decades in the treatment of MPNs and have shown great success as an alternative treatment to hydroxyurea<sup>28,34,35</sup>. While we did not assess the PB level of IFNs, Ptpn1-deficient Jak2<sup>V617F/+</sup> LSK exhibited negative enrichment of both IFN- $\alpha/\gamma$  responses. Similar to the TNF- $\alpha$  situation, this downregulation of IFN responses provides significant resistance to IFNs-induced inhibition that provide Ptpn1-deficient Jak2<sup>V617F/+</sup> cells greater clonal advantages, while hyperphosphorylation of Stat1 provides leverage for MK expansion and erythrocytes reduction. Because of this downregulated response to IFN- $\alpha/\gamma$ , it also raises a potential



question of the efficacy of IFN- $\alpha$  treatment in Ptpn1-deficient Jak2<sup>V617F/+</sup> cells and an inquiry for future assessment.

### **Associated genes in the progression of MPN**

In addition to the previously mentioned reduction in Gata1 expression, RNA-sequencing also reveals a significant reduction in Klf1 and Blvrb, while an increase in the expression of Hmga2, Notch3, Col1a1, and Axl. Kruppel-like factor 1 (KLF1) is associated with erythropoiesis and significantly involved in heme metabolism<sup>36</sup>; however, it antagonizes MK lineages. As such, the downregulation of KLF1 favors megakaryopoiesis over erythropoiesis<sup>37</sup>. Similarly, BLVRB, or biliverdin reductase, also plays a role in heme metabolisms<sup>38</sup>. The deficiency of BLVRB results in MK-bias<sup>39</sup>. Though the role of both of these genes still needs further exploration. Overall, the downregulation of BLVRB and KLF1 indicates diminished heme metabolism that affects erythrocyte differentiation in Ptpn1 deficient Jak2<sup>V617F/+</sup> LSK.

High-mobility group AT-hook 2 (HMGA2) exhibits a significant increase in LSK, which is further elevated in MEP. The gene is found to be upregulated in MF patients<sup>40</sup>. HMGA2 is a non-histone chromatin-binding protein that binds to the minor groove of the DNA helix<sup>41</sup>, and it regulates gene expression by inducing conformational changes on the DNA structure that either repress or promote the binding of transcription factors to the promoter<sup>42</sup>.

Mouse studies have shown that overexpression of HMGA2 with JAK2V617F mutation can enhance megakaryopoiesis and accelerate MF development<sup>43</sup>. The

significant upregulation of Hmga2 in Ptpn1<sup>+/-</sup> Jak2<sup>V617F/+</sup> LSK and MEP indicates that it is one potential source of enhanced megakaryopoiesis.

Upregulation of AXL has been observed in multiple cancers such as non-small cell lung carcinoma and acute myeloid leukemia. These increases are associated with drug resistance in both situations. Therefore, therapeutic targeting of this tyrosine kinase with Bemcentinib is in clinical trials (NCT02424617 [finished – no published results], NCT02488408 [ongoing], NCT03824080 [finished – no published results]).

AXL is a receptor protein tyrosine kinase that gets activated by its ligand, GAS6, and mediates signaling through PI3K/AKT, ERK, and PLC signaling<sup>44</sup>. Although it promotes cell survival and proliferation, its direct role with PTPN1 is still unclear. However, AXL inhibition has shown great efficacy in targeting JAK2 mutated cells<sup>45</sup>, indicating the potential overlapping role of AXL and PTPN1 in drug resistance.

The role of NOTCH3 and COL1A1 (Collagen I) is a bit more unique. NOTCH3 is a receptor protein that mediates cell-cell interaction and plays a significant role in cancer stemness<sup>46</sup> and platelet formation<sup>47</sup>. The signaling enrichment in Ptpn1 deficiency may serve to enhance stemness properties. However, its role in MPNs is poorly understood and requires further assessment to determine the impact.

The increase in Collagen I is interesting because it significantly contributes to bone marrow fibrosis development<sup>48</sup>. However, LSK, MEP, and MK are not major contributors to collagen I production, as it is mainly produced by fibroblast<sup>49</sup>. The source of these bone marrow fibroblasts is mesenchymal stromal cells (MSC) in myelofibrosis<sup>50</sup>. Therefore, it would be more relevant to determine collagen expression from MSCs than LSK, MEP, or MK. The increased expression and secretion of collagen in fibroblasts are

induced by growth factors such as platelet-derived growth factor (PDGF) and TGF $\beta$ , which are produced by megakaryocytes and platelets<sup>51,52</sup>. It is because of this and the expansion of MK in MF patients that the model of how myelofibrosis develops is tied together.

To assess this connection, we cultured MK from our experimental cohort for 48 hours and transferred its media to wild-type MSC cultures. After another 48 hours in this MK-derived media, we assessed the MSC for changes in collagen expression. We observed a significant increase in collagen I expression in MSCs that were incubated in media derived from Ptpn1-deficient MK.

Overall, the signature of these genes revealed a genetic landscape that is biased towards megakaryopoiesis in differentiation and promotes fibrosis development.

### **The role of PTPN1 substrates, PLC $\gamma$ 2 and PTK2B**

We also examined the JAK signaling and showed that Ptpn1 deficiency elevates STAT5, STAT3, STAT1, and ERK1/2 in PTPN1-deleted JAK2<sup>V617F</sup>-positive hematopoietic cells, as well as mouse Ptpn1-deficient Jak2<sup>V617F/+</sup> bone marrow. As PTPN1 is a promiscuous enzyme, its absence leads to a large intracellular hyper-tyrosine phosphorylation. Therefore, we aimed to identify more potential targets outside of JAK-STAT signaling that could provide greater depth to explain some of the observed phenotypes. Using our established coimmunoprecipitation (Co-IP) methods, we were able to identify novel targets of PTPN1, such as Ptk2b and Plc $\gamma$ 2.

PLC $\gamma$ 2, a phosphatidylinositol-specific phospholipase C $\gamma$ 2, is a downstream signaling module of multiple cell receptors. Its activation leads to the cleavage of

phospholipid phosphatidylinositol-4,5-bisphosphate (PIP<sub>2</sub>) into diacylglycerol (DAG) and inositol-1,4,5-trisphosphate (IP<sub>3</sub>), which induce intracellular Ca<sup>2+</sup> release and PKC activation<sup>53</sup>. This protein plays a significant role in numerous pathological conditions, including autoimmune<sup>54</sup>, neurological<sup>55</sup>, allergy<sup>56</sup>, and cancer<sup>57</sup>. The role of PLC $\gamma$ 2 is most extensively studied in chronic lymphocytic leukemia (CLL), Hodgkin's lymphoma, and non-Hodgkin's lymphoma due to its heavy involvement in the lymphomagenesis process<sup>58</sup>. In addition, it is phosphorylated by Bruton's tyrosine kinase (BTK)<sup>59</sup>, another target identified in Ptpn1's Co-IP. The acquisition of a gain-of-function mutation in PLC $\gamma$ 2 is associated with resistance to Ibrutinib, a BTK inhibitor used in the treatment of CLL<sup>60</sup>. In large B cell lymphoma, PLC $\gamma$ 2 expression is elevated in 63% of cases. Interestingly, high expression of PLC $\gamma$ 2 is associated with a good overall prognosis; however, inhibition of PLC $\gamma$ 2 inhibits proliferation and serves as a potential therapeutic target in the treatment of large B cell lymphoma<sup>61,62</sup>. PTPN1 also plays a role in B cell lymphoma, and a recurrent mutation of PTPN1, which results reduction of phosphatase activity, is exacerbate the disease<sup>63</sup>. This highlights a potential interaction role of PTPN1 and PLC $\gamma$ 2 in lymphoid malignancies.

While the role of PLC $\gamma$ 2 in lymphoid malignancies has been extensively explored, its role in the context of myeloid diseases has been less studied. Macrophage colony-stimulating factor (M-CSF) preferentially activates PLC $\gamma$ 2 signaling and subsequently ERK, which may play a role in hyper ERK activation in addition to JAK-STAT induced signaling<sup>64</sup>. Interestingly, PLC $\gamma$ 2-deficient mice do not appear to affect myeloid cell production but do impair cytokine secretion<sup>56</sup>. This may support the production of inflammatory cytokines induced by PTPN1 deficiency. Another study found that PLC $\gamma$ 2-

deficient megakaryocytes (MK) result in a significant reduction in TPO mRNA expression, which in turn results in the reduced growth potential of MK and HSC<sup>65</sup>. However, as TPO is not primarily produced by MK but rather by the liver and kidney, this finding diminishes the impact of the study. Further investigation is needed to understand the role of PLC $\gamma$ 2 in the context of MK, as well as the interaction between PLC $\gamma$ 2 and PTPN1 in myeloid hematopoiesis and malignancies.

PTK2B, also known as protein tyrosine kinase 2 beta, has several other prevalent names, including proline-rich tyrosine kinase 2 (PYK2) and focal adhesion kinase 2 (FAK2). Although sharing structural domain similarity with FAK1, the two proteins are only 46% homologous<sup>66</sup>, indicating a potentially unique role between them. Notably, while FAK1 is essential for embryogenesis, PTK2B is not<sup>67,68</sup>. PTK2B plays a significant role in the cytoskeletal dynamic, and as such, it is well associated with the epithelial-to-mesenchymal transition (EMT) process<sup>69</sup>. Moreover, overexpression of PTK2B is also associated with numerous cancers<sup>70</sup>.

In terms of myeloid hematopoiesis and malignancies, PTK2B has a significant role in platelet function. PTK2B-deficient mice exhibit a prolonged bleeding time but were protected from thrombosis<sup>71</sup>. Additional studies, as well as human studies using PTK2B inhibition, validate this protection from thrombosis<sup>72,73</sup>. Furthermore, the activation of PLC $\gamma$ 2 induces downstream activation of PTK2B through PI3K activation, promoting thrombus formation<sup>74</sup>. While PTK2B's involvement in the progression of MPN or MK-bias is unclear, it has demonstrated a remarkable role in the thrombosis process. Thrombosis is the biggest morbidity risk in MPNs and the major deciding factor in patients' treatment options<sup>75</sup>. We observed a significant increase in PTK2B

phosphorylation as a consequence of PTPN1 deficiency. Along with thrombocytosis, this might explain the increased morbidity observed in mice with PTPN1 deficiency.

Although this property has not been explored, we were able to determine that the increase of PTK2B expression can induce increased proliferation in HEL cells. Furthermore, in the absence of PTPN1, PTK2B activity becomes an impactful driver of proliferation, as demonstrated when PTPN1-deleted cells exhibit a significant reduction in proliferation in the absence of PTK2B. However, in isolation, PTK2B deletion does not exhibit this reduction in proliferation.

### **JAK2 inhibitor insensitivity**

The hyperactivation of JAK-STAT signaling raised a question about the efficacy of ruxolitinib, a JAK1/2 inhibitor, in PTPN1-deficient cells. In both PTPN1-deficient HEL and SET2 cells, we observed a 2 to 3-fold decrease in sensitivity to ruxolitinib. This reduction in sensitivity was also observed in non-clonal cells, as well as lineage-depleted BM cells. Upon assessing the JAK-STAT signaling, we found that the phosphorylation signals of STAT1, STAT3, STAT5, and ERK1/2 were better preserved when challenged with ruxolitinib in PTPN1-deficient cells, compared to native HEL and SET2 cells. In contrast, the phosphorylation of PTK2B was minimally impacted by ruxolitinib. This reduction in ruxolitinib sensitivity poses a great concern for patients undergoing treatment with the drug.

PTPN1 deficiency significantly elevates AXL expression in LSK and MEP as well as both hematopoietic cell lines, HEL and SET2. AXL expression has been heavily implicated in drug resistance in multiple cancer treatments<sup>76-79</sup>. We found that AXL

overexpression promotes increased proliferation in HEL and SET2 cells, while also reducing PTPN1 expression. This interesting dynamic interaction between AXL and PTPN1 expression that could be further explored. To see if the AXL inhibition could provide an alternative treatment to ruxolitinib, we evaluated the properties of two different AXL inhibitors, bemcentinib and dubermatinib, in native and PTPN1-deficient HEL cells. We found that both native and PTPN1-deficient cells exhibited similar sensitivity to bemcentinib and dubermatinib indicating no or minimal impact when targeting AXL in PTPN1 deficiency. As such, targeting the AXL signaling axis may provide a therapeutic option when targeting JAK/STAT signaling axis is compromised, such as in the situation of PTPN1 deficiency. Future examinations can be made to address the potential efficacy of combination therapy with AXL inhibitors and ruxolitinib, as well as the potency of targeting AXL in a direct ruxolitinib-resistant cell.

In this study, we have demonstrated the ramification of chromosome 20q deletion involving the loss of PTPN1 when the JAK2V617F mutation is present. Such an opportunistic event not only provides a clonal advantage to the cells, it aggressively drives JAK2V617F-induced MPN disease progression toward myelofibrosis. We have also demonstrated the nature of this pathogenicity through a combination of robust expansion of HSC, myeloid cells, and megakaryocytes that contributes to the inflammatory environment and drive fibrosis development. The insight from this study will help advance our understanding of the risk involved in the presence of this karyotype abnormality and readjust our therapeutic approach.

## Future works

For our future work, we aim to identify additional contributors to del20q in addition to PTPN1. Previously explored targets, such as SGK2 and L3MBTL1, have been shown to cause dysregulation of erythropoiesis and megakaryopoiesis<sup>80</sup>, processes that are also affected by PTPN1 deficiency. Therefore, we plan to investigate the synergistic potential of these targets and establish a more comprehensive model of del20q in MPN. Based on the resulting phenotype, we will examine the signaling pathway and gene expression to elucidate the mechanism underlying the observed phenotype.

Another important interaction is the interplay between PTPN1 and AXL. The knockout of PTPN1 induced a significant increase in AXL expression and the overexpression of AXL reduces PTPN1 expression. This inverse relationship is poorly understood and we want to determine the mediator that defines this property and connects their signaling pathway. We would also examine the expression of PTPN1 upon treatment with AXL inhibitors to see if the relation is expression-dependent or activity-dependent and if the change is dose-dependent. As both are involved in therapeutic resistance, we want to further explore the dynamic between these two and their contribution to processes.

The activities of PLCG2 and PTK2B were not deeply explored in this study, and their potential involvement in the thrombosis process and increased morbidity in Ptpn1-deficient Jak2<sup>V617F/+</sup> mice will require further investigation. However, their potential as therapeutic targets raises the possibility of using PTK2B inhibitors to reduce morbidity risk in PV and MF patients, especially those with del20q and reduced PTPN1 expression. Additionally, their contribution to the megakaryopoiesis process and therapeutic impact



have not been fully examined. We can explore their involvement in megakaryopoiesis through in vitro overexpression studies using cultured MK, as well as in vivo BMT to assess the phenotypic outcome.

Finally, we aim to investigate the effects of cytokine activity on the nature of the disease. Since we observed a reduction in IFN response in Ptpn1-deficient Jak2<sup>V617F/+</sup> LSK, we question the efficacy of IFN- $\alpha$  treatment in this context if the response is significantly repressed. We also hypothesize that clonal advantages of PTPN1 could be due to prolonged exposure to TNF $\alpha$ , IFN- $\alpha$ , and IFN- $\gamma$  signaling, which diminished the responses to these signals and provide proliferative advantages to HSC. To examine this, we plan to utilize a TNF $\alpha$ /IFN blocker/antagonist, such as adalimumab used in the treatment of rheumatoid arthritis<sup>81</sup>, or IFN- $\alpha$  kinoid which is used in the treatment of lupus<sup>82</sup>, to see if it negates the advantages PTPN1-deficient clone has and reverses the consequences of Ptpn1 deficiency in the context of Jak2V617F mutation.

Overall, the impact of our study provides invaluable knowledge of the disease modality associated progression of PV to MF and the risk imposed by del20q. This knowledge will be crucial to advancing our current therapeutic approaches, as we strive to improve the quality of life for every impacted patient.

## References

1. Villeval, J. L. *et al.* High thrombopoietin production by hematopoietic cells induces a fatal myeloproliferative syndrome in mice. *Blood* **90**, 4369–83 (1997).
2. Emmons, R. V *et al.* Human thrombopoietin levels are high when thrombocytopenia is due to megakaryocyte deficiency and low when due to increased platelet destruction. *Blood* **87**, 4068–71 (1996).
3. Vyas, P., Ault, K., Jackson, C. W., Orkin, S. H. & Shivdasani, R. A. Consequences of GATA-1 deficiency in megakaryocytes and platelets. *Blood* **93**, 2867–75 (1999).
4. Zingariello, M. *et al.* The thrombopoietin/MPL axis is activated in the Gata1low mouse model of myelofibrosis and is associated with a defective RPS14 signature. *Blood Cancer J.* **7**, e572–e572 (2017).
5. Tsang, A. P., Fujiwara, Y., Hom, D. B. & Orkin, S. H. Failure of megakaryopoiesis and arrested erythropoiesis in mice lacking the GATA-1 transcriptional cofactor FOG. *Genes Dev.* **12**, 1176–1188 (1998).
6. Sangiorgio, V. F. I., Nam, A., Chen, Z., Orazi, A. & Tam, W. GATA1 downregulation in prefibrotic and fibrotic stages of primary myelofibrosis and in the myelofibrotic progression of other myeloproliferative neoplasms. *Leuk. Res.* **100**, 106495 (2021).
7. Vannucchi, A. M. *et al.* Abnormalities of GATA-1 in Megakaryocytes from Patients with Idiopathic Myelofibrosis. *Am. J. Pathol.* **167**, 849–858 (2005).
8. Shin, E. *et al.* The Gata1 murine megakaryocyte–erythroid progenitor cells expand robustly and alter differentiation potential. *Biochem. Biophys. Res. Commun.* **528**, 46–53 (2020).
9. Tsai, S.-F. *et al.* Cloning of cDNA for the major DNA-binding protein of the erythroid lineage through expression in mammalian cells. *Nature* **339**, 446–451 (1989).
10. Al-Ali, H. K. & Vannucchi, A. M. Managing patients with myelofibrosis and low platelet counts. *Ann. Hematol.* **96**, 537–548 (2017).
11. Ciurea, S. O. *et al.* Pivotal contributions of megakaryocytes to the biology of idiopathic myelofibrosis. *Blood* **110**, 986–993 (2007).
12. Arber, D. A. *et al.* The 2016 revision to the World Health Organization classification of myeloid neoplasms and acute leukemia. *Blood* **127**, 2391–2405 (2016).
13. Chen, L. *et al.* Inflammatory responses and inflammation-associated diseases in organs. *Oncotarget* **9**, 7204–7218 (2018).
14. Koschmieder, S. *et al.* Myeloproliferative neoplasms and inflammation: whether to

- target the malignant clone or the inflammatory process or both. *Leukemia* **30**, 1018–1024 (2016).
15. Wang, Y. & Zuo, X. Cytokines frequently implicated in myeloproliferative neoplasms. *Cytokine X* **1**, 100005 (2019).
  16. Čokić, V. P. *et al.* Proinflammatory Cytokine IL-6 and JAK-STAT Signaling Pathway in Myeloproliferative Neoplasms. *Mediators Inflamm.* **2015**, 1–13 (2015).
  17. Rahman, M. F.-U. *et al.* Interleukin-1 contributes to clonal expansion and progression of bone marrow fibrosis in JAK2V617F-induced myeloproliferative neoplasm. *Nat. Commun.* **13**, 5347 (2022).
  18. Scheller, J., Chalaris, A., Schmidt-Arras, D. & Rose-John, S. The pro- and anti-inflammatory properties of the cytokine interleukin-6. *Biochim. Biophys. Acta - Mol. Cell Res.* **1813**, 878–888 (2011).
  19. Hollen, C. W., Henthorn, J., Koziol, J. A. & Burstein, S. A. Elevated serum interleukin-6 levels in patients with reactive thrombocytosis. *Br. J. Haematol.* **79**, 286–290 (1991).
  20. Tanaka, T. & Kishimoto, T. The Biology and Medical Implications of Interleukin-6. *Cancer Immunol. Res.* **2**, 288–294 (2014).
  21. Bataller, A., Montalban-Bravo, G., Soltysiak, K. A. & Garcia-Manero, G. The role of TGF $\beta$  in hematopoiesis and myeloid disorders. *Leukemia* **33**, 1076–1089 (2019).
  22. Zauli, G. *et al.* Reduced responsiveness of bone marrow megakaryocyte progenitors to platelet-derived transforming growth factor  $\beta$ 1, produced in normal amount, in patients with essential thrombocythaemia. *Br. J. Haematol.* **83**, 14–20 (1993).
  23. Vannucchi, A. M. *et al.* A pathobiologic pathway linking thrombopoietin, GATA-1, and TGF- $\beta$ 1 in the development of myelofibrosis. *Blood* **105**, 3493–3501 (2005).
  24. Tracey, M.D, K. J. & Cerami, Ph.D, A. TUMOR NECROSIS FACTOR: A Pleiotropic Cytokine and Therapeutic Target. *Annu. Rev. Med.* **45**, 491–503 (1994).
  25. Bryder, D. *et al.* Self-Renewal of Multipotent Long-Term Repopulating Hematopoietic Stem Cells Is Negatively Regulated by FAS and Tumor Necrosis Factor Receptor Activation. *J. Exp. Med.* **194**, 941–952 (2001).
  26. Fleischman, A. G. *et al.* TNF $\alpha$  facilitates clonal expansion of JAK2V617F positive cells in myeloproliferative neoplasms. *Blood* **118**, 6392–6398 (2011).
  27. Steensma, D. P., Mesa, R. A., Li, C.-Y., Gray, L. & Tefferi, A. Etanercept, a soluble tumor necrosis factor receptor, palliates constitutional symptoms in patients with myelofibrosis with myeloid metaplasia: results of a pilot study. *Blood*
-

- 99, 2252–2254 (2002).
28. Elliott, M. & Tefferi, A. Interferon- $\alpha$  Therapy in Polycythemia Vera and Essential Thrombocythemia. *Semin. Thromb. Hemost.* **23**, 463–472 (1997).
  29. Yang, L. *et al.* IFN- $\gamma$  Negatively Modulates Self-Renewal of Repopulating Human Hemopoietic Stem Cells. *J. Immunol.* **174**, 752–757 (2005).
  30. de Bruin, A. M., Demirel, Ö., Hooibrink, B., Brandts, C. H. & Nolte, M. A. Interferon- $\gamma$  impairs proliferation of hematopoietic stem cells in mice. *Blood* **121**, 3578–3585 (2013).
  31. Tsuji, K., Muraoka, K. & Nakahata, T. Interferon- $\gamma$  and Human Megakaryopoiesis. *Leuk. Lymphoma* **31**, 107–113 (1998).
  32. Huang, Z. *et al.* STAT1 promotes megakaryopoiesis downstream of GATA-1 in mice. *J. Clin. Invest.* **117**, 3890–3899 (2007).
  33. Libregts, S. F. *et al.* Chronic IFN- $\gamma$  production in mice induces anemia by reducing erythrocyte life span and inhibiting erythropoiesis through an IRF-1/PU.1 axis. *Blood* **118**, 2578–2588 (2011).
  34. Yacoub, A. *et al.* Pegylated interferon alfa-2a for polycythemia vera or essential thrombocythemia resistant or intolerant to hydroxyurea. *Blood* **134**, 1498–1509 (2019).
  35. Abu-Zeinah, G. *et al.* Interferon-alpha for treating polycythemia vera yields improved myelofibrosis-free and overall survival. *Leukemia* **35**, 2592–2601 (2021).
  36. Bieker, J. EKLF and the development of the erythroid lineage. in *Transcription Factors: Normal and Malignant Development of Blood Cells* (eds. Ravid, K. & Licht, J.) 71–84 (Wiley-Liss, Inc, 2001).
  37. Frontelo, P. *et al.* Novel role for EKLF in megakaryocyte lineage commitment. *Blood* **110**, 3871–3880 (2007).
  38. SHALLOE, F., ELLIOTT, G., ENNIS, O. & MANTLE, T. J. Evidence that biliverdin-IX  $\beta$  reductase and flavin reductase are identical. *Biochem. J.* **316**, 385–387 (1996).
  39. Nesbitt, N. M. *et al.* Divergent erythroid megakaryocyte fates in Blvrb-deficient mice establish non-overlapping cytoprotective functions during stress hematopoiesis. *Free Radic. Biol. Med.* **164**, 164–174 (2021).
  40. Andrieux, J. *et al.* Dysregulation and overexpression of HMGA2 in myelofibrosis with myeloid metaplasia. *Genes, Chromosom. Cancer* **39**, 82–87 (2004).
  41. Fusco, A. & Fedele, M. Roles of HMGA proteins in cancer. *Nat. Rev. Cancer* **7**, 899–910 (2007).
  42. Thanos, D. & Maniatis, T. The High Mobility Group protein HMG I(Y) is required
-

- for NF- $\kappa$ B-dependent virus induction of the human IFN- $\beta$  gene. *Cell* **71**, 777–789 (1992).
43. Dutta, A., Hutchison, R. E. & Mohi, G. Hmga2 promotes the development of myelofibrosis in Jak2V617F knockin mice by enhancing TGF- $\beta$ 1 and Cxcl12 pathways. *Blood* **130**, 920–932 (2017).
  44. Gay, C. M., Balaji, K. & Byers, L. A. Giving AXL the axe: targeting AXL in human malignancy. *Br. J. Cancer* **116**, 415–423 (2017).
  45. Pearson, S., Blance, R., Somerville, T. C. P., Whetton, A. D. & Pierce, A. AXL Inhibition Extinguishes Primitive JAK2 Mutated Myeloproliferative Neoplasm Progenitor Cells. *HemaSphere* **3**, e233 (2019).
  46. Xiu, M. *et al.* The Role of Notch3 Signaling in Cancer Stemness and Chemoresistance: Molecular Mechanisms and Targeting Strategies. *Front. Mol. Biosci.* **8**, (2021).
  47. Dhenge, A., Kuhikar, R., Kale, V. & Limaye, L. Regulation of differentiation of MEG01 to megakaryocytes and platelet-like particles by Valproic acid through Notch3 mediated actin polymerization. *Platelets* **30**, 780–795 (2019).
  48. Kuter, D. J., Bain, B., Mufti, G., Bagg, A. & Hasserjian, R. P. Bone marrow fibrosis: pathophysiology and clinical significance of increased bone marrow stromal fibres. *Br. J. Haematol.* **139**, 351–362 (2007).
  49. Cattoretti, G., Schiró, R., Orazi, A., Soligo, D. & Colombo, M. P. Bone marrow stroma in humans: anti-nerve growth factor receptor antibodies selectively stain reticular cells in vivo and in vitro. *Blood* **81**, 1726–38 (1993).
  50. Decker, M. *et al.* Leptin-receptor-expressing bone marrow stromal cells are myofibroblasts in primary myelofibrosis. *Nat. Cell Biol.* **19**, 677–688 (2017).
  51. GROOPMAN, J. E. The Pathogenesis of Myelofibrosis in Myeloproliferative Disorders. *Ann. Intern. Med.* **92**, 857 (1980).
  52. Martyré, M. C. *et al.* Transforming growth factor- $\beta$  and megakaryocytes in the pathogenesis of idiopathic myelofibrosis. *Br. J. Haematol.* **88**, 9–16 (1994).
  53. Berridge, M. J. Inositol trisphosphate and calcium signalling. *Nature* **361**, 315–325 (1993).
  54. Cremasco, V., Graham, D. B., Novack, D. V., Swat, W. & Faccio, R. Vav/Phospholipase C $\gamma$ 2-mediated control of a neutrophil-dependent murine model of rheumatoid arthritis. *Arthritis Rheum.* **58**, 2712–2722 (2008).
  55. Andreone, B. J. *et al.* Alzheimer’s-associated PLC $\gamma$ 2 is a signaling node required for both TREM2 function and the inflammatory response in human microglia. *Nat. Neurosci.* **23**, 927–938 (2020).
  56. Wen, R., Jou, S.-T., Chen, Y., Hoffmeyer, A. & Wang, D. Phospholipase C $\gamma$ 2 Is
-

- Essential for Specific Functions of FcεR and FcγR. *J. Immunol.* **169**, 6743–6752 (2002).
57. Landau, D. A. *et al.* The evolutionary landscape of chronic lymphocytic leukemia treated with ibrutinib targeted therapy. *Nat. Commun.* **8**, 2185 (2017).
  58. Wen, R. *et al.* Essential Role of Phospholipase Cγ2 in Early B-Cell Development and Myc-Mediated Lymphomagenesis. *Mol. Cell. Biol.* **26**, 9364–9376 (2006).
  59. Kim, Y. J., Sekiya, F., Poulin, B., Bae, Y. S. & Rhee, S. G. Mechanism of B-Cell Receptor-Induced Phosphorylation and Activation of Phospholipase C-γ2. *Mol. Cell. Biol.* **24**, 9986–9999 (2004).
  60. Jones, D. *et al.* PLCG2 C2 domain mutations co-occur with BTK and PLCG2 resistance mutations in chronic lymphocytic leukemia undergoing ibrutinib treatment. *Leukemia* **31**, 1645–1647 (2017).
  61. Huynh, M. Q. *et al.* Expression and pro-survival function of phospholipase Cγ2 in diffuse large B-cell lymphoma. *Leuk. Lymphoma* **56**, 1088–1095 (2015).
  62. Yang, C. *et al.* Tyrosine kinase inhibition in diffuse large B-cell lymphoma: molecular basis for antitumor activity and drug resistance of dasatinib. *Leukemia* **22**, 1755–1766 (2008).
  63. Gunawardana, J. *et al.* Recurrent somatic mutations of PTPN1 in primary mediastinal B cell lymphoma and Hodgkin lymphoma. *Nat. Genet.* **46**, 329–335 (2014).
  64. Jack, G. D., Zhang, L. & Friedman, A. D. M-CSF elevates c-Fos and phospho-C/EBPα(S21) via ERK whereas G-CSF stimulates SHP2 phosphorylation in marrow progenitors to contribute to myeloid lineage specification. *Blood* **114**, 2172–2180 (2009).
  65. Nakamura-Ishizu, A., Takubo, K., Kobayashi, H., Suzuki-Inoue, K. & Suda, T. CLEC-2 in megakaryocytes is critical for maintenance of hematopoietic stem cells in the bone marrow. *J. Exp. Med.* **212**, 2133–2146 (2015).
  66. Hall, J. E., Fu, W. & Schaller, M. D. Focal Adhesion Kinase. in 185–225 (2011). doi:10.1016/B978-0-12-386041-5.00005-4.
  67. Furuta, Y. *et al.* Mesodermal defect in late phase of gastrulation by a targeted mutation of focal adhesion kinase, FAK. *Oncogene* **11**, 1989–95 (1995).
  68. Okigaki, M. *et al.* Pyk2 regulates multiple signaling events crucial for macrophage morphology and migration. *Proc. Natl. Acad. Sci.* **100**, 10740–10745 (2003).
  69. Verma, N. *et al.* PYK2 sustains endosomal-derived receptor signalling and enhances epithelial-to-mesenchymal transition. *Nat. Commun.* **6**, 6064 (2015).
  70. Shen, T. & Guo, Q. Role of Pyk2 in Human Cancers. *Med. Sci. Monit.* **24**, 8172–8182 (2018).
-

71. Canobbio, I. *et al.* Impaired thrombin-induced platelet activation and thrombus formation in mice lacking the Ca<sup>2+</sup>-dependent tyrosine kinase Pyk2. *Blood* **121**, 648–657 (2013).
72. Guidetti, G. *et al.* Novel pharmacological inhibitors demonstrate the role of the tyrosine kinase Pyk2 in adhesion and aggregation of human platelets. *Thromb. Haemost.* **116**, 904–917 (2016).
73. Momi, S. *et al.* Proline-rich tyrosine kinase Pyk2 regulates deep vein thrombosis. *Haematologica* **107**, 1374–1383 (2022).
74. Consonni, A. *et al.* Role and regulation of phosphatidylinositol 3-kinase  $\beta$  in platelet integrin  $\alpha 2\beta 1$  signaling. *Blood* **119**, 847–856 (2012).
75. Tefferi, A. & Barbui, T. Polycythemia vera and essential thrombocythemia: 2019 update on diagnosis, risk-stratification and management. *Am. J. Hematol.* **94**, 133–143 (2019).
76. Huang, L. & Fu, L. Mechanisms of resistance to EGFR tyrosine kinase inhibitors. *Acta Pharm. Sin. B* **5**, 390–401 (2015).
77. Lotsberg, M. L. *et al.* AXL Targeting Abrogates Autophagic Flux and Induces Immunogenic Cell Death in Drug-Resistant Cancer Cells. *J. Thorac. Oncol.* **15**, 973–999 (2020).
78. Sen, T. *et al.* Targeting AXL and mTOR Pathway Overcomes Primary and Acquired Resistance to WEE1 Inhibition in Small-Cell Lung Cancer. *Clin. Cancer Res.* **23**, 6239–6253 (2017).
79. Kariolis, M. S. *et al.* Inhibition of the GAS6/AXL pathway augments the efficacy of chemotherapies. *J. Clin. Invest.* **127**, 183–198 (2016).
80. Aziz, A. *et al.* Cooperativity of imprinted genes inactivated by acquired chromosome 20q deletions. *J. Clin. Invest.* **123**, 2169–2182 (2013).
81. Furst, D. E. *et al.* Adalimumab, a fully human anti tumor necrosis factor-alpha monoclonal antibody, and concomitant standard antirheumatic therapy for the treatment of rheumatoid arthritis: results of STAR (Safety Trial of Adalimumab in Rheumatoid Arthritis). *J. Rheumatol.* **30**, 2563–71 (2003).
82. Paredes, J. L. & Niewold, T. B. Type I interferon antagonists in clinical development for lupus. *Expert Opin. Investig. Drugs* **29**, 1025–1041 (2020).

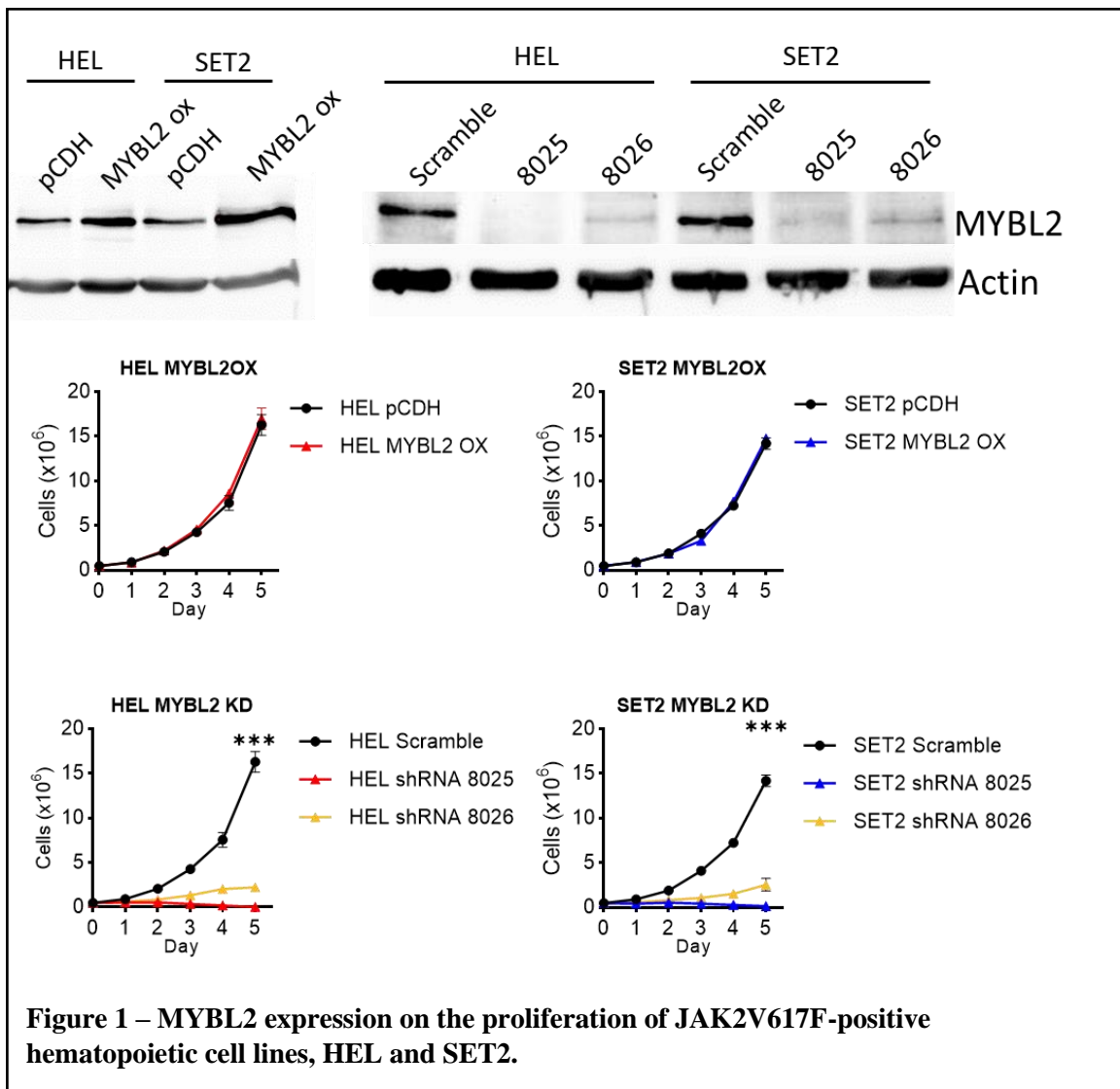
## **APPENDIX**

### **The role of MYBL2 in myeloproliferative neoplasms**

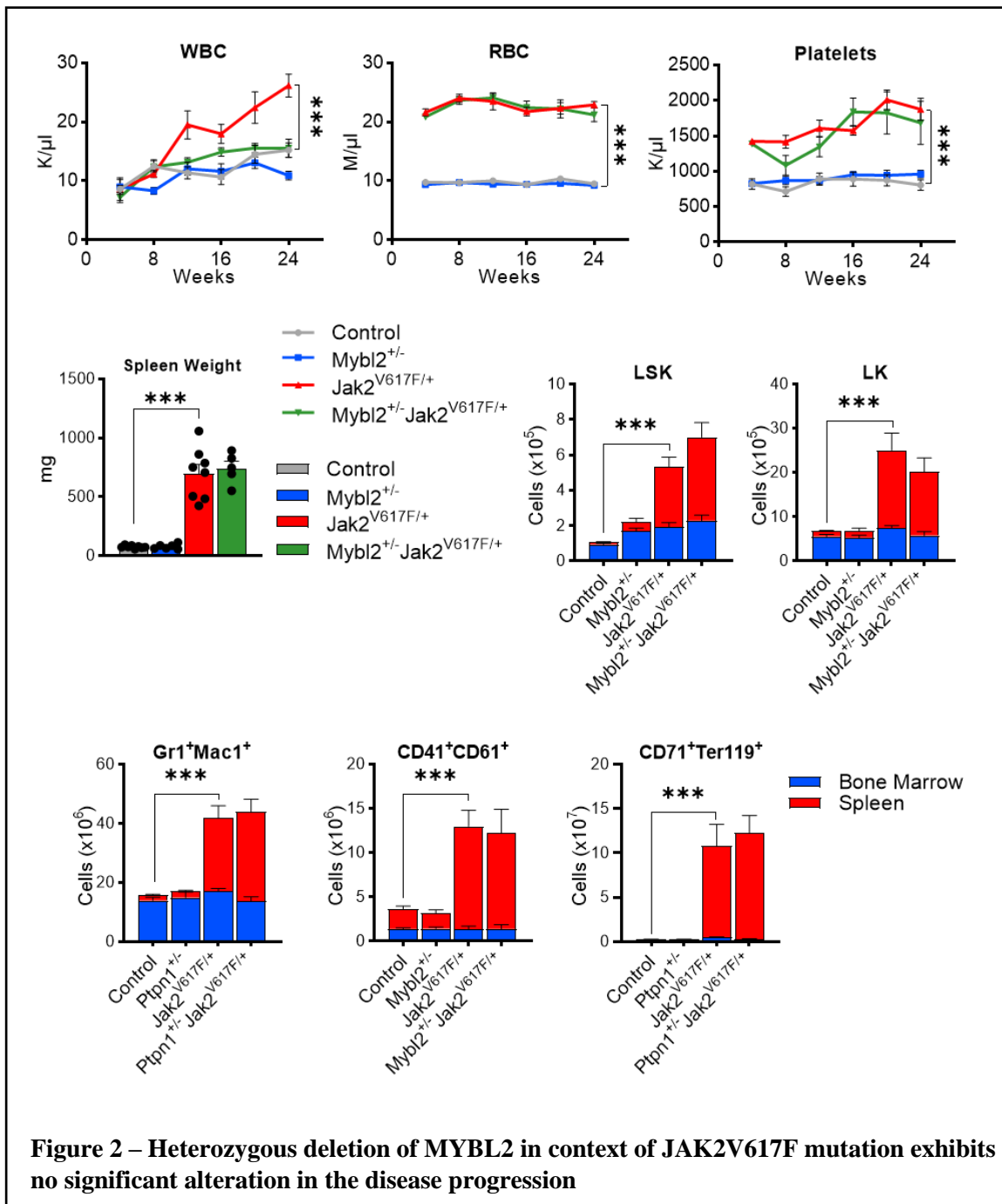
Bao Le and Golam Mohi

Besides PTPN1, we have investigated other genes deleted in 20q deletion syndrome, including MYBL2, a nuclear protein involved in cell cycle progression. We studied the role of MYBL2 in both hematopoietic cell lines and a murine model, which allowed us to determine its essential role in the survival of hematopoietic cell lines. However, unlike PTPN1, MYBL2 appears to have no involvement in the pathogenesis of myeloproliferative neoplasms (MPNs).





We overexpressed and knocked down MYBL2 in both HEL and SET2 cells and validated the expression changes by Western blotting. The cells overexpressing MYBL2 did not show any significant changes in proliferation. However, knocking down MYBL2 in HEL and SET2 using two different shRNAs resulted in a significant reduction in the proliferation of both cell lines. These results indicate the essential role of MYBL2 in cell survival.



To investigate the phenotypic effects of Mybl2 deficiency in the context of JAK2V617F mutation, we established an experimental cohort of control, Mybl2<sup>+/-</sup>, Jak2<sup>V617F/+</sup>, and Mybl2<sup>+/-</sup>Jak2<sup>V617F/+</sup> mice. Blood parameter assessment revealed a significant reduction in white blood cell (WBC) count in Mybl2<sup>+/-</sup>Jak2<sup>V617F/+</sup> mice

compared to Jak2<sup>V617F/+</sup> alone, whereas red blood cell (RBC) and platelet counts were unaffected by the Jak2V617F mutation. The splenic size was also unchanged in Mybl2-deficient mice with the Jak2V617F mutation. Analysis of the hematopoietic compartment of the bone marrow and spleen showed no significant alteration in the populations of hematopoietic stem and progenitor cells (LSK and LK), myeloid cells (Gr1<sup>+</sup>Mac1<sup>+</sup>), megakaryocytes (CD41<sup>+</sup>CD61<sup>+</sup>), or erythroid cells (CD71<sup>+</sup>Ter119<sup>+</sup>). These results suggest that while MYBL2 is essential for hematopoietic cell survival, heterozygous deficiency of Mybl2 does not contribute to the development of myeloproliferative neoplasms (MPNs).

**Interleukin-1 contributes to clonal expansion and progression of bone marrow fibrosis in JAK2V617F-induced myeloproliferative neoplasm**

Mohammed Ferdous-Ur Rahman, Yue Yang, Bao T. Le, Avik Dutta, Julia Posyniak, Patrick Faughnan, Mohammad A. Sayem, Nadine S. Aguilera, & Golam Mohi

Nature Communications 2022

[doi: <https://doi.org/10.1038/s41467-022-32928-3>]

This publication investigates the roles of interleukin-1 (IL-1) and inflammation in the pathogenesis of myeloproliferative neoplasms (MPNs). Our study shows that genetic deletion of IL-1 receptor normalizes blood parameters induced by the Jak2V617F mutation, reduces splenomegaly, and ameliorates bone marrow fibrosis. My role in the project involved supporting the bioinformatic analysis, which included evaluating the expression of interleukin-1 in MPN patients with different driver mutations and analyzing the populations of hematopoietic stem and progenitor cells (LSK) and mesenchymal stromal cells (MSCs) derived from mice treated with PBS and IL-1 $\beta$ .

## Expression of IL-1 is elevated in MPN

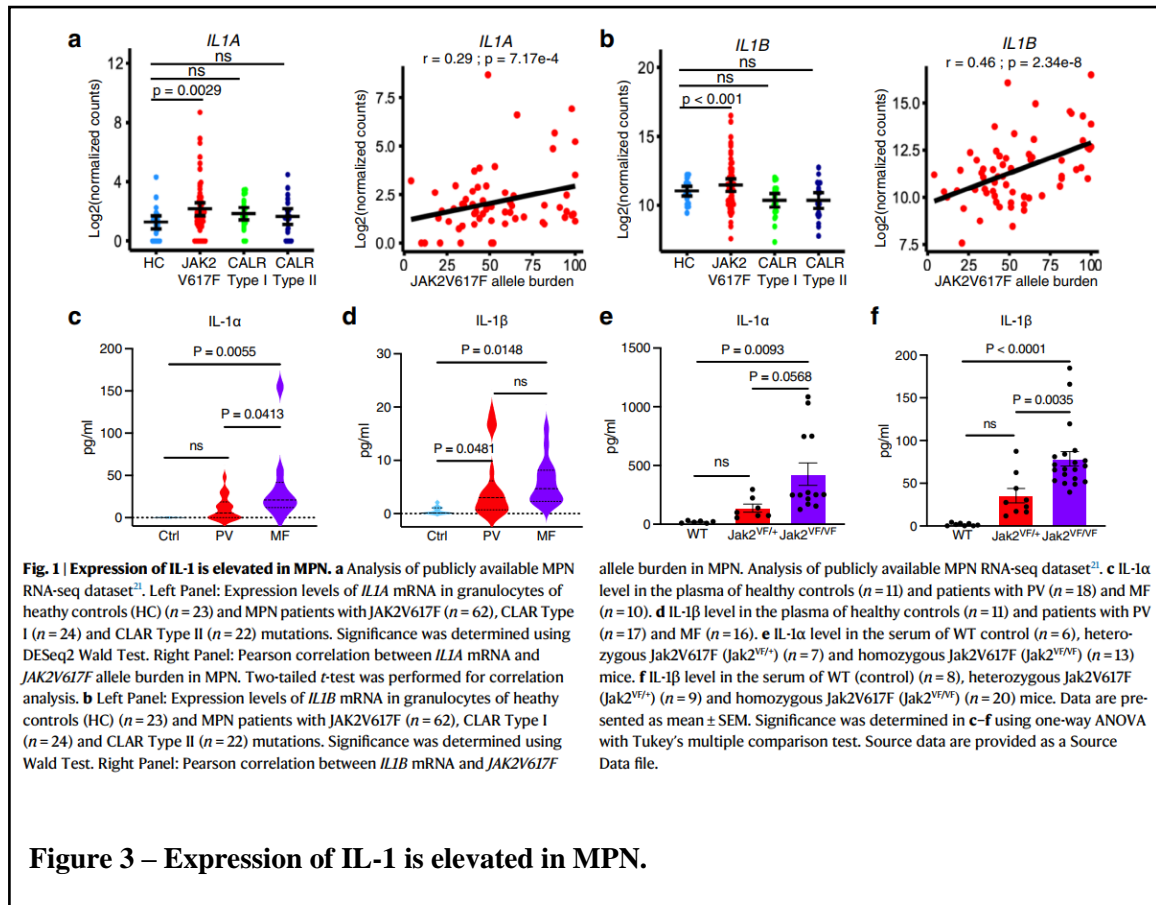


**Figure 3 – Expression of IL-1 is elevated in MPN.**

I used the publicly available MPN RNA-seq dataset to extract normalized read counts for both IL1A and IL1B genes. The expression levels of both genes were stratified based on the presence of JAK2V617F mutation, CALR Type 1 mutation, and CALR Type 2 mutation in MPN patients, in order to identify any significant elevation of IL1A and IL1B expression. Furthermore, I plotted the expression levels of IL1A and IL1B against the JAK2V617F allele burden and found a significant positive correlation between the two.

## Effects of IL-1 $\beta$ on gene expression in Jak2V617F mice hematopoietic progenitors.

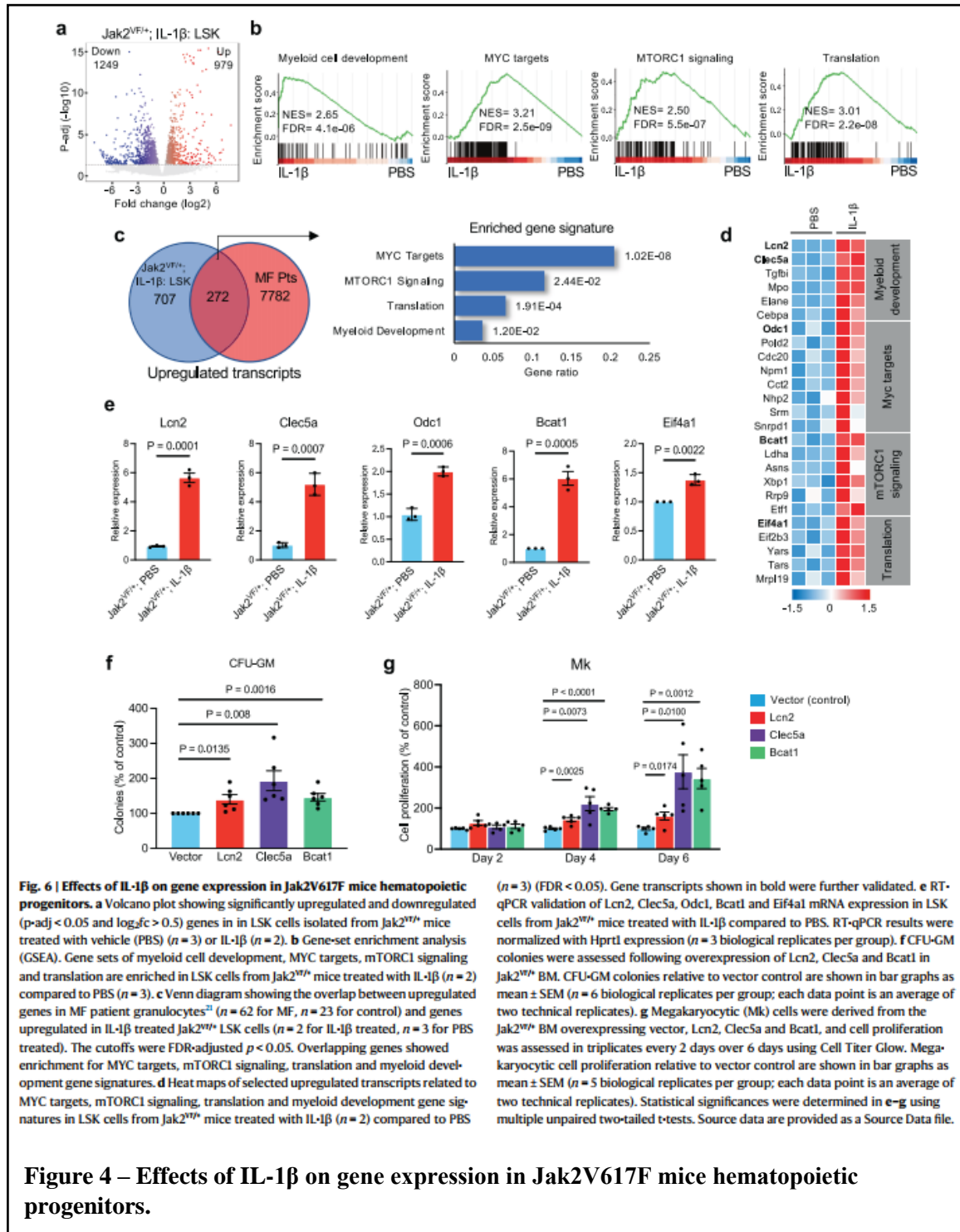


**Fig. 6 | Effects of IL-1 $\beta$  on gene expression in *Jak2V617F* mice hematopoietic progenitors.** **a** Volcano plot showing significantly upregulated and downregulated ( $p$ -adj < 0.05 and  $\log_2fc > 0.5$ ) genes in LSK cells isolated from *Jak2<sup>V617F</sup>* mice treated with vehicle (PBS) ( $n = 3$ ) or IL-1 $\beta$  ( $n = 2$ ). **b** Gene-set enrichment analysis (GSEA). Gene sets of myeloid cell development, MYC targets, mTORC1 signaling and translation are enriched in LSK cells from *Jak2<sup>V617F</sup>* mice treated with IL-1 $\beta$  ( $n = 2$ ) compared to PBS ( $n = 3$ ). **c** Venn diagram showing the overlap between upregulated genes in MF patient granulocytes<sup>21</sup> ( $n = 62$  for MF,  $n = 23$  for control) and genes upregulated in IL-1 $\beta$  treated *Jak2<sup>V617F</sup>* LSK cells ( $n = 2$  for IL-1 $\beta$  treated,  $n = 3$  for PBS treated). The cutoffs were FDR-adjusted  $p < 0.05$ . Overlapping genes showed enrichment for MYC targets, mTORC1 signaling, translation and myeloid development gene signatures. **d** Heat maps of selected upregulated transcripts related to MYC targets, mTORC1 signaling, translation and myeloid development gene signatures in LSK cells from *Jak2<sup>V617F</sup>* mice treated with IL-1 $\beta$  ( $n = 2$ ) compared to PBS

( $n = 3$ ) (FDR < 0.05). Gene transcripts shown in bold were further validated. **e** RT-qPCR validation of Lcn2, Clec5a, Odc1, Bcat1 and Eif4a1 mRNA expression in LSK cells from *Jak2<sup>V617F</sup>* mice treated with IL-1 $\beta$  compared to PBS. RT-qPCR results were normalized with Hprt1 expression ( $n = 3$  biological replicates per group). **f** CFU-GM colonies were assessed following overexpression of Lcn2, Clec5a and Bcat1 in *Jak2<sup>V617F</sup>* BM. CFU-GM colonies relative to vector control are shown in bar graphs as mean  $\pm$  SEM ( $n = 6$  biological replicates per group; each data point is an average of two technical replicates). **g** Megakaryocytic (Mk) cells were derived from the *Jak2<sup>V617F</sup>* BM overexpressing vector, Lcn2, Clec5a and Bcat1, and cell proliferation was assessed in triplicates every 2 days over 6 days using Cell Titer Glow. Megakaryocytic cell proliferation relative to vector control are shown in bar graphs as mean  $\pm$  SEM ( $n = 5$  biological replicates per group; each data point is an average of two technical replicates). Statistical significances were determined in **e-g** using multiple unpaired two-tailed t-tests. Source data are provided as a Source Data file.

**Figure 4 – Effects of IL-1 $\beta$  on gene expression in *Jak2V617F* mice hematopoietic progenitors.**

We isolated LSK cells from the bone marrow of mice that were treated with PBS and IL-1 $\beta$ , and then sent them for RNA-sequencing. Differential gene expression analysis was performed, and the results were visualized using a volcano plot. Gene-set enrichment analysis (GSEA) was then conducted to reveal the enrichment signature of myeloid development, MYC targets, MTORC1 signaling, and translation. By overlapping the upregulated genes of IL-1 $\beta$ -treated murine LSK cells with those of MF patients, we identified shared genes that exhibit similar gene signatures to the GSEA. We then selected genes from these enriched pathways and visualized them using a heatmap, with the highlighted genes further validated using qPCR.

# Effects of IL-1 on gene expression changes and collagen expression in BM mesenchymal stromal cells

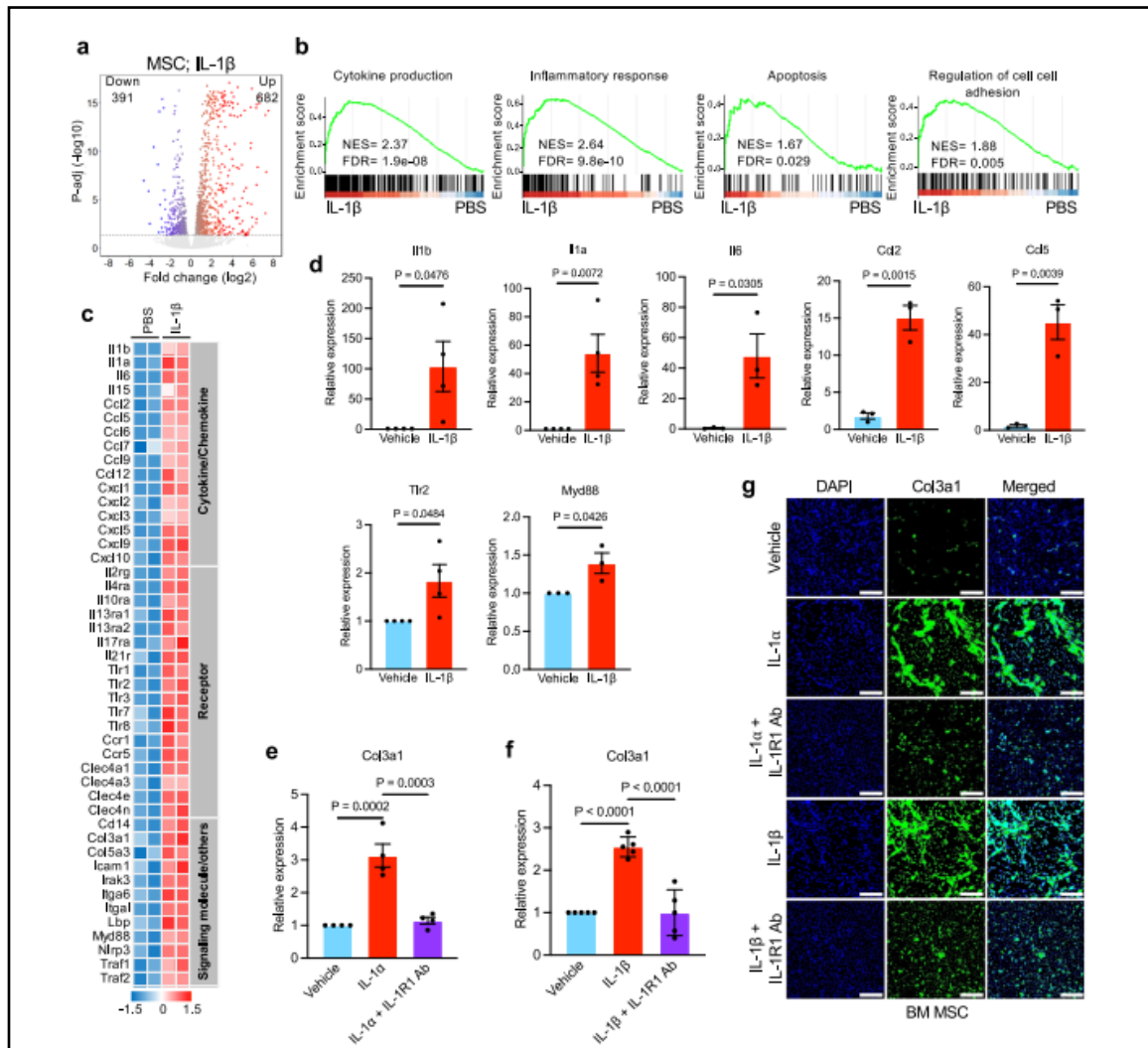


**Fig. 7 | Effects of IL-1 on gene expression changes and collagen expression in BM mesenchymal stromal cells.** **a** Volcano plot showing significantly upregulated and downregulated ( $p\text{-adj} < 0.05$  and  $\log_2fc > 0.5$ ) genes in IL-1 $\beta$  (5 ng/mL) treated MSCs ( $n = 2$ ) compared to PBS treated MSCs ( $n = 2$ ). **b** Gene-set enrichment analyses (GSEA) show significant increase in expression of genes related to cytokine production, inflammatory response, apoptosis and regulation of cell-cell adhesion in IL-1 $\beta$  treated MSCs ( $n = 2$ ) compared to PBS treated MSCs ( $n = 2$ ). Enrichment plots with normalized enrichment score (NES) and false discovery rate (FDR) are shown. **c** Heat map of selected genes upregulated in IL-1 $\beta$  treated MSCs ( $n = 2$ ) compared to PBS treated MSCs ( $n = 2$ ) with expression changes more than 1.5-fold (FDR < 0.05). **d** RT-qPCR validation of increased mRNA expression of Il1b ( $n = 4$ , 4 biological replicates), Il1a ( $n = 3$ , 3), Ccl2 ( $n = 3$ , 3), Ccl5 ( $n = 3$ , 3), Tlr2 ( $n = 4$ , 4) and Myd88 ( $n = 3$ , 3) in IL-1 $\beta$  treated MSCs compared with PBS treated MSCs. Data were

normalized with Hprt1 expression. Data are shown in bar graphs as mean  $\pm$  SEM. Statistical significances were determined using two-tailed unpaired  $t$ -test. **e, f** BM MSCs were treated with vehicle (PBS), IL-1 $\alpha$  (5 ng/mL) or IL-1 $\alpha$  (5 ng/mL) + IL-1RI Ab (1  $\mu$ g/mL) ( $n = 4$  biological replicates per group) (**e**) and vehicle (PBS), IL-1 $\beta$  (5 ng/mL) or IL-1 $\beta$  (5 ng/mL) + IL-1RI Ab (1  $\mu$ g/mL) ( $n = 5$  biological replicates per group) (**f**) for 72 h. Col3a1 mRNA expression was assessed using RT-qPCR. Fold change of Col3a1 expression is shown in bar graphs as mean  $\pm$  SEM. Statistical significance was determined using one-way ANOVA with Tukey's multiple comparison test. **g** Immunofluorescence images showing increased Col3a1 expression in MSCs upon IL-1 $\beta$  (5 ng/mL) and IL-1 $\alpha$  (5 ng/mL) stimulation and, IL-1RI Ab (1  $\mu$ g/mL) treatment abolished IL-1 $\alpha$ / $\beta$ -induced Col3a1 expression in the BM MSCs. Col3a1 (green) and DAPI (blue); scale bars, 100  $\mu$ m. Representative images from 3 independent experiments are shown. Source data are provided as a Source Data file.

**Figure 5 – Effects of IL-1 on gene expression changes and collagen expression in BM mesenchymal**



We performed a similar RNA-sequencing analysis on mesenchymal stromal cells that were treated with either PBS or IL-1 $\beta$ . Differential analysis was visualized using a volcano plot, with the gene signature showing enrichment in cytokine production, inflammatory response, apoptosis, and cell-cell adhesion. Key genes from the selected enrichment were then shown in a heatmap.

## **U2af1 is required for survival and function of hematopoietic stem/progenitor cells**

Avik Dutta, Yue Yang, Bao T. Le, Yifan Zhang, Omar Abdel-Wahab, Chongzhi Zang, &

Golam Mohi

Leukemia 2021

[doi: <https://doi.org/10.1038/s41375-020-01116-x>]

This project investigates the role of U2AF1 in normal hematopoiesis. Conditional deletion of U2af1 in mice results in defective hematopoiesis characterized by pancytopenia and ablation of hematopoietic stem and progenitor cells (HSPCs), which leads to early lethality due to bone marrow failure. In this project, I provided bioinformatic analysis support, which included RNA sequencing analysis and alternative splicing analysis.

## Effect of U2af1 deletion on gene expression profile in HSPC

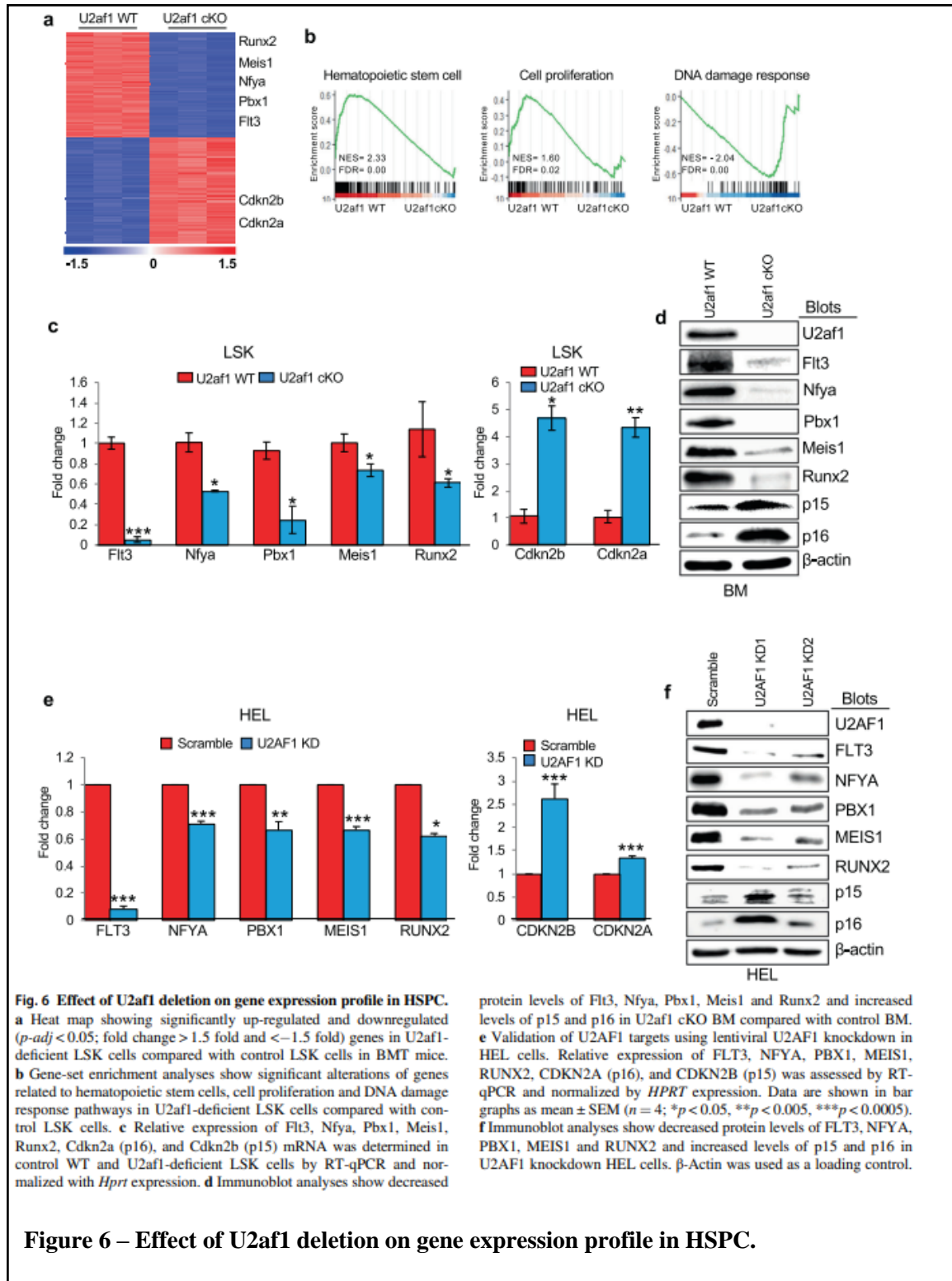


**Fig. 6 Effect of U2af1 deletion on gene expression profile in HSPC.** **a** Heat map showing significantly up-regulated and downregulated ( $p$ -adj < 0.05; fold change > 1.5 fold and < -1.5 fold) genes in U2af1-deficient LSK cells compared with control LSK cells in BMT mice. **b** Gene-set enrichment analyses show significant alterations of genes related to hematopoietic stem cells, cell proliferation and DNA damage response pathways in U2af1-deficient LSK cells compared with control LSK cells. **c** Relative expression of Flt3, NfyA, Pbx1, Meis1, Runx2, Cdkn2a (p16), and Cdkn2b (p15) mRNA was determined in control WT and U2af1-deficient LSK cells by RT-qPCR and normalized with *Hprt* expression. **d** Immunoblot analyses show decreased

protein levels of Flt3, NfyA, Pbx1, Meis1 and Runx2 and increased levels of p15 and p16 in U2af1 cKO BM compared with control BM. **e** Validation of U2AF1 targets using lentiviral U2AF1 knockdown in HEL cells. Relative expression of FLT3, NFYA, PBX1, MEIS1, RUNX2, CDKN2A (p16), and CDKN2B (p15) was assessed by RT-qPCR and normalized by *HPRT* expression. Data are shown in bar graphs as mean  $\pm$  SEM ( $n = 4$ ; \* $p < 0.05$ , \*\* $p < 0.005$ , \*\*\* $p < 0.0005$ ). **f** Immunoblot analyses show decreased protein levels of FLT3, NFYA, PBX1, MEIS1 and RUNX2 and increased levels of p15 and p16 in U2AF1 knockdown HEL cells.  $\beta$ -Actin was used as a loading control.

**Figure 6 – Effect of U2af1 deletion on gene expression profile in HSPC.**

We performed an RNA sequencing analysis on murine LSK populations, comparing U2af1 knockout and U2af1 wild-type. Differential analysis was shown through a heatmap, which displayed the top upregulated and downregulated genes. Gene-set enrichment analysis revealed that the loss of U2af1 resulted in negative enrichment of hematopoietic stem cells and proliferation signature, while having a positive enrichment of DNA damage response.

## Effect of U2af1 deletion on RNA splicing

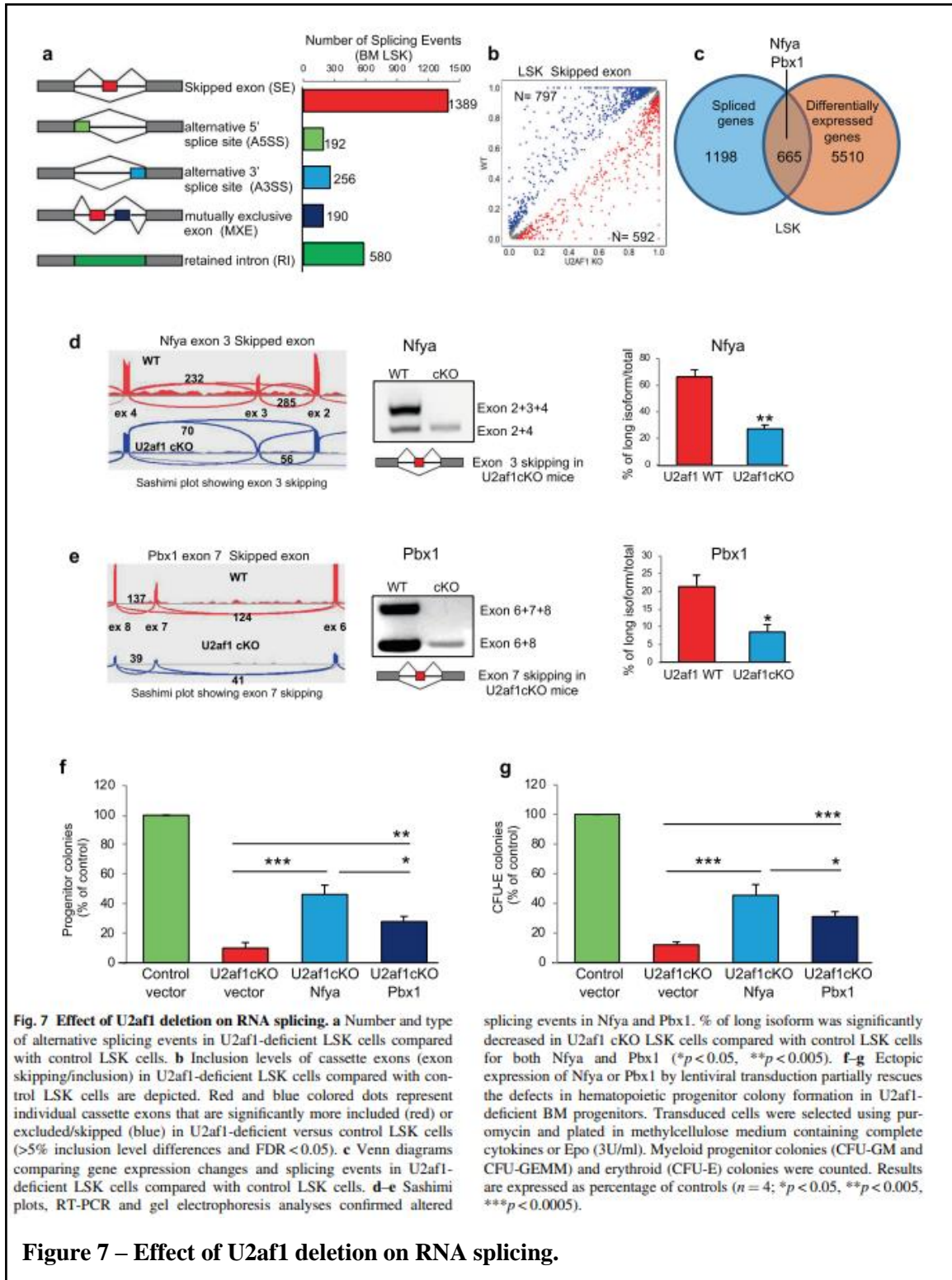


**Fig. 7 Effect of U2af1 deletion on RNA splicing.** **a** Number and type of alternative splicing events in U2af1-deficient LSK cells compared with control LSK cells. **b** Inclusion levels of cassette exons (exon skipping/inclusion) in U2af1-deficient LSK cells compared with control LSK cells are depicted. Red and blue colored dots represent individual cassette exons that are significantly more included (red) or excluded/skipped (blue) in U2af1-deficient versus control LSK cells (>5% inclusion level differences and FDR < 0.05). **c** Venn diagrams comparing gene expression changes and splicing events in U2af1-deficient LSK cells compared with control LSK cells. **d-e** Sashimi plots, RT-PCR and gel electrophoresis analyses confirmed altered

splicing events in Nfya and Pbx1. % of long isoform was significantly decreased in U2af1 cKO LSK cells compared with control LSK cells for both Nfya and Pbx1 (\* $p$  < 0.05, \*\* $p$  < 0.005). **f-g** Ectopic expression of Nfya or Pbx1 by lentiviral transduction partially rescues the defects in hematopoietic progenitor colony formation in U2af1-deficient BM progenitors. Transduced cells were selected using puromycin and plated in methylcellulose medium containing complete cytokines or Epo (3U/ml). Myeloid progenitor colonies (CFU-GM and CFU-GEMM) and erythroid (CFU-E) colonies were counted. Results are expressed as percentage of controls ( $n$  = 4; \* $p$  < 0.05, \*\* $p$  < 0.005, \*\*\* $p$  < 0.0005).

**Figure 7 – Effect of U2af1 deletion on RNA splicing.**

We processed the RNA sequencing data using rMATS to determine significantly altered splicing events. The resulting data showed a significant number of exon skipping and intron retention events. We mapped the level of exon inclusion between U2af1 KO and WT and identified genes with both significant splicing events and differential expression. These genes were shown in a Venn diagram, with the highlighted genes being further examined using a sashimi plot to visualize the specific exon-skipping events.